CHEMICAL REVIEWS

pubs.acs.org/CR

Review

Antifouling Strategies for Selective *In Vitro* and *In Vivo* Sensing

Cheng Jiang,[¶] Guixiang Wang,[¶] Robert Hein,[¶] Nianzu Liu, Xiliang Luo,[*] and Jason J. Davis[*]

Cite This: https://dx.doi.org/10.1021/acs.chemrev.9b00739

Read Online

ACCESS | Metrics & More | Article Recommendations

ABSTRACT: The ability to fabricate sensory systems capable of highly selective operation in complex fluid will undoubtedly underpin key future developments in healthcare. However, the abundance of (bio)molecules in these samples can significantly impede performance at the transducing interface where nonspecific adsorption (fouling) can both block specific signal (reducing sensitivity) and greatly reduce assay specificity. Herein, we aim to provide a comprehensive review discussing concepts and recent advances in the construction of antifouling sensors that are, through the use of chemical, physical, or biological engineering, capable of operating in complex sample matrix (e.g., serum). We specifically highlight a range of molecular approaches to the construction of solid sensory interfaces (planar and nanoparticulate) and their characterization and performance in diverse *in vitro* and *in vivo* analyte (e.g., proteins, nucleic acids, cells, neuronal transmitters) detection applications via derived selective optical or electrochemical strategies. We specifically highlight those sensors that are capable of detection in complex media or those based on novel architectures/approaches. Finally, we provide perspectives on future developments in this rapidly evolving field.

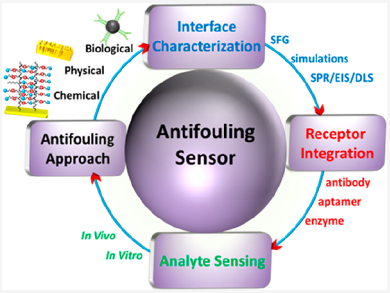

CONTENTS

1. INTRODUCTION

It is undoubtedly the case that an early diagnosis and treatment of disease can dramatically reduce mortality and human suffering. A detection of markers shed from tumors, for example, provides a potent opportunity to diagnose cancer early and disease management.[1−4] However, one major challenge is that in complex biological fluids (such as serum, saliva, urine, etc.) or in the *in vivo* circulating environment, the concentration of disease markers (e.g., specific proteins) is often very low in comparison to the large number of coexisting background species (e.g., proteins, cells) that can adsorb onto a sensing interface nonspecifically. This can cause serious

Received: November 13, 2019

https://dx.doi.org/10.1021/acs.chemrev.9b00739
Chem. Rev. XXXX, XXX, XXX−XXX

operational interference such as false positives, lowered signal-to-noise, and impairing specific recognition/response.[5−7] Further side effects can arise for implantable sensors by, for example, thrombus formation.[8,9] There are a number of ways of combatting this issue by preventing nonspecific binding (fouling) while retaining specific binding. The primary one that does not require sample pretreatment is to integrate nonfouling chemistry into the assaying surfaces.[10,11] The use of such materials has received increasing attention in recent years, where poly(ethylene glycol) (PEG) and its derivatives,[12−14] zwitterionic materials,[15−17] peptides and peptoids,[18−20] and others candidates (e.g., hyaluronic acid (HA), polyoxazoline, etc.)[21−24] have all been applied. Significantly, this has facilitated a quantification of clinically relevant targets in complex media via a number of transducer modalities and with minimal sample pretreatment. In general terms, it is worth noting that no existing antifouling strategy can completely prevent fouling, and indeed this is not a requirement so long as functionality is primarily retained over the relevant time frame of application and any signal-generating "background noise" that arises from nonspecific surface association falls well below the required detection limits. Moreover, as *in vivo* biofouling (i.e., protein corona) is inherent in the action of the immune system, complete inhibition may lead to unintended physiological responses and even damage to the host.[25,26] It should also be noted that different sensory formats suffer differently from fouling. For example, sandwich assays are much less sensitive to fouling so long as fouling does not impede the primary (capture) antibody. In contrast, label-free sensors, such as those based on surface-plasmon resonance (SPR) or electrochemical impedance spectroscopy (EIS), cannot distinguish between specifically bound target analytes and other adsorbed interferents and are, then, particularly sensitive to the deleterious impact of fouling. It is thus imperative that, for any desired sensing application, the potential impact of nonspecific adsorption is carefully considered. In general, a large variety of relevant characteristics should be considered and optimized for; these include sensitivity, selectivity, reproducibility, dynamic range, lifetime, baseline stability, ease-of-fabrication, and response time. In different sensor formats, the impact of fouling on these parameters can be considerably different such that it will often be necessary to rank parameters that are more or less crucial to the chosen application. For example, in an implantable sensor, its lifetime and toxicology are of crucial importance, while, in ultrasensitive single molecule sensors, the sensitivity (signal-to-noise) at ultralow concentrations is more important (see Table 1).

In this review, we focus on recent advances in the construction of solid-phase sensors capable of operation in complex biological fluid. We comprehensively discuss a range of antifouling approaches with a particular focus on the most commonly used zwitterion- and PEG-based highly hydrated chemical surface modifiers. In addition to these chemical approaches, physical (e.g., substrate topography engineering or membrane filtration) and biological approaches (e.g., bio-affinity depletion or enzyme catalyzed degradation) will be discussed. Construction methods, including those based on self-assembly, (electro)polymerization, and electrografting, will be highlighted as well as the integration of specific (bio)-recognition elements. The experimental and theoretical methods that have been employed to study these architectures and their associated antifouling performance are also described. Lastly, we discuss a number of specific applications of so derived *in vitro* and *in vivo* sensors capable of sensing clinically relevant target analytes such as proteins, nucleic acids, or circulating small molecules like dopamine or glucose.

Table 1. Overview of Important Sensory Parameters in the Context Specific Sensor Antifouling Performance

sensor type	principle challenges[a]
general sensors, PoC/disposable sensors	sensitivity
	selectivity
	reproducibility
	response time
	fabrication cost
	degree of user intervention
ultrasensitive and single molecule sensors	high signal/noise at ultralow concentration
	data magnitude
	scalability
durable (e.g., implantable, wearable) sensors	selectivity
	operation duration
	immunogenicity

[a]It is important to note we have highlighted the principle challenges that are (uniquely) associated with the specific sensor type. Many general assay characteristics, such as a required sensitivity and selectivity, will be common to all.

2. CHEMICAL ANTIFOULING STRATEGIES AND THEIR SENSING APPLICATIONS

One of the most commonly employed strategies to endow sensory interfaces with antifouling properties is the use of chemical modifiers that render the interface strongly hydrated. This hydration has been associated with a resistance to fouling (as discussed in more detail in Section 2.2) and is generated by decorating the sensory interfaces with highly polar, hydrated chemical groups/materials. In this section, we will discuss the most commonly used chemical agents, their incorporation into sensors, and the evaluation of their antifouling properties.

2.1. Selection and Immobilization of Antifouling Agents

2.1.1. Choice of Antifouling Agent. As shown in Figure 1, a wide range of molecular systems, such as polyethyleneglycol (PEG, >10 EG units) and its derivatives, zwitterionic species (phosphorylcholine (PC), sulfobetaine (SB), and carboxybetaine (CB)), peptides with alternating or random mixed-charge (based on glutamic or aspartic acid (E/D) and lysine (K), e.g., EKEKEKEC),[27] and other polymers like polysaccharides, polyoxazolines, poly(hydroxy acrylates), hyperbranched polyglycerol (HPG), or hybrid materials (e.g., PEG-SB) have been shown to possess significant antifouling properties that arise primarily from their strong hydration (see Section 2.2).[28−31] All of these systems have been employed for a variety of purposes and possess specific features and advantages/disadvantages in terms of derived specific sensing (discussed in more detail in Section 2.3). We will first introduce the means by which these chemistries can be incorporated into interfaces and then how this can be characterized.

2.1.2. Immobilization Strategies. As shown in Figure 2, the immobilization of an antifouling coating onto a solid substrate can be achieved through a range of methods. Most commonly, self-assembly,[32−34] electrografting,[35,36] or polymerization (e.g., electropolymerization,[37,38] atom transfer radical polymerization (ATRP),[39−43] or reversible addition−fragmen-

https://dx.doi.org/10.1021/acs.chemrev.9b00739
Chem. Rev. XXXX, XXX, XXX−XXX

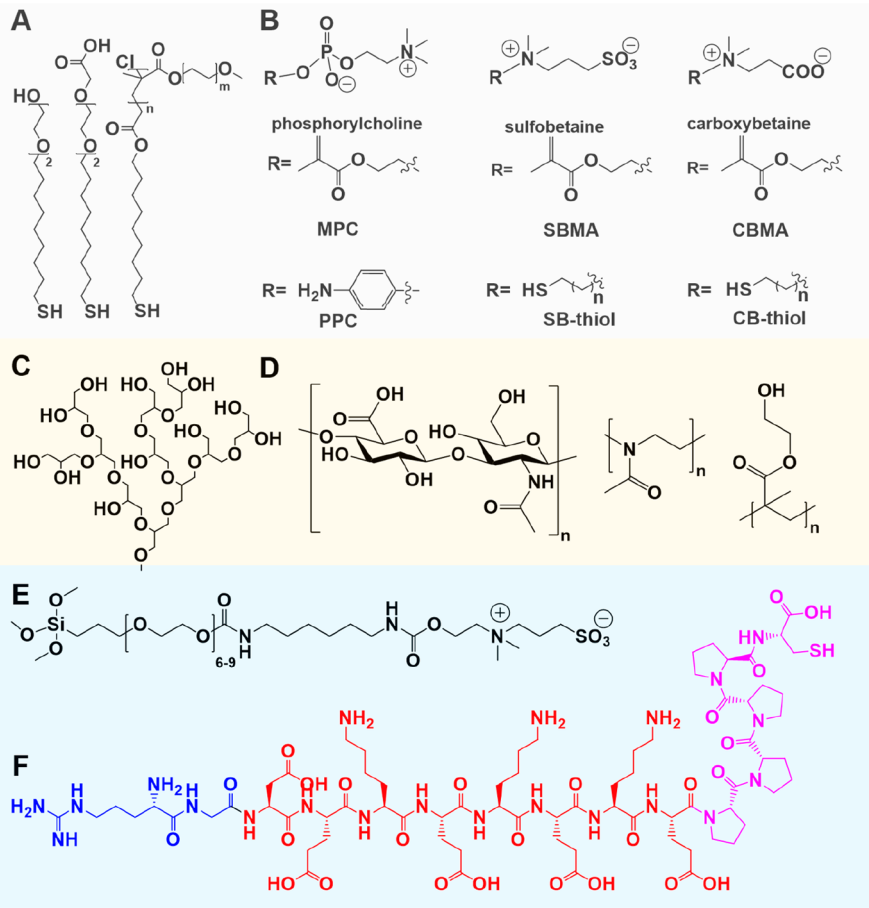

Figure 1. Chemical structures of (A) OEG/PEG based thiols, (B) zwitterionic molecular systems, (C) hyperbranched polyglycerol (HPG), (D) hyaluronic acid (HA), poly(2-methyl-2-oxazoline) and poly(2-hydroxyethyl methacrylate) (pHEMA) (from left to right), (E) PEG-SB silane, and (F) an all-in-one natural mixed peptide containing a cell recognition sequence (RGD, blue), antifouling unit (EKEKEKE, red), and an anchoring sequence (CPPPP, magenta).

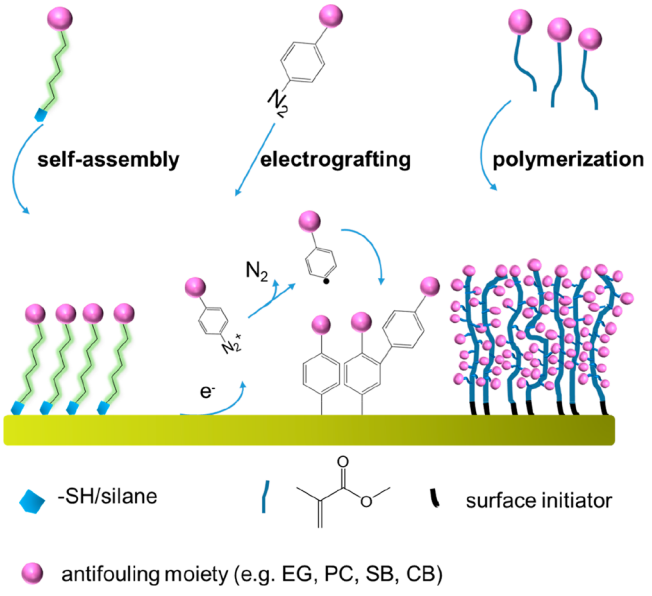

Figure 2. Common approaches for surface functionalization with antifouling molecular systems, from left to right: self-assembly, electrografting, and polymerization.

tation chain transfer (RAFT)[44,45]) methodologies are applied. Importantly, an extensive variety of nonfouling architectures can be incorporated into sensors utilizing these approaches if they are endowed with the appropriate chemical functionalities (e.g., thiols, silanes, or (meth)acrylates). In prior considering an immobilization protocol, both the specific underlying substrate and the required film characteristics (hydration, chemical stability, biological functionalization etc.) should be taken into account. One of the most common methods to immobilize antifouling components is self-assembly *via* "thiolate" bonding at noble metal surfaces.[33,34,46,47] This well-established methodology offers easy access to well-defined, monolayer architectures *via* simple exposure of clean (commonly gold) substrates to solutions or vapors of thiol-derived organics. Though deemed simple and undoubtedly ubiquitous, it is, however, limited in terms of substrate scope. In contrast, polymeric antifouling materials have been explored extensively and can be applied to a broad range of interfaces *via* graft-to and graft-from strategies whereby not only various monomers (most commonly (meth)acrylates) can be used but various film parameters, such as thickness and density can often be controlled easily.[12,48−50]

Another commonly used strategy to functionalize conductive interfaces (relevant to electronic/electrochemical or plasmon resonance sensing) is electrografting.[51] For example, the reductive grafting of diazonium salts, which can be presynthesized or generated *in situ* from the corresponding aniline, is a convenient method to functionalize a variety of

https://dx.doi.org/10.1021/acs.chemrev.9b00739
Chem. Rev. XXXX, XXX, XXX−XXX

(electrode) materials such as carbon, gold, or platinum. Specifically, the electrografting of arydiazonium salts proceeds *via* the formation of an aryl radical, which spontaneously reacts with the substrate to form a covalent bond.[52] Depending on the grafting conditions (time, potential range, concentration, etc.), films of variable thickness can be obtained. This methodology can be applied to form homogeneous (single component)[53] or heterogeneous films (multiple components).[54] Antifouling moieties, for example, ethylene glycol (EG)[55] or zwitterionic groups (phosphoryl choline (PC), sulfobetaine (SB), carboxybetaine (CB)),[35,56,57] at the *para*-position of the corresponding aniline precursors can be grafted and can endow the resultant interface with the desired antifouling properties.

2.2. Characterization of Antifouling Surfaces

In recent years, great progress has been made in elucidating the processes that govern fouling interactions at interfaces and how these can be modulated through (chemical) modification. The widely accepted view is that entropic loss associated with surface group mobility upon fouling (steric suppression) and the intrinsic strong hydration of these films play key roles wherein a tightly bound water layer, that is, hydration layer, forms a physical and energetic barrier to (protein) adsorption (Figure 3).[15,58] Where neutral hydrophilic components are

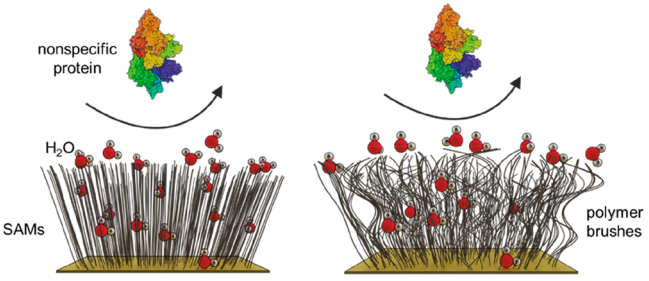

Figure 3. Antifouling molecular films present highly hydrated functionalities (e.g., EG, zwitterionic PC/SB/CB), which are implicit in protein resistance.

used (such as PEG chains), this hydration is tethered *via* hydrogen bonding.[12,59] When charged (e.g., zwitterionic) interfaces are used, the hydration layer has a large electrostatic component.[60−62] These are generalized observations/assumptions that populate an accepted picture without providing mechanistic detail. Understanding the specific structure of surface hydration and other interfacial processes/characteristics is valuable in guiding the design of new and effective nonfouling materials for robust sensing in complex environments. The following section will briefly discuss nonfouling mechanisms and the correlation between interfacial structure and nonspecific surface association as supported by simulations and experimental studies. It should be noted that most of these studies are carried out on chemical antifouling systems but that the experimental techniques that will be discussed can often also be utilized to evaluate the performance of other (nonchemical) systems such as that provided by porous electrodes (Section 3.1).

2.2.1. Probing Antifouling Mechanism. *2.2.1.1. Experimental Analyses.* A number of studies have been reported to directly probe the hydration layer of a range of nonfouling chemical entities. In solution nuclear magnetic resonance (NMR) spectroscopy has been utilized to, for example, study the hydration of poly (sulfobetaine methacrylate) (pSBMA) or PEG, however it is it is unclear to what extent these results are transferable to a solid/liquid nonfouling interface where film thickness, packing density, chain conformation and local chain flexibility effects are very likely to be significant.[63−65] A direct insight into the hydration of interfaces can be provided by sum frequency generation (SFG) vibrational spectroscopy. SFG vibrational spectroscopy is surface-sensitive technique[66] and, unlike other methods, which cannot distinguish between interfacial and bulk water, it facilitates a selective investigation of the properties of the former. This is achieved by irradiation of the surface with two laser beams which generate a mixed output signal offering information complementary to that offered by more standard IR and Raman spectroscopies (Figure 4).[67,68] This has for example been exploited by Leng et

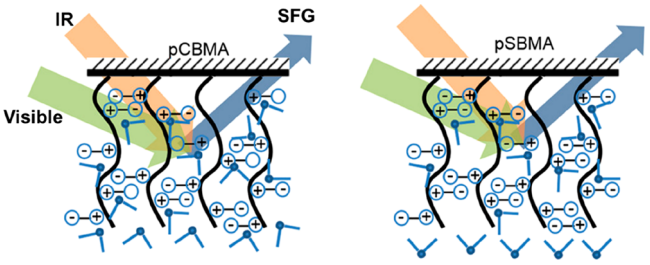

Figure 4. Schematic representation of the investigation of water molecules on pCBMA and pSBMA coated silica prism by SFG. Reproduced with permission from ref 76. Copyright 2018 American Chemical Society.

al., who used SFG for an in situ and real-time assessment of the surface hydration of pSBMA and OEG methacrylate (OEGMA) polymer brushes at SiO_2/liquid interfaces exposed to protein solution.[69,70] The SFG intensity is correlated with the ordering of the dipole moments of the interfacial functional groups selected and thus allows a direct interrogation of water molecule ordering at the interface; a strong SFG signal for water thus indicates both high levels of ordering and of hydration.[71−74] In Leng's work, it was observed that, although strongly bonded water exists at both interfaces, the surface hydration of pSBMA remained unaffected while the water ordering at the pOEGMA surface was disturbed upon exposure to protein (1 mg mL^{-1} of bovine serum albumin (BSA), lyzosome or fibrinogen).[70] Wang et al. have similarly applied SFG to confirm that interfacial water molecule presence within EG based self-assembled monolayer (SAM) films.[75]

In another study from Leng et al., water molecules were shown to be strongly hydrogen-bonded to zwitterionic interfaces (poly (carboxybetaine acrylamide) (pCBAA) and pSBMA), much more than at pOEGMA (which contained a detectable amount of weakly hydrogen-bonded water).[69] Chen and co-workers further elucidated the water structure on nonfouling poly(carboxybetaine methacrylate) (pCBMA) and poly(sulfobetaine methacrylate) pSBMA-modified silica prisms using SFG (Figure 4) at different solution pH values showing that, depending on pH-induced protonation/deprotonation of the zwitterionic groups, the water molecules adopt different orientations.[76] This work thus provides important insights on the relationship between nonfouling behavior and the external environment (such as pH), which might be applied in pH-responsive nonfouling interfaces. Further studies of the hydration of SBMA as well as acrylamide and polysaccharide

https://dx.doi.org/10.1021/acs.chemrev.9b00739
Chem. Rev. XXXX, XXX, XXX−XXX

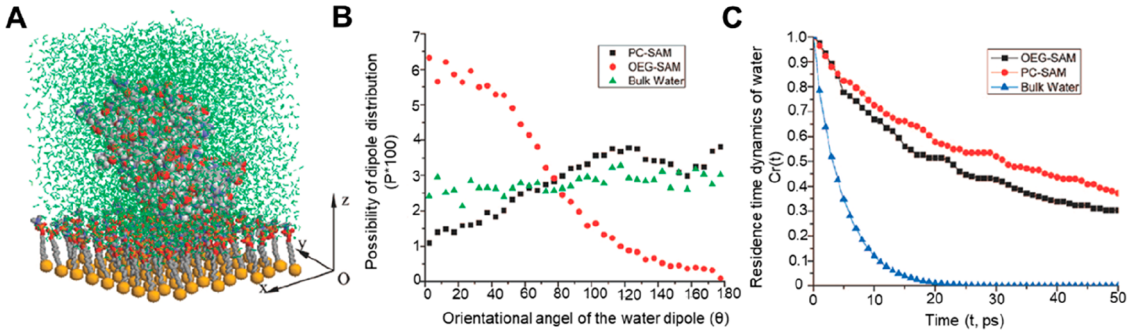

Figure 5. Simulation of water structure at PC and OEG SAMs. (A) Simulated structure, including water, of PC SAMs and model protein (lysozyme) (B) Water dipole distribution near the PC and OEG-SAM and in bulk water and (C) Water residence times of SAMs and bulk water. Adapted with permission from ref 81. Copyright 2008 American Chemical Society.

(alginate and hyaluronic acid) based polymers have further reinforced the stronger hydrogen-bonding water association with SB in comparison to the neutral hydrophilic polymers.[77] Recently, the same group used SFG vibrational spectroscopy to study the interfacial water structure of mixed charged polymers generated by surface initiated-ATRP (SI-ATRP) on a silica prism revealing that only the net neutral 1:1 mixed charge interface shows significant antifouling properties in single protein solutions, reinforcing the importance of high hydrophilicity and low net charge (polymer thickness: 20 nm).[78] In summary, we have a picture, then, that surface hydration, as can be assessed by SFG vibrational spectroscopy, has a large impact on the subsequently resolved antifouling performance of the interface.

2.2.1.2. Molecular Simulations. Computational studies are valuable in both supporting these experimental observations and in potentially aiding interfacial design without the need for prior acquisition of specific data. In 1991, Jeon et al. reported the first theoretical study of protein adsorption onto PEG-decorated interfaces. They noted that steric repulsion resulting from the compression of PEG chains upon approach of the protein to the surface was the main driving force preventing adsorption. It was concluded that longer chains and higher surface densities would lead to better protein resistance.[79] However, in this study no atomic-level information of hydration was considered. To directly correlate film hydration with antifouling performance, Zheng et al. have reported a restrained molecular dynamics (MD) simulation to calculate the interaction forces exerted onto a protein from an OEG-SAM and its associated water, as the protein approaches the surface. Their force−distance profiles show that the strength of repulsive force acting on the protein decreases across OEG-SAMs > OH-SAMs > CH_3−SAMs. Moreover, this work appeared to confirm that the total repulsive force is composed of two contributions: one from the SAM surface (loss of conformational entropy) and the other from interfacial water with the latter contributing more.[80]

In another study, He et al. compared the structural and dynamic properties of water molecules near the SAMs of zwitterionic PC and nonionic EG using MD simulations (Figure 5A). They showed that water molecules near the PC-SAMs have a lower mobility, wider dipole orientation distribution and residence time than those near the EG-SAMs (Figure 5B,C).[81] In another paper, Shao et al. calculated the hydration free energies of CB, SB, and EG_4 moieties in SAMs using the free energy perturbation method.[82] The hydration free energy of zwitterionic CB and SB moieties was observed to be much larger (−404 and −519 kJ mol^{-1}, respectively) than that of nonionic EG_4 moieties (−182 kJ mol^{-1}), indicating that, as fully expected and noted already, zwitterionic materials exhibit stronger hydration.[61] In a recent study the difference in self-association between oppositely charged moieties in zwitterionic pSBMA and pCBMA was investigated using MD simulations (at 1.5 M in solution).[83] Results indicated more and stronger interactions (associations) between the oppositely charged groups in pSBMA due to the similar charge density of the sulfonate and ammonium moieties. In contrast, the larger discrepancy in charge density of carboxylate and ammonium in pCBMA leads, apparently, to fewer/weaker interactions but facilitates a stronger hydration.

When nonfouling interfaces are applied within field-effect transistors (FETs) or other electroanalytical configurations, the influence of field on molecular orientation is worthy of consideration. In MD simulation studies by Xie et al. PC-SAMs were found to be electrically responsive such that protein-resistance could be controllably modulated.[84] Results specifically indicated that PC-SAMs can exhibit three states with different charge distributions, namely, one where both negatively charged phosphate groups and positively charged choline groups are exposed to solution (state 1, no electric field), only the phosphate groups are exposed with the choline groups buried (state 2, positive electric field), and choline groups exposed to the solution when the PC chains are stretched (state 3, negative electric field). As a result, the interaction between the model protein cytochrome c (isoelectric point of 9.6) and the surface was deemed tunable. In state 1, adsorption was predicted to be reversible, while in states 2 and 3, adsorption was enhanced and retarded, respectively, due to electrostatic interactions between the positively charged protein and the exposed groups. Such findings potentially enable an enhancement of antifouling properties by tuning the external electric field and provide a note of caution in assuming native characteristics are retained when surface-imposed fields are actioned.

The presented computational studies, then, support the picture developed by spectroscopic analysis that a strongly bound hydration layer plays a pivotal role in preventing interfacial fouling and offer a fundamental view into the behavior of antifouling molecular systems. It is sensible to note that current simulation studies are both limited in chemical scope and usually conducted with model protein solutions; they do not offer a full picture on the real-world behavior of the antifouling interfaces. For example, the impact of the antifouling components on specific binding events at

https://dx.doi.org/10.1021/acs.chemrev.9b00739
Chem. Rev. XXXX, XXX, XXX−XXX

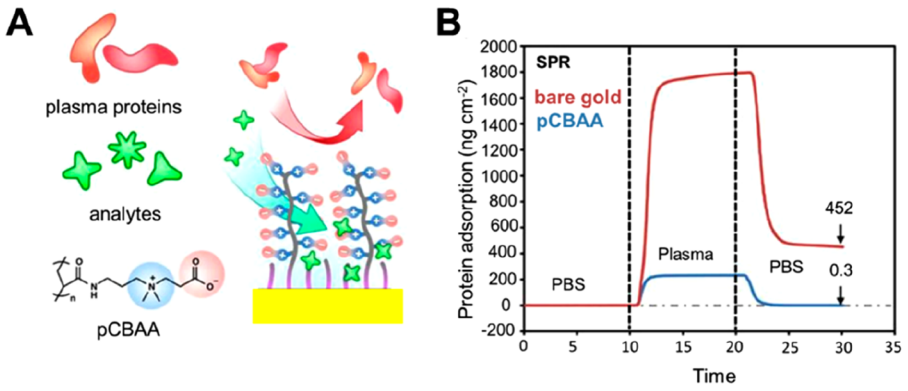

Figure 6. (A) Schematic of a hierarchical pCBAA-based zwitterionic nonfouling modification on a gold surface. (B) Typical SPR sensogram of protein adsorption from undiluted plasma on bare gold and a pCBAA-modified gold surface. Reproduced with permission from ref 87. Copyright 2016 Springer Nature.

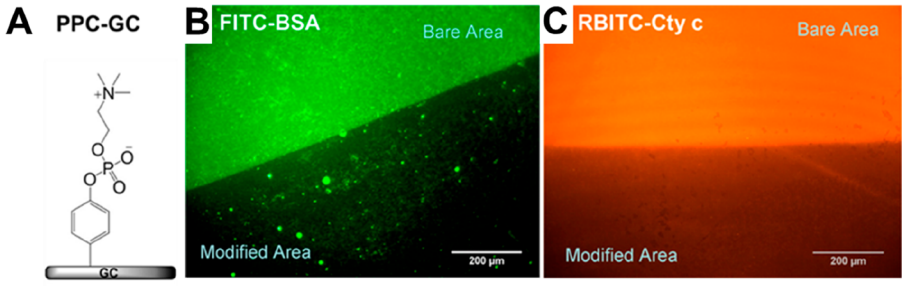

Figure 7. (A) Chemical structure of PPC on glassy carbon electrode. Evaluation of protein adsorption of (B) FITC-BSA and (C) RBITC-Cyt on PPC-GC surface by fluorescence imaging. Scale bars are 200 μm. Reproduced with permission from ref 88. Copyright 2013 American Chemical Society.

incorporated bioreceptors has not been investigated at any depth nor have analyses been carried out to model more complex solutions where a broad range of intermolecular interactions are present. This gap in data will undoubtedly close with increasing computational power.

2.2.2. Evaluation of Antifouling Behavior. In seeking to apply some of the above principles in an analytical format that additionally enables selective target recruitment, careful component selection needs to be married to a prior (chemical, physical, spectroscopic) analysis of the nonfouling interface. In this section, we focus on the experimental methods that have been routinely used to examine interactions at functionalized solid surfaces (e.g., flat electrodes, spherical particles).

2.2.2.1. Surface Plasmon Resonance. Surface Plasmon Resonance (SPR) has been extensively used to examine protein adsorption at chemically decorated interfaces, enabling a real time and quantitative probing without the necessity for labeling. SPR takes advantage of surface plasmons generated by incident light excitation in thin metal layers. It is specifically sensitive to dielectric constant change above the metal layer and can thus report on binding events (including kinetics).[85] This enables a facile evaluation of specific and nonspecific adsorption events and has thus been heavily utilized not only for biosensing but also evaluation of protein adsorption at PEG,[11,12] zwitterion[15−17] or peptide-based[20] antifouling interfaces. For example, a direct comparison of fibrinogen adsorption on five SAMs (OEG, PC, oligo-PC and mixed-charge SAMs) as well as three polymer brushes (pCBMA, pSBMA, pOEGMA) on gold has been reported.[86] All interfaces exhibit a low fibrinogen adsorption (from single protein solution, 1 mg mL^{-1}); 3.8 ng cm^{-2} for PC SAMs, and <0.3 ng cm^{-2} for the other surfaces), but adsorption from undiluted human blood plasma was observed to vary widely, with polymer brushes exhibiting fouling levels some 25−30 times lower than the SAMs and pCBMA having the lowest levels of total protein adsorption (0.4 ng cm^{-2}). Moreover, decreasing the number of EG or PC units in the SAMs was observed to lead to an expected increase in adsorption from both fibrinogen solution and plasma (see also Section 3.1.2).[86] As shown in Figure 6, very low fouling levels from undiluted plasma, assessed by SPR, has also recently been reported for a gold substrate decorated with SAMs of pCBAA (0.3 ng cm^{-2} vs 452 ng cm^{-2} for bare gold).[87]

2.2.2.2. Fluorescence Imaging. Fluorescence imaging offers a very convenient and accessible way of examining the spatial distribution and status (such as aggregation) of adsorbed fluorophore-labeled materials such as proteins or cells and can thereby directly report on interfacial fouling.[88−91] The Gooding group, for example, have employed fluorescence imaging to compare protein adsorption levels on glassy carbon (GC) and gold surfaces modified with zwitterionic phenyl-phosphoryl choline (PPC)[88,91] using fluorescein isothiocyanate labeled BSA (FITC-BSA) and rhodamine B labeled cytochrome c (RBITC-Cyt c) (Figure 7). BSA and Cyt c were chosen as representative anionic and cationic proteins at physiological pH and it was demonstrated that the protein-resistance of electrodeposited zwitterionic PPC was superior to that of electrodeposited OEG and bare surfaces with a reduction of protein adsorption of 83% and 90%, respectively. In other work, Zhang et al. modified planar gold with a SI-ATRP generated polymer containing pHEMA and a HWRGWVA peptide (an immunoglobulin G (IgG) recep-

https://dx.doi.org/10.1021/acs.chemrev.9b00739
Chem. Rev. XXXX, XXX, XXX−XXX

tor).[92] Fluorescence experiments then showed that FITC-IgG did not foul on a pHEMA control but was specifically recruited to the pHEMA-receptor interface.

Similarly, Cao et al. have applied fluorescence imaging to evaluate cell adhesion on poly(sulfobetaine-3,4-ethylenedioxythiophene) (pSB-EDOT) coated gold surface.[93] Adhered cells were directly stained with fluorescein diacetate showing negligible cell attachment on pSB-EDOT while the unmodified poly(3,4-ethylenedioxythiophene) (PEDOT) control showed significant cell fouling. While offering simple visual, qualitative assessment of fouling it should be taken into consideration that fluorescence imaging requires the conjugation (and subsequent purification) of suitable fluorophores onto the model fouling agent (e.g., protein) which can be cumbersome and not readily extendable to a refined analysis of complex samples containing a broad range of different proteins.

2.2.2.3. Quartz Crystal Microbalance with Dissipation. A Quartz Crystal Microbalance with Dissipation (QCM-D) constitutes another sensitive label-free technique, in which an alternating voltage is applied to drive the oscillation of a quartz substrate at its resonance frequency.[94] Relevant parameters, such as the mass of adsorbed protein, including associated solvent molecules and the viscoelastic properties of the adsorbed layer, can be determined from frequency (Δf) and dissipation change (ΔD). A combination of the two factors can be used to determine the interaction between underlying nonfouling materials and potential adsorbates.[95−97]

Utilizing QCM-D, the protein resistance of simple zwitterionic SAMs of L-cysteine, L-methionine, and glutathionine (GSH) has, for example, been evaluated.[94] The data demonstrated that, of these interfaces, the GSH-SAM showed lowest fouling when exposed to 1 mg mL^{-1} BSA at physiological pH (37 ng cm^{-2} vs 749 ng cm^{-2} for bare Au) and that the fouling of all SAMs was predictably pH-dependent. For example, the GSH film showed high fouling at pH 4.0 and relatively low fouling at pH 5.0. This is due to electrostatic attraction between BSA and GSH at pH 4.0, due to the pI of BSA and immobilized GSH of 4.7 and 3.9, respectively; they are oppositely charged at this pH. This nicely highlights the attention that should be given to the pH-dependence of nonspecific electrostatic associations. Recently, Li et al. investigated the construction of an effective antifouling layer *via* electrodeposition.[98] The gold electrode was modified with zwitterionic SB *via* diazonium chemistry and fouling studies to 10% fetal bovine serum (FBS) carried out by QCM-D. The authors showed that this film possessed similar antifouling capabilities as the analogous SB-SAM.

In another study, QCM was used to evaluate the antifouling performance of zwitterionic peptides immobilized on polydopamine (PDA)-treated gold substrates.[99] The alternating glutamic acid- and lysine-based peptide interface was observed to show adequate fouling resistance (~110 ng cm^{-2}) to human serum, significantly better than bare gold (~700 ng cm^{-2}), PDA/Au (~870 ng cm^{-2}) and PEG/PDA/Au (~270 ng cm^{-2}).

2.2.2.4. Electrochemical Impedance Spectroscopy. Electrochemical impedance spectroscopy (EIS) is a technique that can be applied to the characterization of electrode interfaces and sensitively report on interfacial change such as those associated with binding events (specific or nonspecific).[100] In recent work from Jiang and co-workers, EIS was applied to evaluate the interactions between proteins and zwitterionic PPC-modified indium tin oxide (ITO) electrodes, in which HSA was selected as a nonspecific model protein.[36] Upon exposure to HSA (1 mg mL^{-1}) the charge transfer resistance (R_{ct}) of the interface did not change, indicating negligible fouling. Similar results were also obtained by Bryan et al. at PEG SAMs.[47] Davis and co-workers have applied non-Faradaic EIS to evaluate protein adsorption on cysteamine/graphene oxide-modified gold microelectrodes.[101] They found that after 30 min exposure to 100% serum or 1 μM BSA in phosphate buffered saline (PBS) for 30 min, the relative change in impedimetric modulus (Z) is considerably lower for cysteamine/GO composite electrodes (<1%) than that of simple cysteamine SAMs (~24%), indicating a significant contribution of GO to overall antifouling performance. Non-Faradaic EIS has also been applied to the ultrasensitive quantification of insulin in neat serum using pCBMA-modified gold electrodes (see also Section 2.3.2).[102] Similarly, the fouling of HSA (1 mM) on ferrocene-tagged peptide SAMs has been evaluated by impedance-derived redox-capacitance.[103] In other examples, Luo's group have assessed the antifouling performance of sensors based on PEG-aptamer-modified PDA/GC[104] and zwitterionic peptide (EKEKEKE-PPPPC)-modified gold electrodes[33,105] using Faradaic EIS, indicating negligible protein adsorption from single protein solution and in diluted plasma in both cases.

2.2.2.5. Dynamic Light Scattering. Through appropriate decoration with antifouling layers (nano)particle-based platforms have gain increasingly intense levels of attention as promising diagnostic and therapeutic tools.[106] In this context, dynamic light scattering (DLS) is a useful technique not only for determination of particle size and size distribution but also for examination of subsequent fouling/absorption or aggregation events. Upon fouling at the liquid−solid interface, a change in the hydrodynamic diameter (D_h) of the particle can be measured. Wang et al. have, for example, reported an analysis of zwitterion functionalized spherical nanoparticles (size).[107] Specifically, silica nanoparticles were conjugated with natural amino acids (L-lysine, L-cysteine, L-arginine) and their antifouling properties indirectly evaluated in BSA and FBS solution, whereby protein adsorption is accompanied with an increase in D_h. It was shown that all of the tested amino acid-functionalized silica nanoparticles can effectively resist protein adsorption under these conditions. Among them, lysine-functionalized silica nanoparticles had the best antifouling performance, showing an increase of (D_h) of only 10% after incubation for up to 24 h in 1 mg mL^{-1} BSA solution and 20% after incubation in 10% FBS solution (initial $D_h \approx 65$ nm). In another paper reported by Sanchez-Salcedo et al. the same approach was applied to evaluate the antifouling performance of zwitterionic 2-methacryloyl posphorylcholine (MPC)-coated mesoporous silica nanoparticles in 1 mg mL^{-1} BSA and 10% FBS solutions.[108] Results showed that D_h remained stable over 72 h. More recently, the antifouling behavior of silica nanoparticles decorated with different compositions of (3-aminopropyl)triethoxysilane (APTES) and zwitterionic SB-silane was assessed (Figure 8).[109] After exposure to FBS, only a slight increase (~2−3 nm) in size of the nanoparticles containing large proportions of zwitterionic moieties (100% SB and 75% SB) was noted. This technique is readily applicable for the evaluation of well-dispersed and homogeneous nanoparticles, but limitations arise for larger beads that aggregate or sediment which can severely interfere with the scattering measurements.

https://dx.doi.org/10.1021/acs.chemrev.9b00739
Chem. Rev. XXXX, XXX, XXX−XXX

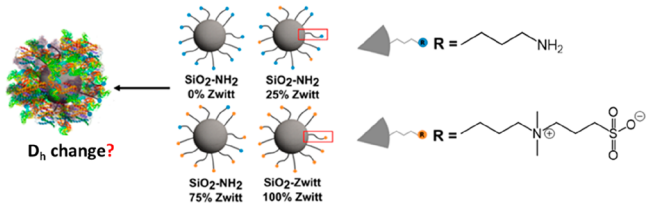

Figure 8. Nanoparticles modified with mixed silanes terminated with amine and zwitterionic SB groups where protein adsorption is evaluated by DLS. Adapted with permission from ref 109. Copyright 2018 American Chemical Society.

2.2.2.6. Bicinchoninic Acid Assay. The Bicinchoninic Acid (BCA) assay is a quantitative colorimetric assay for total soluble protein and can be used to indirectly study protein adsorption at a solid−liquid interface by monitoring solution depletion. For example, the protein-resistance of pSBMA-modified magnetic nanobeads has been assessed this way,[110] where the bead surface modification was, as expected, shown to dramatically reduced nonspecific BSA adsorption (<10 μg adsorption/mg beads). Similarly, BSA fouling resistance (from single protein solution, 4.5 mg mL^{-1}) was demonstrated for PC-coated hydroxyapatite with fouling reduction of 50% in comparison to the unmodified particles.[111] Estupiñán et al. recently prepared a magnetic multifunctional silica particle platform containing antifouling moieties (SB) as well as anchor groups for receptor conjugation (amine and alkene terminated silanes). The protein resistance in undiluted FBS was assessed with the BCA assay after particle incubation revealing only moderate (<60 ng cm^{-2}) fouling. Furthermore, it was demonstrated that the presence of SB did not prohibit subsequent controlled conjugation of an IgG antibody.[112]

There are then, a number of sensitive interfacial techniques available to allow characterization of antifouling materials and their performance on diverse solid supports (conducting or nonconducting, flat or nanoparticle). Some of these allow a direct quantification of adsorbed mass on the interface (e.g., SPR, QCM) while others can serve as a useful qualitative tool to assess fouling (DLS, electrochemistry, (fluorescence) spectroscopy, etc.). In addition to the highlighted approaches, a number of other techniques such as isothermal titration calorimetry (ITC),[113] ellipsometry[114] or differential pulse voltammetry (DPV)[115,116] can also be readily utilized to investigate surface adsorption events. Through the appropriate selection of these complementary techniques, a detailed evaluation of fouling performance can be entertained through the use of (ideally) realistically complex test solutions. This data can then guide the design of sensing interfaces with improved performance, most notably selectivity and robustness.

2.3. Sensors Based on Chemical Antifouling Interfaces

2.3.1. Incorporation of Receptive Elements. In any specific downstream sensory application, functional (bio)-recognition elements need to be incorporated into antifouling surface architectures. It is, of course, imperative (or at least ideal) that the performance of these additional functionalities is not impeded by the nonfouling support and, equally, that the incorporation of significant amounts of such elements can be carried out with minimal perturbation of the supporting antifouling performance.[30] Therefore, the appropriate (co)-incorporation of receptor/anchor and antifouling units is a crucial part of the sensor design. If both functionalities are inherently present in one component such as CB or peptides or functional group terminated OEGs,[34] then direct assembly of this component will yield a modifiable interface in one step (Figure 9A). If the antifouling component is not easily functionalizable, like phosphorylcholine or sulfobetaine, then an additional anchor component must be immobilized simultaneously or consecutively to form a mixed interface (Figure 9B). This can usually be achieved by, for example, self-assembly, electrografting or copolymerization. Importantly, if (bio)recognition and nonfouling elements are coimmobilized their surface ratio must be tuned to obtain the best sensor performance in terms of antifouling performance, target capture efficacy and interfacial selectivity. Depending on the specific tethering method, and the relative reactivity of the different components, this tuning can usually be carried out by

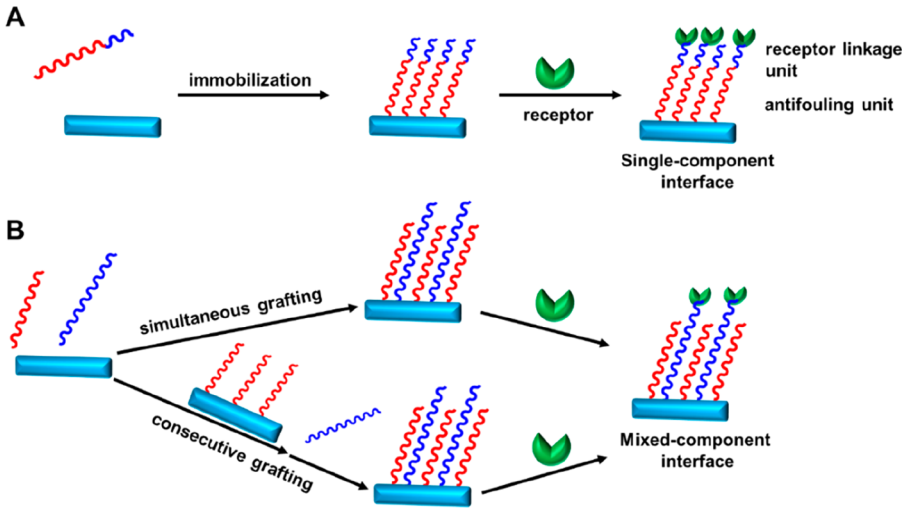

Figure 9. General construction principle of antifouling sensors with anchor sites for receptor immobilization. (A) Antifouling unit (orange) and anchor site for (bio)receptor conjugation (blue) are present in the same component and can thus be assembled in one step to form a "homogeneous" film. (B) Antifouling and anchor units are immobilized separately by either simultaneous or consecutive grafting to form a "heterogeneous" sensory interface.

https://dx.doi.org/10.1021/acs.chemrev.9b00739
Chem. Rev. XXXX, XXX, XXX−XXX

adjusting the immobilization protocol (e.g., concentration, time).[56]

In a typical example, as shown in Figure 10, a mixture of functional elements can also be immobilized by electrografting.

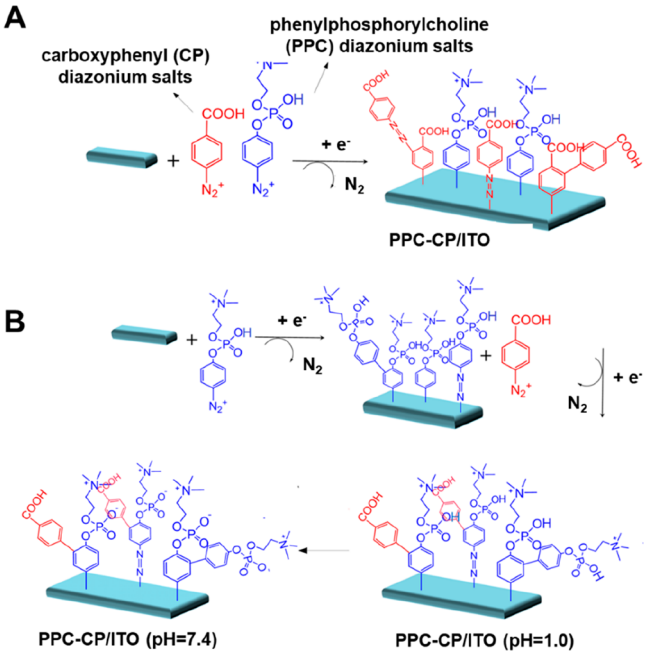

Figure 10. Electrografting mixed layers of PPC and CP on ITO using (A) simultaneous electrografting strategy and (B) consecutive electrografting strategy. Reproduced with permission from ref 36. Copyright 2016 American Chemical Society.

For example, simultaneous and consecutive electrografting of zwittterionic PPC diazonium salts with carboxyphenyl diazonium salts onto ITO electrodes has been investigated by Jiang et al.[36,54] The authors demonstrated that, with the employment of consecutive electrografting, the surface ratio of mixed films can be tuned and antifouling abilities retained through the conjugation of high levels of bioreceptive elements (anti-TNF-α antibody).

Regardless of the specific immobilization protocol that is utilized, attention must be given to the compatibility of all immobilized anchor/receptive/nonfouling components. This includes, but is not limited to, their stability, reactivity, and spatial arrangement. The latter is particularly important, where care must be taken to ensure that the integration of any antifouling components does not (significantly) affect the operation of the sensor (e.g., signal transduction and binding selectivity). For example, when receptive elements are incorporated into the interface, the nonfouling support should not sterically (or electrostatically) impede target binding nor present a chemical environment that is otherwise not conducive to binding (such as a particularly high dielectric where target binding has a large electrostatic component). A sterically imposed "filtering" of background can be beneficial in very specific cases (see Sections 3 and 5).[117] One notable exception to these steric considerations is when receptive units are temporarily embedded within the antifouling interface and controllably exposed upon the application of a stimulus (e.g., electric field, temperature, light).[118−120]

Another important consideration is the effect receptor coupling has on the underlying "native" fouling characteristics of the supporting film; the commonly utilized tethering to film exposed anionic carboxyls, for example, will render an initially zwitterionic moiety cationic. In addition to both the effect of nonfouling chemistry on target capture and the potential impact of receptor integration on nonfouling character, one most also consider signal transduction. If, for example, comparatively thick nonfouling films are married with low levels of receptor; one may then be in a regime where target capture is not effectively transduced to an underlying mass, optical, or electrochemical sensor.

On the basis of the above analyses and general design principles, a broad range of electrochemical or optical sensors for a variety of analytes have been constructed and utilized *in vitro* and *in vivo*. These examples will be discussed in the following sections. It should be noted (again) that label-free approaches are significantly more sensitive to nonspecific adsorption because they cannot natively distinguish non-specific from specific binding events and thus almost inevitably require the integration of antifouling approaches when sensing in complex biological media is sought. Sensors based on multistep labeled-designs (e.g., enzyme-linked immunosorbent assay (ELISA)) are less prone to this nonspecificity (though it undoubtedly remains) and very often contain no predesigned antifouling components; they are thus not the main focus herein.

2.3.2. *In Vitro* Sensing Based on Antifouling Chemistries. Optical or electrochemical sensor formats have long been the most commonly used in applications in complex biological fluids. In the following sections, we will highlight relevant recent examples of such sensors and discuss their analytical performance. We will specifically focus on those presenting novel architectures capable of operating in real-life samples such as serum.

2.3.2.1. PEG. Since the 1970s, polyethylene glycol (PEG; >10 EG units) and its derivatives such as oligoethylene glycol (OEG, $n \approx 3-10$) have undoubtedly been the most accessible and frequently applied antifouling materials[121] and have been utilized in numerous sensory formats. Particularly common are sensors based on PEG-based SAMs such as a recently developed multiplex SPR sensor for the simultaneous detection of three human pancreatic islets peptide hormones, that is, insulin, glucagon, and somatostatin.[122] In this work, a mixed SAM of CH_3O-PEG-SH and 16-mercaptohexadecanoic acid (molar ratio of 3:2) was utilized as an antifouling support and for antibody attachment, respectively. Antibody functionalized spots on the sensor chips showed high specificity to the corresponding hormones with negligible interference from 1 mg mL^{-1} BSA or lyzosome and adequate detection limits for insulin (1 nM), glucagon (4 nM), and somatostatin (246 nM). While it was not demonstrated that this sensor is capable of operating in real-life samples, the multiplexed detection of different markers with high throughput is of large interest in clinical applications. In another study, Xu et al. reported a label-free impedimetric sensor to detect insulin using a simple SAM of SH-$(EG)_4$-COOH as simultaneous antifouling layer and antibody anchoring support.[123] They demonstrated that this sensor is capable of insulin detection in 50% serum with minimal interference (3%), a limit of detection (LoD) of 1.2 pM, and a clinically relevant linear range (from 5 pM to 50 nM). Notably, the obtained sensor could be regenerated and reused by disassociation of insulin antibody−antigen complex using 0.2 M Gly-HCl buffer.

https://dx.doi.org/10.1021/acs.chemrev.9b00739
Chem. Rev. XXXX, XXX, XXX−XXX

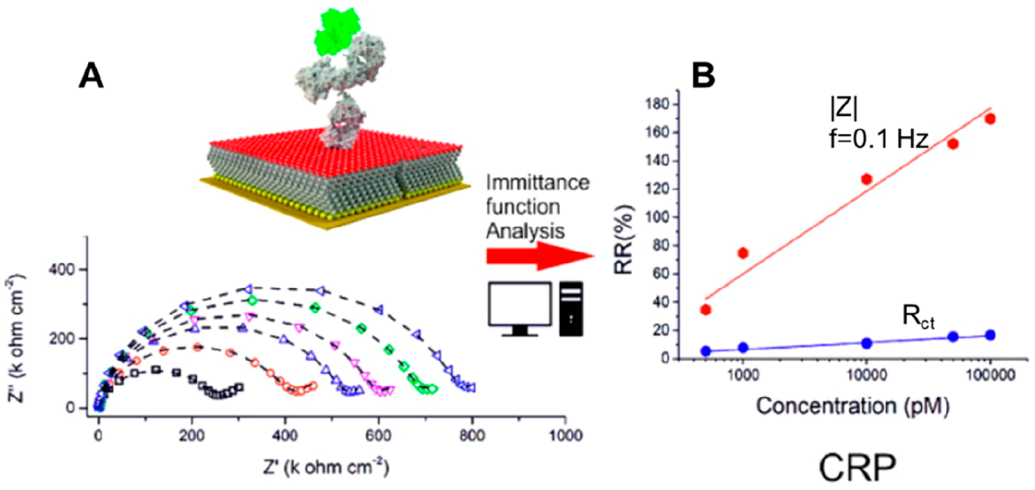

Figure 11. (A) PEG thiol (HS-C11-$(EG)_3$-OCH_2−COOH) based interface for label-free immittance electroanalysis of CRP. (B) Optimized analytical response curve for impedimetric CRP detection showing that |Z| is a 12× more sensitive analytical parameter than the more commonly used Rct. Adapted with permission from ref 125. Copyright 2015 American Chemical Society.

Other impedimetric sensors based on PEG chemistries have also been reported by the Davis group. For example, α-synuclein antibodies (markers for Parkinson's disease, PD) have been quantified in blood at a α-synuclein antigen-modified SAM of HS-C_{11}-$(EG)_3$-OCH_2−COOH (EG-SAM) on gold.[47,124] This format was then applied to serum samples of Parkinson's disease (PD) patients and healthy controls demonstrating pM levels of sensitivity and good levels of disease-relevant selectivity. Similar sensors for the detection of C-reactive protein (CRP, an important marker of potential cardiac stress and inflammation) at anti-CRP modified the EG-SAMs using impedance based electrochemical capacitance spectroscopy (ECS) have also been developed, where an immittance function approach has been employed to extract the most sensitive analytical parameter (Figure 11).[125−128] Recently, the same group has applied EIS at EG-SAMs on gold bead electrodes to assay the exosomal proteins CD 9 and Syntenin with picomolar sensitivity in exosomal lysate.[129] Mixed SAMs of EG-thiol and ferrocene-thiol have also been utilized as supports for the redox capacitive detection of nonstructural protein 1 (NS1), IgG, or human prostatic acid phosphatase (PAP) in 20% serum.[130] The multiplexed impedimetric sensing of insulin and CRP has also been reported at PEG-modified gold electrode arrays. Specifically 4-armed PEG-amine and 4-armed PEG-epoxide were physisorbed onto the electrode surface and then thermally cross-linked prior to antibody tethering. This platform was capable of the detection of insulin and CRP in undiluted human serum with fM and pM detection limits respectively, a capability then applied to real patient sample analysis.[131]

The Gooding group has investigated antifouling electrochemical sensors based on mixed layers of electrografted OEG and molecular wires (MWs). It is worth noting here that while OEG can effectively resist nonspecific protein adsorption, it can, if densely packed, significantly hinder electron transfer to the underlying electrode impeding its use in various electrochemical sensors. Thus, additional oligo(phenylethynylene) based MWs were used to switch on the electrochemical communication between an immobilized redox probe (ferrocene) and the electrode.[55,132] To apply this design, they further incorporated an epitope of biotin into the wire to allow amperometric biotin sensing *via* a displacement assay, taking advantage of the difference in the affinity of biotin to the antibiotin antibody or its synthetic epitope (Figure 12). Five different combinations of MWs/OEG (1:0, 1:20, 1:50, 1:75, and 1:100) were tested in the detection of the model analyte (biotin) whereby the ratio of 1:50 was found to give the highest sensitivity. This OEG/MW mixed-layer platform was then successfully applied to detect glycosylated hemoglobin (HbA1c) in undiluted human serum by incorporating a recognition epitope (an N-glycosylated pentapeptide) into the wire.[55,132] A good linear relationship between the relative Faradaic current associated with ferrocene and the concentration of HbA1c from 4.5% to 15.1% of total hemoglobin in serum without the need for washing or rinsing steps was achieved, indicating its applicability for point-of-care (PoC) use.[133] The major limitation of these systems is the relative complexity of the MW synthesis.

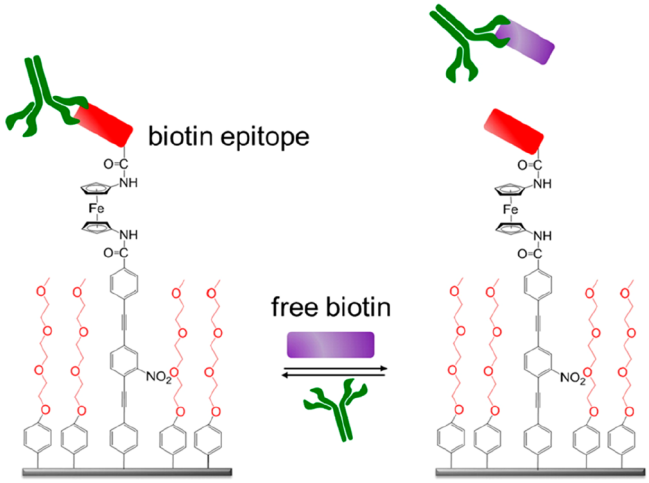

Figure 12. Schematic representation of a mixed OEG/molecular-wire based electrochemical biosensor for detection of biotin. Adapted with permission from ref 54. Copyright 2011 Elsevier.

The Luo and Davis groups have also developed a series of label-free DNA biosensors based on PEG antifouling chemistry to electrochemically detect the breast cancer susceptibility gene 1 (BRCA1) in human serum. In one example, they drop-

https://dx.doi.org/10.1021/acs.chemrev.9b00739
Chem. Rev. XXXX, XXX, XXX−XXX

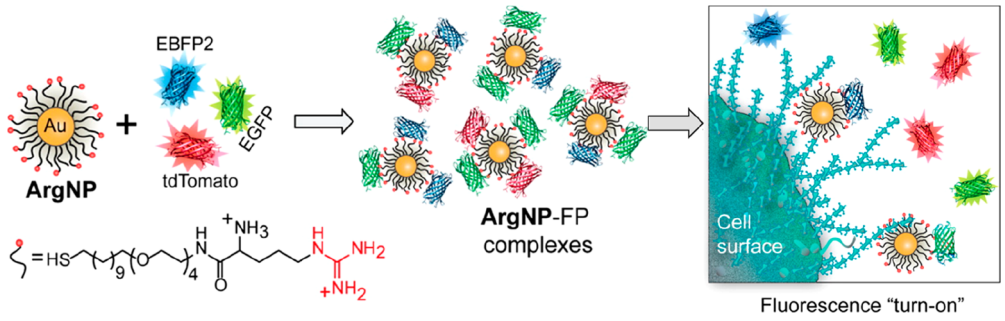

Figure 13. Fabrication of a fluorescent displacement nanosensor based on the reversible binding of fluorescent proteins (FPs) onto ArgNPs. In binding to the arginine head groups of the PEGylated AuNP, the FP fluorescence is initially quenched by the underlying gold. Displacement by specific cell surface proteins restores their fluorescence. Adapted with permission from ref 137. Copyright 2015 American Chemical Society.

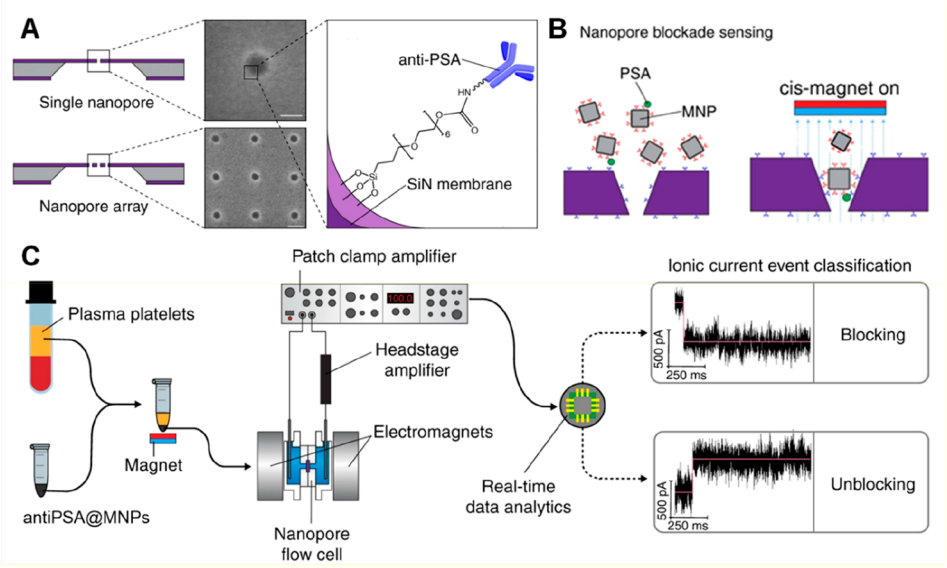

Figure 14. (A) Schematic representation and scanning electron micrographs of a solid-state nanopore modified with silane-EG6-anti-PSA. (B) Removal of nonspecific nanopore blockade events (i.e., anti-PSA-MNP without target) was through the application of a magnet, whereas (anti-PSA)-MNP with bound PSA will remain in the pore, thus blocking it. (C) Flowchart for assay of PSA. After incubation and separation of the MNPs, they were exposed to the nanopore flow cell. A potential difference was applied between both sides of the nanopore and the ionic current analyzed by an event classifier where three distinct event types: translocation, blocking, and unblocking can be observed. Adapted with permission from ref 142. Copyright 2019 Nature Publishing Group.

coated 4-armed PEG-amine and 4-armed PEG-epoxide onto a GC electrode forming a cross-linked PEG film onto which oligonucleotide probe immobilizing gold nanoparticles were deposited.[134] Upon binding of the BRCA1 DNA, an increase in the charge transfer resistance of the sensory interface was measured by EIS. The sensor exhibited a three orders linear range with a fM LoD. Spiking of undiluted serum with target (1, 10, and 100 pM) showed a recovery rate ranging from 92.6% to 100.6%, indicating a robust nonfouling performance. In another study by the same group, a 4-armed-PEG-COOH based nonfouling sensor for BRCA1 electroanalytical detection in serum was developed.[38] Specifically, polyaniline (PANI) nanowires were introduced onto GC through electropolymerization. Subsequently, this interface was modified with PEG on which the amino functionalized methylene blue-modified DNA capture probes were coupled. Upon target capture, the hybridization of complementary target DNA and DNA probe displaced the MB out of the duplex structure, leading to a reduction in current with a LoD of 0.01 pM. Similarly, Chen et al. investigated an antifouling support of PEG/tannic acid/PDA on GC onto which gold nanoparticles (AuNPs) were electrodeposited to allow attachment of thiolated probe DNA. Impedimetric BRCA1 detection in 10% serum was achieved with a sub femtomolar LoD.[135] PEG adlayer methodologies can also be applied to the modification of particulate systems to enable optical based target detection in complex media. For example, Luo's group has investigated PEGylated Au/Fe_3O_4 particles for the optical detection of human papilloma virus (HPV).[136] In this study, the additional decoration of the PEG-based particles with chondroitin sulfate (CSA) resulted in enhanced colloidal stability and endowed the particles with apparent excellent fouling-resistance. A DNA probe for HPV was then immobilized onto the particles. After hybridization (target capture), a fluorescent dye (Hoechst 33258, which exclusively binds to the minor groove of double-stranded DNA) was utilized as a transducer. This fluorescent sensor was observed to possess a wide linear range and a pM LoD.[136]

Another fluorescent nanosensor platform has been developed by the Rotello group, using functional PEG-thiol SAMs on small AuNPs (~2.6 nm diameter), where the head groups, for example, arginine (Arg), served as noncovalent anchor sites for three different fluorescent proteins (FPs, (EBFP2 (blue),

https://dx.doi.org/10.1021/acs.chemrev.9b00739
Chem. Rev. XXXX, XXX, XXX−XXX

EGFP (green), and tdTomato (red)) (Figure 13).[137] This configuration was then utilized in a displacement assay for the sensing of target analytes that can compete with the FPs for the headgroup binding sites. Depending on the binding properties of the target analytes, the system generates different fluorescence finger prints, which can be analyzed by a linear discrimination assay (LDA). This was then successfully utilized to investigate the physicochemical changes of cell surfaces (as "analyte") upon exposure to chemotherapeutic drugs with unique fluorescent signatures for different response mechanisms. This PEG-based nanoparticle platform was also successfully translated to protein sensing in serum (in addition to bacterial sensing in culture media) by endowing the head groups with specific interaction sites.[138−141] These particles allowed the high-throughput screening of multiple targets without additional sample preprocessing, thus offering a convenient approach for drug discovery, protein screening, and cell-based sensing.

Kyloon et al. utilized OEG-based antifouling chemistry in a silicon nitride nanopore sensor for the sensitive detection of prostate specific antigen (PSA) in blood.[142] Sensing was carried out by capturing PSA from patient blood with anti-PSA antibody-modified OEG-modified magnetic nanoparticles (MNPs, 50 nm). These MNPs were then further captured at anti-PSA antibody-modified photolithographically generated nanopores (27 nm) whereby the blocking of the pore results in a modified current response (Figure 14). Importantly, the MNPs can be magnetically driven whereby those particles that have not captured the analyte can be magnetically removed, which together with the antifouling OEG modification reduces fouling/nonspecific response. This sandwich format afforded a very high sensitivity (LoD 0.8 fM) and showcased both the importance of antifouling design and a viable extension to other trace analyte detection.[143,144] In different work, Giamblanco et al. demonstrated that (5 kDa) PEG-modified 20 nm nanopore sensors can be used to study protein aggregate morphology. The intensity of the relative current blockade (aggregate vs translocating) enabled the detection and discrimination of the morphology of ß-lactoglobulin, lysozyme, and BSA.[145]

Despite its ubiquitous use as an antifouling material, it is important to note that PEG chemistry suffers from a number of major drawbacks such as those associated with chemical tailorability and a noted susceptibility to oxidative damage[146,147] and decomposition in the presence of oxygen and transition metal ions (impeding long-term stability/functionality) (as summarized in Table 4).[12,121,148] They are also only rarely capable of a prolonged operation in high levels of blood or serum. Under such circumstances, alternatives are required.

2.3.2.2. Zwitterions. In recent years, zwitterionic materials, which possess high oxidative resistance and hydrolytic stability, have attracted considerable attention as promising alternatives to PEG in developing high performance antifouling interfaces.[147,149−151] As discussed in Section 2.2, their hydration not only arises from hydrogen-bonding (as is the case for PEG) but also has an appreciable electrostatic component (a key element of their antifouling properties). A range of functional groups can be readily incorporated into zwitterionic surface-confined architectures; most commonly, quaternary ammonium groups are combined with phosphates/phosphonates (phosphorylcholine),[152,153] sulfone/sulfate groups (sulfobetaine),[154,155] or carboxylates (carboxybetaine) (Figure 1B).[150,156] The latter can furthermore serve as convenient anchor groups for subsequent (bio)conjugation *via*, for example, esterification or amidation as discussed further.[157]

In analogy to the PEG-based systems, zwitterionic chemistries can be easily incorporated into (subsequently) sensory interfaces *via* self-assembly or polymerization. The former has been used by Wang et al., who investigated mixed zwitterionic antifouling SAMs of SB and CB-modified thiols on a gold SPR chip for the detection of rabbit polyclonal IgG.[158] The SAM possessed a high fouling resistance whereby the CB also served as an anchor point for antibody immobilization. The sensor exhibited high sensitivity (LoD of 0.4 nM) and high target specificity without interference from chicken polyclonal IgG. As shown in Figure 15, a CB-based SPR sensory system for the detection of Hepatitis B antibody in clinical saliva has also been reported by Riedel et al.[43] In this case, poly[(N-(2-hydroxypropyl)methacrylamide)-co-(carboxybetaine methacrylamide)] (poly[HPMA-co-CBMAA]) brushes were synthesized on an initiator-modified Au surface *via* ATRP and the Hepatitis B antigen, then immobilized through standard methods. Upon exposure to saliva, the target antibody is bound followed by addition of a fluorophore-labeled secondary antibody (IgG) enabling detection *via* surface plasmon-enhanced fluorescence. This sandwich immunosensor showed excellent antifouling properties in saliva and was capable of distinguishing between positive clinical saliva samples (respective serum ELISA response >1 IU mL^{-1}) and negative clinical saliva samples (respective serum ELISA response <0.01 IU mL^{-1}).

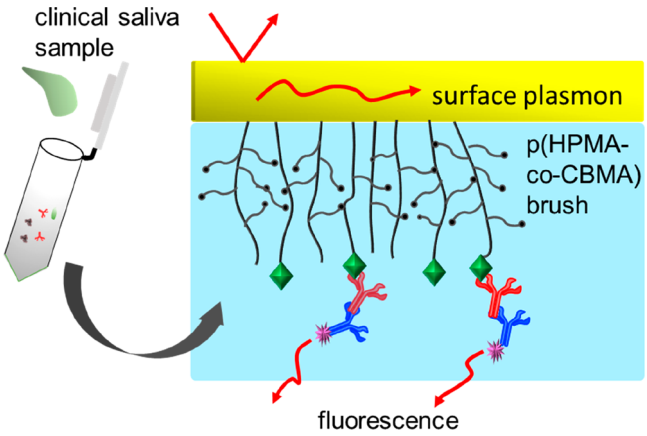

Figure 15. Schematic depiction of a plasmonically enhanced fluorescence biosensor where a gold sensor chip functionalized with a poly(HPMA-co-CBMAA) brush functions as a nonfouling support for Hepatitis B antigen. After anti-Hepatitis B capture, a second fluorophore labeled antibody is introduced enabling sensitive detection anti-Hepatitis B *via* plasmonically enhanced fluorescence. Adapted with permission from ref 43. Copyright 2017 American Chemical Society.

A broad range of optical sensors based on zwitterionic antifouling chemistries have also been reported. In one example, pCB functionalized cellulose paper has been applied to detect glucose in undiluted human serum.[156] To this end, pCB brushes were first grafted from cellulose paper *via* SI-ATRP, which was incorporated into a microfluidic device. The subsequent colorimetric glucose assay was based on the enzymatic oxidation of iodide to iodine. Compared to bare cellulose paper, the pCB-modified cellulose showed an improved performance (color intensity and response time)

https://dx.doi.org/10.1021/acs.chemrev.9b00739
Chem. Rev. XXXX, XXX, XXX−XXX

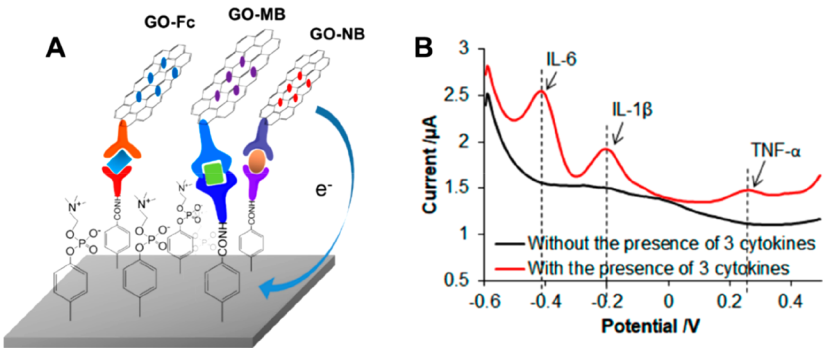

Figure 16. (A) Zwitterionic sandwich immunosensor for the multiplexed detection of three cytokines IL-6, IL-1β, and TNF-α in serum. (B) Square wave voltammetry response at the interface before and after incubation with three cytokines IL-6, IL-1β, and TNF-α, followed by incubation of anti-IL-6 Ab-GO-NB, anti-IL-1β Ab-GO-MB, and anti-TNF-α Ab-GO-Fc. Adapted with permission from ref 161. Copyright 2018 American Chemical Society.

for all glucose concentrations (0.5−5.0 mM), particularly in undiluted human serum samples. In other work, optical sensors based on a bifunctionalized silica nanoparticle modified with −CB and −COOH terminated silanes were developed by Hu et al.[113] This short-chained interface showed effective antifouling properties in both BSA based model protein solution and 50% FBS as assessed by the BCA assay. These functionalized nanoparticles were then successfully applied for chemiluminescent detection of human chorionic gonadotrophin in 50% FBS by formation of a sandwich complex on the horseradish peroxidase antibody-modified particles.

Brault et al. extended the application of pCB to the development of an SPR sensor interface capable of the multiplexed profiling of protein targets.[159] pCB brushes were coated on a gold chip through ATRP and were then functionalized with three antibodies *via* microcontact printing. Human monoclonal antibody against the activated leukocyte cell adhesion molecule (anti-ALCAM), an antibody against thyroid stimulating hormone (anti-TSH), and an antibody against β-human chorionic gonadotropin (anti-hCG) were used to generate the printed antibody spots on pCB films. The authors demonstrated that such a configuration exhibited similar sensitivities to conventional SPR sensors with the same pCB films (10 ng mL^{-1} vs 7.8 ng mL^{-1}) but with high-throughput capabilities. This work represents the first demonstration of a low fouling pCB-based antibody sensing array for analysis of undiluted human plasma and shows great potential for the assaying of a wide range of protein analytes.[159] Similarly, Homola's group has presented a multichannel SPR sensor coated with a functionalizable and low-fouling pCBAA brush for simultaneous detection of *E. coli* O157:H7 and *Salmonella sp.* in hamburger and cucumber samples.[39] The SPR chips were based on a sandwich format of capture Ab-analyte-streptavidin-labeled detection Ab on pCBAA brushes. Recognition and binding of biotinylated gold nanoparticles were used to enhance the SPR sensor response and amplify the signal. The limits of detection for the two species of bacteria in cucumber and hamburger extracts were determined to be 57 colony-forming unit (CFU) mL^{-1} and 17 CFU mL^{-1} for *E. coli*, 7.4 × 10^3 CFU mL^{-1} and 11.7 × 10^3 CFU mL^{-1} for *Salmonella sp.*, respectively.

Vaisocherová et al. reported an extraction-free (no pretreatment) and polymerase chain reaction (PCR)-free sensor based on a zwitterionic pCBAA SPR array that enabled the direct multiplexing of four miRNAs (miR-16, miR-181, miR-34a, and miR-125b) in crude erythrocyte lysates (EL).[41] pCBAA brushes approximately 40 nm thick (generated by ATRP) were able to load ∼9.8 × 10^{12} probes per cm^2 and showed a strong resistance to fouling from EL. samples (<2 ng cm^{-2}). Different capture probes for the four miRNAs were immobilized onto this support facilitating RNA quantification after hybridization with biotinylated detection probes (the signal of the sandwich hybridization assay can be further amplified with the aid of streptavidin-functionalized AuNPs). The developed sensor successfully assayed for miRNA biomarkers of myelodysplastic syndrome in clinical EL samples enabling detection of miRNAs at levels <0.5 pM.

Other electrochemical sensors have been explored by Jiang et al., who modified electrodes with short and low-impedance binary aryl layers constructed *via* the electrodeposition of aryldiazonium salts containing zwitterionic PC or carboxy groups for anchoring biorecognition units.[36,56] For example, an electrochemical sensor for TNF-α detection has been constructed by in situ simultaneous electrografting of PPC and phenyl butyric acid (PBA) onto indium tin oxide (ITO).[54] This was employed in an amperometric sandwich assay with a low LoD (<1 pM) reported for TNF-α in whole blood. A similar approach has utilized reduced graphene oxide immobilized onto a gold electrode through diazonium chemistry.[160] This interface was then further decorated with mixed zwitterionic PPC and carboxyphenyl groups *via* diazonium reduction onto which anti-TNF-α was coupled. Subsequent amperometric detection of targets was then carried out by a sandwich method whereby the recruited analytes were exposed to ferrocene and anti-TNF-α-modified rGO. This electrochemical immunosensor was successfully used for the detection of secreted TNF-α from BV-2 cell lines (in cell media). In a more recent study, the same group reported a similar sensor capable of multiplexed sensing of cytokines TNF-α, IL-6, and IL-1β in serum.[161] As shown in Figure 16, mixed layers of PPC and CP were electrodeposited, followed by antibody immobilization. Analyte detection was carried out amperometrically with the rGO both analyte antibody and redox reporter (nile blue (NB), methylene blue (MB), or ferrocene (Fc))-modified. Because of the distinct redox peaks associated with these reporters (−0.4 V, − 0.2 and 0.2 V, respectively), a simultaneous sensing of all three analytes was deemed possible in undiluted mouse serum. This study demonstrates a promising adaptive methodology for multiplexed sensing in complex media by rational selection and evaluation of redox labels. In another study, electrochemical sensors based on a zwitterionic polymer interface were

https://dx.doi.org/10.1021/acs.chemrev.9b00739
Chem. Rev. XXXX, XXX, XXX−XXX

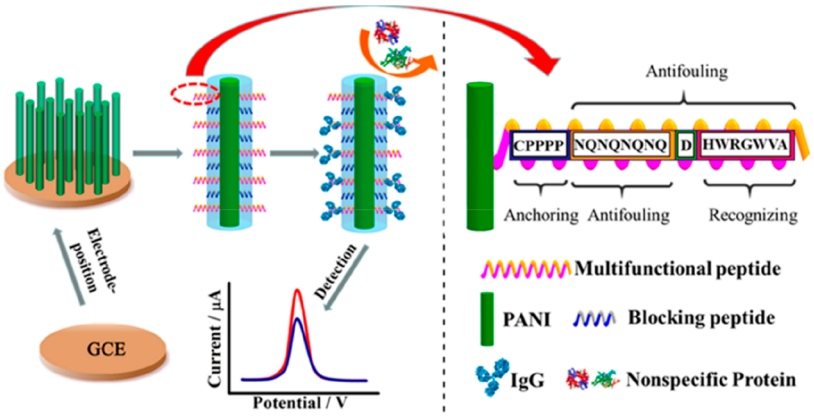

Figure 17. Multifunctional peptide-polyaniline nanowire based sensor for the detection of IgG in serum. Reproduced with permission from ref 164. Copyright 2018 American Chemical Society.

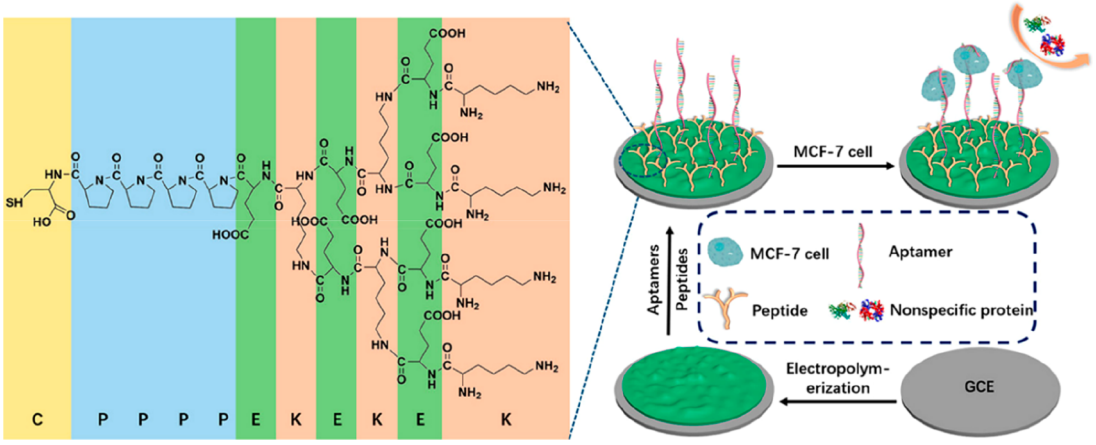

Figure 18. Schematic illustration of the preparation of a PANI-supported branched peptide-based amperometric cell sensor (C, cysteine; P, proline; E, glutamic acid; K, lysine.) Reproduced with permission from ref 168. Copyright 2019 American Chemical Society.

reported by Davis and co-workers who developed a pCBMA based label-free biosensor to support the fM detection of insulin (LoD = 40 fM) in neat serum, which, some years later, still represents a benchmark in the selective label free electrochemical detection of protein targets in complex fluid.[102] In spite of their frequent use and excellent antifouling capabilities, few zwitterionic compounds are commercially available necessitating the often complicated synthesis and purification of these highly charged molecules. Furthermore, it should be taken into account that the external pH as well as electric field (e.g., in electrochemical sensing) may influence the overall interfacial charge status and thus the antifouling behavior.

2.3.2.3. Peptides. Peptides are natively biocompatible with physicochemical characteristics (hydrophilicity, charge, conformational rigidity, anchor groups) tunable through their specific sequence. With the high hydrogen bond-donor/acceptor abilities of their polar functional groups and their zwitterionic charge, peptides are usually strongly hydrated.[18,162] Charged side chains (glutamic acid (E), lysine (K), aspartic acid (D), histidine (H), and arginine (R)) or surface anchor groups (cysteine (C)) are usually incorporated in derived applications,[27,34,163] with nonfouling character also being reported on noncharged hydrophilic[164] and amphiphilic peptides.[165] Peptides of various length and sequence have been assembled onto a range of planar and nanoparticulate surfaces most commonly by incorporation of a cysteine motif at the peptide terminus to facilitate the formation of ("thiolate") SAMs on gold. The influence of complex amphiphilic and zwitterionic peptide structures on the resistance of protein adsorption has been investigated by He and co-workers. Specifically, two different heptapeptides, the noncharged CYSYSYS and the zwitterionic CRERERE, have been synthesized and self-assembled on gold.[165] Ultralow levels of protein adsorption (1.97−11.78 ng cm^{-2}) on these surfaces were quantified by SPR with single proteins (BSA, lysozyme, and β-lactoglobulin) as well as biological media (serum, soybean milk, and cow milk) confirming an improved performance of the zwitterionic peptide interface (over the amphiphilic noncharged peptide) for both single protein solutions and natural complex fluids.

On the basis of such background observations, a number of peptide-based sensors have been constructed. In one recent study, a SPR sensor for the detection of platelet-derived growth factor (PDGF-BB) was developed.[166] To this end, a gold coated optical fiber has been modified with mixed SAMs of the antifouling CPPPP-EKEKEKE peptide and an aptamer by simultaneous self-assembly to produce a film that was then employed in a sandwich format using AuNPs as signal amplifiers. This enabled PDGF-BB sensing in 10% human serum with a sub pM LoD.

https://dx.doi.org/10.1021/acs.chemrev.9b00739
Chem. Rev. XXXX, XXX, XXX−XXX

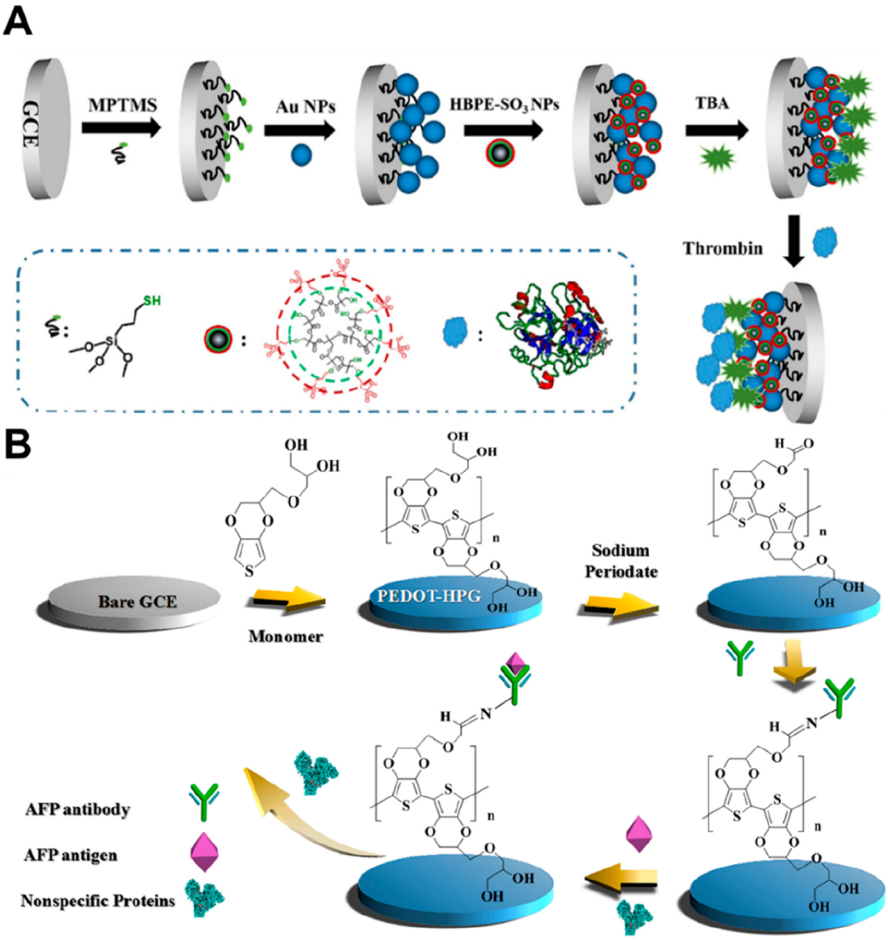

Figure 19. (A) Schematic illustration of the fabrication of a hyperbranched polyester-sulfonic acid nanoparticle-based aptasensor for electrochemical sensing of thrombin in undiluted serum. Reproduced with permission from ref 170. Copyright 2017 Elsevier. (B) Schematic illustration of the fabrication of the AFP biosensor interface using HPG. Reproduced with permission from ref 175. Copyright 2019 Elsevier.

Peptide films have also been used in a range of electrochemical sensor formats. Luo's group, for example, recently reported a peptide-based nonfouling interface for the sensitive detection of IgG in clinical human serum using DPV.[164] As illustrated in Figure 17, PANI nanowire arrays were first constructed on GC electrodes *via* electropolymerization. Immobilization of a multifunctional peptide onto this modified electrode was then carried out *via* covalent cross-linking of the amino groups of PANI and thiol groups of the peptide *via* sulfo-SMCC. The peptide was specifically designed to contain an anchoring unit (CPPPP), a nonfouling sequence (NQNQNQNQ), and a specific IgG recognition sequence (HWRGWVA). This aptasensor was capable of selective IgG detection *via* DPV in neat serum and real clinical samples with a low pM LoD. The analysis of patient samples was resolved to be in good agreement with hospital nephelometry IgG quantifications. The same group employed a EKEKEKE peptide sequence in assays of BRCA1.[33,167] Specifically, PEDOT was electrodeposited onto GC to anchor the zwitterionic peptide *via* nickel cation coordination. Receptive DNA probes were immobilized *via* EDC/NHS facilitating the detection of BRCA1 in 5% human plasma with a sub fM sensitivity by DPV.[145] A similar sensing interface on gold has been utilized for the impedimetric detection of BRCA1 in 10% human serum.[27]

In a recent study, a novel branched peptide has been explored, wherein a mucin1 aptamer (for capture of MCF-7 cancer cell) and a branched zwitterionic peptide (CPPPPEK-$(EK)_2(EK)_4$) were simultaneously immobilized on PANI coated GC to generate the sensory interface (Figure 18). The branch-structured peptide was shown to offer better antifouling performance than that of linear analogues or PEG (likely related to conformational entropy and higher levels of hydration). The developed sensor was capable of detecting cancer cell with a LoD of 20 cells mL^{-1} in spiked human serum.[168]

These studies clearly demonstrate the potential of peptide based antifouling interfaces in sensors whereby their chemical tunability (i.e., amino acid sequence) can be rationally designed for a given specific applications. Comparatively little analysis has been done of the operational mechanisms active at such, but it is likely that hydration levels exceed those at PEG or CB/SB/PC-based interfaces. Caution should also be applied to the use of sequences containing cysteine or methionine residues where oxidative degradation is possible. Depending on application, protease degradation may also result in a compromised antifouling performance (Table 4).

2.3.2.4. Other Antifouling Chemistries. In addition to the aforementioned chemistries, a myriad of other hydrated molecular systems have been employed in sensors designed to recruit targets selectively under testing conditions. For

https://dx.doi.org/10.1021/acs.chemrev.9b00739
Chem. Rev. XXXX, XXX, XXX−XXX

example, hyaluronic acid (HA, Figure 1D), an anionic glycosaminoglycan of polysaccharides, has been explored as antifouling decoration in several studies.[37,169] The disaccharide unit in HA contains amide and carboxylic acid groups are believed to provide hydrogen-bond donor/acceptor and thus enhance the hydration that ultimately presents a thermodynamic repulsion to proteins.[169] In the meantime, hyperbranched polymers, a class of synthetic dendritic macromolecules with irregularly dense branched structures, and a large number of functional end groups, are promising antifouling materials. The surface-immobilization of these polymers, *via*, for example, polymerization of glycidol, can introduce a high density of hydrophilic functional groups on surfaces facilitating both further functionalization as well as the formation of a strong hydration layer.

In a recent study, the detection of carcinoembryonic antigen (CEA) in human serum was demonstrated by construction of a sensor based on HA and PANI nanowires.[31] By modification of HA with conducting PANI, the label-free anti-CEA/HA/PANI sensor was capable of sensitive amperometric detection of CEA with $a > 3$ order of magnitude linear response and a fM detection limit in buffer and a high recovery (~100%) in serum samples.

The use of a heparin-mimicking hyperbranched polyester nanoparticle based aptasensor for the detection of thrombin in whole blood has been explored by Niu et al.[170] As shown in Figure 19A, the proposed sensor interface was obtained through a layer-by-layer self-assembly approach, with 3-mercaptopropyltrimethoxysilane (MPTMS) first grafted onto the surface of GC to enable Au NPs anchoring. Then hyperbranched polyester-sulfonic acid nanoparticles (HBPE-SO_3 NPs) were attached *via* electrostatic adsorption, followed by immobilization of a 5′-amino thrombin aptamer by physisorption. This sensing interface showed good resistance to nonspecific proteins and blood cell adhesion compared to MPTMS- or HBPE−OH-modified interfaces and was applied to detect thrombin (TB) in whole blood by DPV with comparable performance to that of the aptamer-based fluorescence assay. There are also reports of hyperbranched polyglycerol (HPG) antifouling coatings on glass, silicon, porous silicon, and GC electrodes.[171−175] In one recent example, HPG-EDOT was electropolymerized onto GC, which was then partially oxidized by periodate to an antibody anchoring aldehyde (Figure 19B).[175] This sensory interface permitted the sensitive detection of α-fetoprotein (AFP) with a fM LoD in serum by square wave voltammetry (SWV).

Qi et al. have studied a ternary monolayer based TB aptasensor created by the coassembly of dithiothreitol (DTT), a thiolated TB aptamer, and 6-mercapto-1-hexanol (MCH) backfilling on gold.[176] The hydroxyl groups on DTT and MCH provide a hydrophilic microenvironment most likely highly relevant to the observed nonfouling properties. It was demonstrated that (within an impedimetric assay) the increase in the electron transfer resistance was linearly proportional to the concentration of thrombin in the range from 28 to 556 pM with a detection limit of 8 pM. The direct quantification of extrinsic thrombin in undiluted serum samples was subsequently achieved.

In other work, McQuistan et al. have explored negatively charged oligonucleotides as antifouling components together with a methylene blue (MB) labeled peptide epitope (from HIV p24 antigen) as probe for a HIV antibody (Figure 20).[177] When the target antibody binds to the peptide, the MB probe

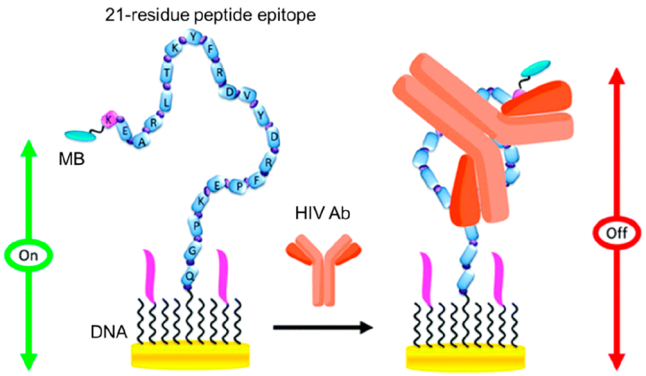

Figure 20. Electrochemical peptide-based sensor with DNA as antifouling diluent for the detection of a HIV antibody in saliva. Before analyte binding the peptide epitope is flexible ("on state") resulting in a measurable methylene blue (MB) tag derived faradaic current. After analyte binding, the associated conformational change results in an attenuated electrochemical response ("off" state). Reproduced with permission from ref 177. Copyright 2014 Royal Society of Chemistry.

flexibility is significantly reduced, leading to a conveniently resolved reduction in measured current. Different surface ratios of the mixed layers were investigated revealing an optimal DNA/peptide surface ratio of 1.37×10^3:1 in enabling a low nM sensitivity assay in saliva. Significantly, the oligonucleotide was shown to play a crucial role in preventing fouling; replacement with 6-mercaptohexanol was observed to result in significant fouling and substantial faradaic signal suppression. Liús and Meyeŕs groups have recently expanded the scope of DNA-based antifouling interfaces by immobilizing DNA triangle nanostructures on SiO_2 through DNA-lithography and formation of layer-by-layer assemblies with polycations (i.e., poly(ethyleneimine), PEI) on glass, respectively.[178,179] Both interfaces have been observed to effectively resist biofilm formation. In related work, DNA tetrahedra on gold have been shown to exhibit excellent antifouling performance (≤8.0 ng cm^{-2}) even in neat serum.[180] These and related configurations are likely to be of value in further extending DNA based interfaces for highly selective biosensing in complex biofluids.

In contrast to the aforementioned negatively charged DNA-based antifouling interfaces, a recent report investigated the performance of the positively charged lipid bilayer mimic, 2-dioleoyl-sn-glycero-3-ethylphosphocholine (EPC^+), as a nonfouling support.[181] As shown in Figure 21A, a gold chip was first modified with a mixed SAM of 3-mercapto-1-propanol (MPO) and protein A. The latter was utilized for the subsequent oriented recruitment of anti-IgG after which a nonfouling lipid membrane was introduced. Interestingly, the natural, zwitterionic, 1-palmitoyl-2-oleoyl-sn-glycero-3-phosphocholine (POPC) membrane displayed higher fouling than the positively charged EPC membrane, which was subsequently utilized to support the detection of IgG in undiluted mouse serum in a sandwich format *via* SPR (Figure 21B). Special attention should be drawn to the necessary precise control over the lipid bilayer formation and antibody integration into this architecture. It should also be noted that in this, and previous examples of permanently charged interfaces, a clear rational for the observed antifouling performance is lacking; while these interfaces are certainly strongly hydrated, biofouling from oppositely charged (bio)-molecules could be expected. These concerns thus require the

https://dx.doi.org/10.1021/acs.chemrev.9b00739
Chem. Rev. XXXX, XXX, XXX−XXX

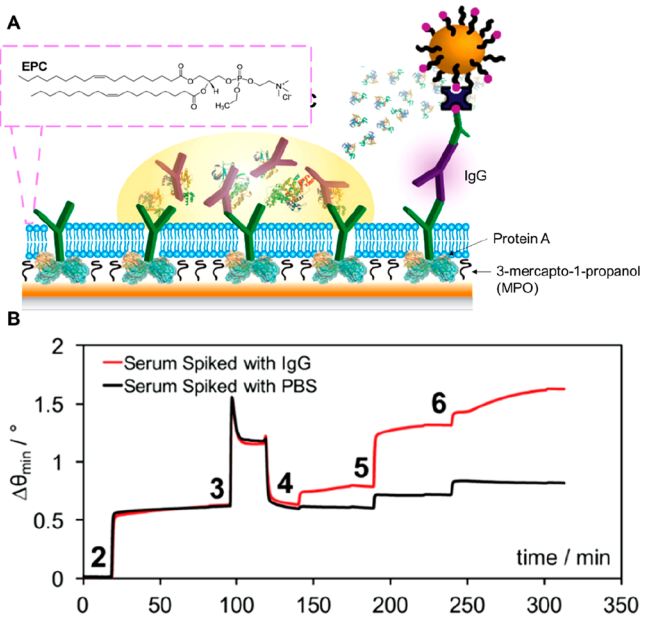

Figure 21. (A) Schematic representation of a sensory interface for IgG detection in undiluted serum based on a positively charged lipid bilayer coating. (B) SPR sensogram showing the assembly of the interface and subsequent IgG detection. After self-assembly of the underlying MPO/protein A/anti-IgG interface, EPC lipid vesicles were utilized to form the lipid bilayer (2), after which serum spiked with mouse IgG was injected (3), followed by a biotinylated detection antibody (4), a streptavidin bridge (5), and biotin-labeled gold nanoparticles (6) for signal enhancement. Adapted with permission from ref 181. Copyright 2019 American Chemical Society.

further theoretical and experimental investigation. It is worth noting that a similar strategy based on biomimetic cell membranes, for example, human platelet membrane-coated poly(lactic-co-glycolic acid) (PLGA) particles[182] or red blood cell membrane-coated gold nanoparticles,[183] has been applied to drug delivery and therapeutics, where the membrane coating apparently confers the nanoparticles with platelet-mimicking properties reducing cellular uptake by macrophage-like cells and securing a prolonged circulation time.

An interesting addition to the chemical antifouling approach was recently reported by Demirci et al.[120] The authors reported a stimuli-responsive sensing interface that can switch between two states: an antifouling/repelling state and a detection state. This was achieved by the formation of a mixed polymeric film on silicon whereby long polymer brushes of poly(2-N-morpholinoethyl methacrylate) (PMEMA) serve as the antifouling decoration, while a shorter beta-cyclodextrin (β-CD)-terminated polymer is utilized as an anchor to immobilize an adamantylamine-modified capture antibody. In this "resting" state, the longer, extended PMEMA chains completely cover the β-CD anchor groups preventing passivating the surface. At temperatures above 37 °C, the PMEMA brush collapses and exposes the β-CD. This interface can then be modified with the capture antibody and utilized to detect the target analyte in a fluorescent sandwich format. As a proof-of-concept, the authors demonstrate that this state can indeed be utilized to qualitatively detect antihepatitis C in PBS. This platform can potentially be adapted to other antifouling/receptor functionalities to create switchable sensing formats.

To summarize so far, a range of antifouling chemistries have been applied in a multitude of electrochemical and optical sensors that are capable of detecting different biomarkers in complex samples and more examples based on the design strategy (illustrated in Figure 9) are summarized in Table 2, whereby different chemical configurations present different advantages and limitations. To overcome the functional chemical or performance limitations that are frequently associated with the use of a single chemical entity, recent work has progressively moved toward the use of combinations. To date, these have included, for example, the use of mixed assemblies based on a combination of, for example, PEG/HA,[184] PC/HA,[185] GSH/HA,[186] or PDA/HA,[187,188] peptide/HA[189] or HA, PC, PDA with lubricin.[190−192] Currently, zwitterionic (including peptidic) and polymeric interfaces currently represent the most tunable high performance platforms encompassing not only significant antifouling properties but also structural adaptability, and it is likely that a continued exploration will furnish a realistic translation to *in vitro* PoC diagnostics. Interestingly, some of the above interfacial designs have also been adapted for the *in vivo* monitoring of a range of analytes, as discussed in the next section.

2.3.3. *In Vivo* Sensing Based on Antifouling Chemistries. *In vivo* sensors are designed to work in the internal microenvironment of the body to sense specific environmental change relevant to health management or an improved understanding of physiological processes.[210−212] In comparison to *in vitro* sensors, *in vivo* sensors encounter harsher, and more prolonged, challenges associated with biofouling (e.g., proteins and cells) as well as potential immune reactions in response to the introduction of the sensor into the active body. These challenges brought about by the complex and dynamic microenvironment can partially or completely impede any pre-engineered sensing capability in terms of accuracy and usable lifetime.[213,214] Antifouling approaches have to be biocompatible with low toxicity and also highly tolerant of the *in vivo* dynamic environment, which includes exposure to dissolved oxygen, transition metals, and enzymes. Thus, the need for high performance nonfouling designs in such work is crucial; to date, functional sensors consist of two main phenotypes: implanted electrochemical sensors and circulating (nanoparticulate) optical sensors. The former are generally capable of high analytical sensitivity and high temporal resolution and are most commonly based on cylindrically shaped wire or multielectrode needle-based microelectrodes (size of a few tens of micrometers or less), which are directly inserted into tissue.[214,215] As with all sensors, biofouling on the sensory interface can result in profound problems associated with loss of analyte mass transport or (electric) communication between the (implantable) *in vivo* sensor and the body.[216,217] A broad range of nanoparticulate platforms such as semiconducting quantum dots (QDs), metallic nanoparticles, mesoporous particles, and metal oxide particles have been designed for *in vivo* applications like drug delivery, sensing, or imaging. The decoration of such solid supports with antifouling chemistry is key to minimizing the formation of an associated protein corona and can be an absolute requirement if both colloidal stability and designed functionality are to be retained *in vivo*.[218,219] For example, PEGylated iron oxide nanoparticles (biotin-PEG, 5 kDa) and zwitterionic dopamine sulfonate coated iron oxide nanoparticles have been shown to possess low levels of toxicity and to prevent phagocytic uptake *in vivo*.[220,221] Similarly, CdSe(ZnCdS) core(shell) QDs with a compact cysteine coating (D_h < 6 nm) were found to prevent

https://dx.doi.org/10.1021/acs.chemrev.9b00739
Chem. Rev. XXXX, XXX, XXX−XXX

Table 2. Fabrication of Sensors Using Different Antifouling Molecular Systems and Their *In Vitro* Sensing Performance[a]

sensor				sensing performance			
antifouling unit	overall composition	analyte	detection method	dynamic range	detection limit	complex sample	ref
OEG	Fc-GO-detection Ab/troponin-I/Ab1/GO-Ph-AuNPs-Ph-OEG/Ph-amine/GC	troponin-I	SWV	2.1−126 pM	2.1 pM	human plasma	193
PEG	Anti-insulin Ab/PEGylated thiol-backfilled BSA/Au	insulin	EIS	5 pM−50 nM	1.2 pM	human serum	123
PEG	Anti-CRP Ab/PEG thiol-Fc/Au	CRP	EIS	0.5 pM−50 nM	1 pM	human serum	125
PEG	Anti-CRP Ab/PEG thiol/Au	CRP	EIS	0.5−50 nM	176 pM	human serum	126
PEG	Ab/PEG/AuNPs/PANI/GC	AFP	DPV	147 aM−14.7 pM	103 aM	human serum	115
PEG	Capture DNA/PEG/PANI/GC	BRCA1	DPV	0.01 pM−1 nM	3.8 fM	human serum	38
PEG	Aptamer-PEG/PDA/GC	ATP	EIS	0.1−1000 pM	0.1 pM	human plasma; cancer cell lysates	194
PEG	Ab/PEG epoxide-PEG amine/Au	insulin, CRP	EIS	0.5−100pM, 0.5−50 nM	171 fM, 150 pM	human serum	131
PEG	Ab1/SH-PEG-COOH/Au	α-synuclein	EIS	0.5−10 nM	55 pM	human serum	47
PEG	Ab/thiolated PEG acid/Au	IL-8	EIS	81 fM−81 nM	8.1 fM	human serum	195
PEG	Brucellosis Ab/OMP31/Fe_3O_4/Au/PEG/HA NPs/GC	Brucellosis Ab	DPV	50 aM−500 fM	18 aM	human serum	196
EGDMA	TB aptamer/p(HEMA-EGDMA-VC)/microbeads/gold chip	thrombin	QCM	1−100 nM	1 nM	human serum	197
PEG	reporter-antiEpCAM/EVs/anti-EpCAM/PEG/Pt	tdEVs	CV	10−10^6 tdEVs μL^{-1}	5 tdEVs μL^{-1}	cell media	198
PPC	HRP-Ab2/analyte/Ab1/PPC−PBA/ITO	TNF-α	CA	0.57 pM−28.5 nM	0.57 pM	human blood	54
PPC	GO-Ab2-redox probes (NB/Fc/MB)/analyte/Ab1/PPC−CP/GC	IL-6, IL-1β, TNF-α	SWV	0.21−6.2 pM, 0.16−6.4 pM, 0.285−11.4 pM	0.21 pM, 0.16 pM, 0.285 pM	mouse serum	161
PPC	Ab2-GO-Ph-Fc/TNF-α /Ab1/PPC−CP/rGO-AuNPs/Ph/Au	TNF-α	SWV	5.7 fM−8.55 pM	5.7 fM	cell conditioned media	160
pCBMA	pCBMA/cysteamine/Au	insulin	EIS	0.1−200 pM	42.6 fM	human serum	102
PVIS	PVIS-GMA-Ab/GO/GC	streptomycin	DPV	0.09−171 nM	3 pM	milk	199
peptide	MCH/Aptamer-Peptide/AuNPs/Au	ATP	EIS	0.1 pM−5 nM	0.1 pM	human whole blood; cancer cell lysates	105
peptide	ssDNA/Peptide/Ni^{2+}/Citrate-PEDOT/GC	BRCA1	DPV	10 fM−10 nM	0.03 fM	human plasma	167
peptide	mixed antifouling peptide-blocking peptide/PANI/GC	IgG	DPV	6.7 pM−67 nM	1.7 pM	human serum	164
peptide	mixed antifouling peptide-AFP aptamer/Au	AFP	DPV	147 aM−1.47 pM	45.6 aM	human serum	200
peptide	MTase/Au@luminol-H1/peptide/AuNPs/PANI/ITO	MTase	ECL	0.05−100 U mL^{-1}	0.02 U mL^{-1}	human serum	201
peptide	Ig E aptamer/zwitterionic peptide/porous gold/GC	Ig E	DPV	5.1 fM−0.51 pM	2.1 fM	FBS	202
peptide	aptamer/MCH/Peptide/$ZnIn_2S_4$/TiO2/ITO	Hela cell	PEC	100−10^6 cells mL^{-1}	34 cell mL^{-1}	cell media	203
peptide	AuNPs@Fe-MOF-detection DNA/target DNA/peptide/capture DNA/Au	T4 PNK	DPV	1.0 × 10^{-3}−10 U mL^{-1}	3.5 × 10^{-4} U mL^{-1}	human serum	204
zwitterion-peptide	sulfophenyl-aminophenyl-S7 peptide/GC	*Streptococcus pneumonia*	EIS	50−5 × 10^4 CFU mL^{-1}	50 CFU mL^{-1}	human serum	205
HA	CEA/anti-CEA Ab/HA/PANI/GC	CEA	DPV	0.56 fM−0.56 nM	0.42 fM	human serum	37
PEG-HA	CD44/PEG-HA-PDA/TiO_2/ITO	CD44	PEC	0.06 pM−6.25 nM	5.5 fM	human serum	184
MCH	aptamer-MCH/PDA/AgNPs/GC	TB	EIS	0.1 pM−5.0 nM	36 fM	human serum	206
backfilled MEA	Ab-MEA/PEDOT-HA/GC	CEA	DPV	56 fM−5.6 nM	16.8 fM	human serum	207
DTT, MCH	aptamer-DTT-MCH/Au	TB	EIS	27.8−556 pM	8.3 pM	human serum	176
DTT, MCH	HRP-aptamer@AuNPs/lysozyme/MCH/DTT/aptamer/Au	lysozyme	DPV	0.71 pM−7.1 nM	0.2 fM	human serum	208
polyglycerol	antiAFP Ab/PEDOT-HPG/GC	AFP	SWV	1.4 fM−14 pM	0.49 fM	human serum	175
PA−PANI	antiCRP Ab/PA−PANI/SPGE	CRP	EIS	2.25 nM−144 nM	4.5 nM	FBS	209

[a]Abbreviations: Fc, ferrocene; GO, graphene oxide; ph, phenyl; CRP, C-reactive protein; EIS, electrochemical impedance spectroscopy; PANI, polyaniline; HA, hyaluronic acid; p(HEMA-EGDMA-VC), poly(2-hydroxyethyl methacrylate-ethylene glycol dimethacrylate-vinylene carbonate); DPV, differential pulse voltammetry; QCM, quartz crystal microbalance; CA, chronoamperometry; CV, cyclic voltammetry; tdEVs, tumor derived extracellular vesicles; SWV, square wave voltammetry; Ag, antigen; Ab1, capture antibody; Ab2, detection antibody; NB, nile blue; MB, methylene blue; ITO, indium tin oxide; AFP, alpha-fetoprotein; PEDOT, poly(3,4-ethylenedioxythiophene); MCH, 6-mercapto-1-hexanol; DTT, dithiothreitol; MEA, monoethanolamine; CEA, carcinoembryonic antigen; IL-6, Interleukin-6; IL-1β, Interleukin-1 β; CP, carboxylic phenyl; MPH, methylparathionhydrolase; Ig E, immunoglobulin E; PVIS, 1-propyl-3-vinylimidazole sulfonate; GMA, glycidyl methacrylate; ECL, electrogenerated chemiluminescence; DNA MTase, DNA methyltransferase; TB, thrombin; PEC, photoelectrochemistry; AgNPs, silver nanoparticles; T4 PNK, T4 polynucleotide kinase; CFU, colony-forming unit; MOF, metal−organic frameworks; HPG, hyperbranched polyglycerol; CRP, C-reactive protein; SPGE, screen-printed graphene nanoplate electrode; PA−PANI, phytic acid-doped polyaniline; FBS, fetal bovine serum.

https://dx.doi.org/10.1021/acs.chemrev.9b00739
Chem. Rev. XXXX, XXX, XXX−XXX

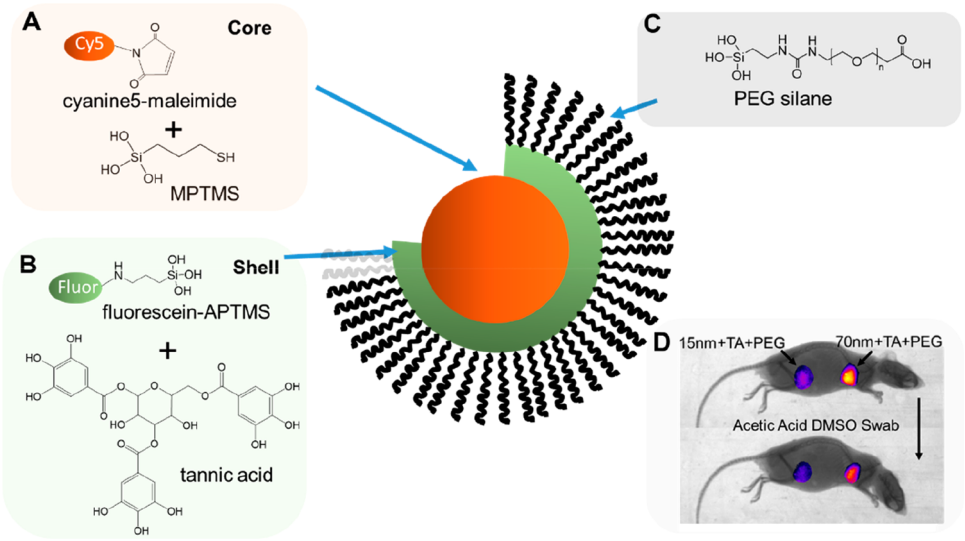

Figure 22. Schematic representation of the synthesis and application of a PEG-coated organosilica core/shell nanoparticle based optical pH sensor. Adapted with permission from ref 233. Copyright 2018 American Chemical Society.

nonspecific serum protein adsorption (as assessed by DLS).[222,223] Breus et al. have further investigated coating CdSe-ZnS core−shell QDs with zwitterionic D-penicillamine and demonstrated an antifouling performance, which was comparable to cysteine coated QDs.[224] Such antifouling *in vivo* nanovectors pave a way for the development of *in vivo* nanosensors when further modification with receptive and transductive elements is carried out. The most successful examples of such sensors based on the two phenotypes will be discussed in the following sections.

2.3.3.1. PEG. Benefiting from a commercial availability, high biocompatibility, and low toxicity, PEG has been the most frequently used antifouling agent for *in vivo* applications. For example, Kozai et al. have reported an ultrasmall implantable composite microelectrode that enabled single-neuron recording in rats.[225] The integrated composite electrode (~8.5 μm diameter) consists of a carbon fiber core (7 μm diameter) coated with 50 nm poly(*p*-xylylene) as well as a 200 nm thick PEG methacrylate polymer as an antifouling layer (both generated by ATRP). The microelectrodes were implanted 1.6 mm into the rat motor cortex to facilitate electrophysiological recordings. They were reported to provide a stable neural signal over 5 weeks in the brain without signal degradation, an important step toward the realization of long-lasting implants.[225] On this note, Schwerdt et al. have reported another ultrasmall sensor capable, apparently, of tracking and monitoring dopamine in the rat brain for up to one year.[226] For this purpose, the authors used an electrode with a diameter as small as individual neuronal cell bodies (10 μm). One advantage of using electrodes of this scale is that they do not produce assay-interfering scar tissue. In the study, a thin layer (0.7−1.3 μm) of parylene-C (a Food and Drug Administration (FDA)-approved biocompatible dielectric) was deposited on a bare carbon fiber, and PEG_{6000} (0.5−1 mm thick) was then cast onto the electrode (by melting) to facilitate implantation into the rat brain. The microelectrode was exposed at the tip and then implanted into the forebrain bundle to monitor the release of DA by fast-scan cyclic voltammetry. It was demonstrated that, with the incorporation of the PEG coating, low noise and high sensitivity amperometric performance could be retained enabling a longitudinal tracking of dopamine over chronic time scales without signal degradation. These sensors could be useful in Parkinson's patients on receipt of deep brain stimulation (with additionally implanted stimulation electrodes). Using a sensor to monitor dopamine levels could help doctors deliver the stimulation more selectively, only when it is needed.[227] Inspiringly, existing commercial systems like closed loop deep brain stimulation systems with sensing electrodes have been tested in clinical research to provide continuous neural signal monitoring and therapy for patients with chronic neuropathic pain.[228−230]

In addition to sensors capable of monitoring neurotransmitters, a range of sensor electrodes have been generated to enable ion level analysis *in vivo*. Machado et al., for example, studied an impedimetric sensor for monitoring extracellular potassium in the mouse brain.[231] Imbalances in $[Na^+]$ and $[K^+]$ have been implicated in numerous central nervous system (CNS) disorders such as epilepsy.[232] In their study, mixed monolayers of 18-crown-6-ether (as the K^+ probe) and thiolated monoethylene glycol with a molar ratio of 1:10 were formed on gold microelectrode arrays allowing real-time *in vivo* non-Faradaic impedimetric measurements of extracellular $[K^+]$ in the mouse brain (although only over multiple minutes).

Robinson et al. proposed an organosilica core−shell ratiometric nanosensor capable of the continuous monitoring of pH in the skin of mice *via in vivo* fluorescence imaging following subcutaneous injection (Figure 22).[233] Both core and shell were formed *via* a silane based hydrolysis−condensation procedure.[234] The pH-sensitive fluorophores Cy5-maleimide or fluorescein-(3-aminopropyl)-trimethoxysilane (APTMS) were mixed into the hydrolyzed (3-mercaptopropyl)trimethoxysilane (MPTMS) solution to allow covalent incorporation into the core and shell structure, respectively. A 1 kDa PEG antifouling layer was then introduced through silanization on the shell. This ratiometric fluorescence sensor was highly sensitive to pH over a physiologically relevant range (pH 4.5−8.0) with a fast response time of <100 ms. The nanosensors were shown to successfully monitor pH changes within a bacterial culture over 15 h. *In vivo* pH sensing was then examined by monitoring the fluorescence after injection of the nanosensors into the

https://dx.doi.org/10.1021/acs.chemrev.9b00739
Chem. Rev. XXXX, XXX, XXX−XXX

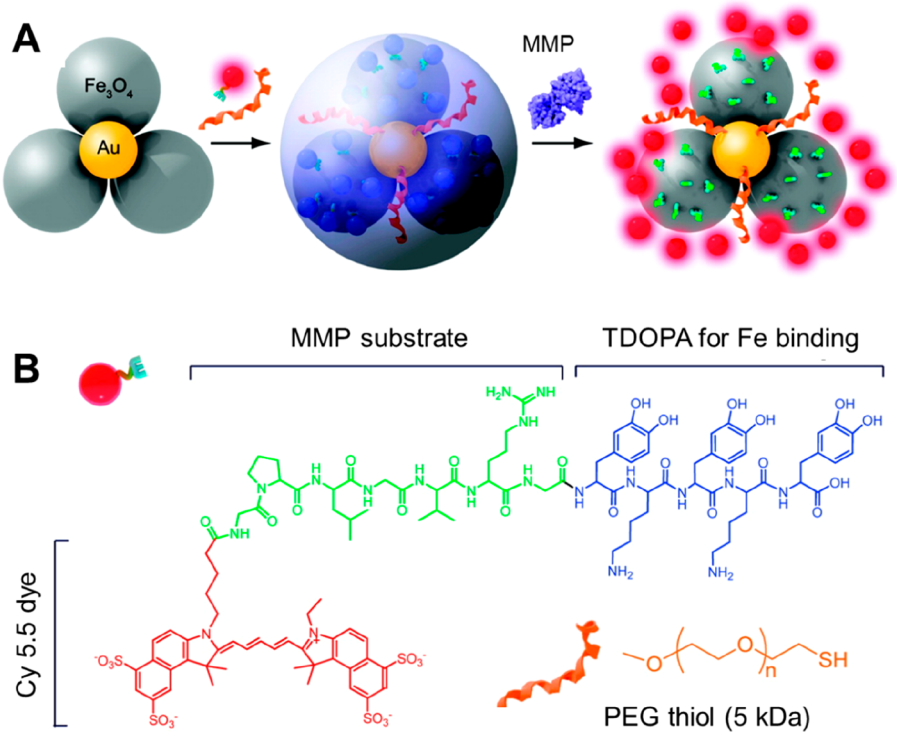

Figure 23. (A) Schematic illustration of the formation of an Au−Fe_3O_4 nanocomposite matrix metalloproteinase (MMP) optical sensor comprising Cy5.5-GPLGVRG-TDOPA and SH-PEG_{5000}. (B) PEG integration into the Au-core endows the particles with fouling resistance while the MMP substrate is tagged with TDOPA for assembly onto the Fe_3O_4 domains. The substrate is furthermore conjugated to a Cy5.5 dye, which, upon cleavage by MMP, is liberated and strongly fluoresces (initially the fluorescence is quenched on the particle through the underlying gold). Adapted with permission from ref 240. Copyright 2011 American Chemical Society.

subcutaneous tissue of mouse flank skin. After injection, the skin surface was swabbed with an acidifying solution prior to imaging at defined times thereafter (to ensure sufficient time for sample diffusion). The fluorescein and Cy5 emissions were isolated using spectral unmixing and overlaid with X-ray images, showing a significant and localized pH response (Figure 22D). Notably, the PEG coating resulted in higher colloidal stability of the optical nanosensor and a better signal-to-noise ratio than for the unmodified control nanoparticles or those nanoparticles containing either tannic acid or PEG alone.

In another use of PEG-based *in vivo* systems, Clark's group studied a phosphorescent nanosensor for the monitoring of histamine.[235] The ∼100 nm sensor particles were fabricated by the encapsulation of a sodium optode, diamine oxidase, Pt(II) meso-tetra(pentafluorophenyl)porphine (PtTPFPP), and a hydrophobic platinum porphyrin dye into amphiphilic PEG lipids *via* an established nanoemulsion approach.[236] In this design, PtTPFPP acts as an oxygen responsive element by exploiting a reversible, oxygen-dependent phosphorescence signal. In the presence of oxygen and histamine, diamine oxidase enzymatically produces ammonia and imidazole-4-acetaldehyde, which lowers the local oxygen concentration resulting in increased phosphorescence. A surface coating with a PEG-lipid (12 EG units) was shown to minimize protein fouling and prolong nanoparticle lifetime (circulation) as revealed by liver or kidney tests. *In vivo* monitoring of phosphorescence every 30 s demonstrated that the injected nanosensor facilitated a continuous monitoring of histamine in live mice across several hours. This study highlights the potential of such approaches to widen the range of measurable analytes by incorporating an enzymatic recognition element; the modular approach applied to histamine sensing is readily extendable to lactate, creatinine, urea, etc. simply by swapping out the enzyme.

Optical sensors with an inbuilt PEGylated polymer coat have also been investigated for *in vivo* detection of reactive oxygen species (ROS) and reactive nitrogen species (RNS), hallmarks of many pathological processes including chronic diseases such as cancer, cardiovascular disease, and arthritis. An ability to detect and track these species would both facilitate our understanding of the etiology of these diseases and support therapeutic intervention.[237] With this in mind, Zhen et al. have reported the development of polymer nanoparticles capable of the sensitive *in vivo* detection of hydrogen peroxide (H_2O_2).[238] These multifunctional nanoparticles were generated by nano-precipitation of a PEG polymer network (subsequently an antifouling shell), a semiconducting polymer (SP), and the chemiluminescent substrate peroxalate bis(2,4,6-trichlorophenyl) oxalate (TCPO). The amphiphilic PEG-b-PPG-b-PEG triblock polymer served as a matrix for the encapsulation of SP and TCPO while also endowing the particles with good fouling resistance, water-solubility, and biocompatibility. The sensor showed excellent colloidal stability in aqueous solution as no precipitation or change in size observed after two months. Doping of the SP with a naphthalocyanine dye leads to intraparticle chemiluminescence resonance energy transfer (CRET), resulting in near-infrared (NIR) luminescence in the presence of H_2O_2. The circulating nanocomposites (∼10 nm) were shown to detect H_2O_2 down to 5 nM in living mice and to exhibit a chemiluminescence quantum yield significantly higher than that of previous nanoparticle probes. Importantly,

https://dx.doi.org/10.1021/acs.chemrev.9b00739
Chem. Rev. XXXX, XXX, XXX−XXX

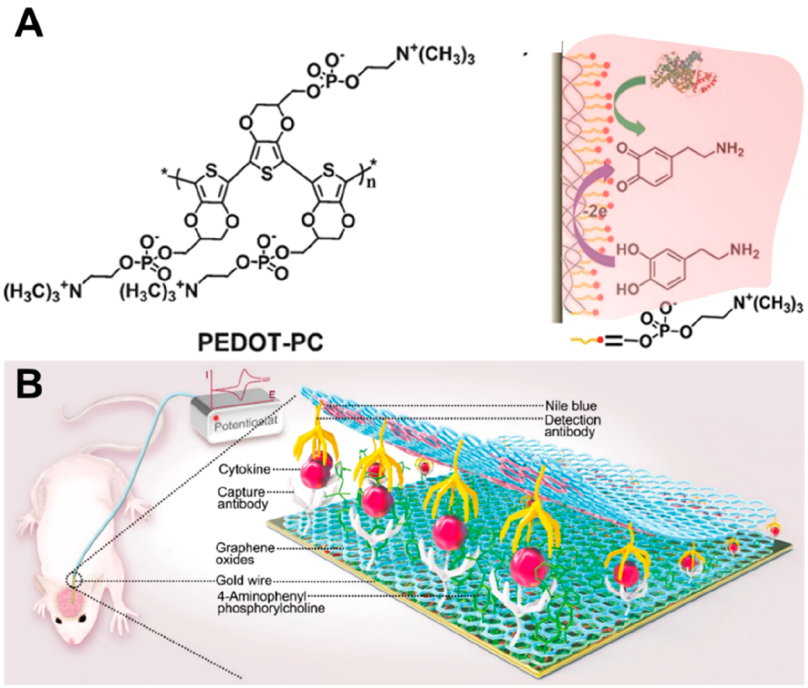

Figure 24. (A) Structure of PEDOC−PC and schematic of the interface between PEDOC−PC/CFE and bloodstream. Adapted with permission from ref 244. Copyright 2017 John Wiley and Sons. (B) Schematic depiction of zwitterionic PPC-GO decorated sensor for electrochemical sandwich sensing of IL-6 cytokine in a mouse brain. Reproduced with permission from ref 245. Copyright 2017 American Chemical Society.

these NIR probes with CRET capability sense H_2O_2 without the need of external light excitation.[238]

Shuhendler et al. have also reported the use of a functionalized PEG polymer within an optical nanosensor for the simultaneous detection of drug (e.g., antipyretic acetaminophen (APAP)) induced RNS and ROS in the liver of living mice to support the evaluation of acute hepatotoxicity in real time.[239] This sensor (average diameter ∼50 nm) is also a nanocomposite generated by coprecipitation, in which the H_2O_2-sensitive chemiluminescent compound bis(2,4,5-trichloro-6-(pentyloxycarbonyl)phenyl)oxalate (CPPO) and a ROS-sensitive fluorescent dye (IR775 S) are integrated into a PEG-polymer. The CPPO enabled the detection of H_2O_2 without external light excitation *via* CRET, and the IR775 S facilitated ratiometric fluorescence resonance energy transfer (FRET) detection of $ONOO^-$ upon light excitation. The nanosensors were injected intravenously through a tail-vein catheter 15 min after drug administration, after which imaging of the liver using an IVIS Spectrum imaging system was performed. The authors assessed the rate of nanosensor uptake and retention in the liver by measurement of the total liver fluorescence intensity for 80 min. The sensor exhibited specific and nanomolar sensitivity toward oxidative and nitrosative species generated during triggered pathophysiological conditions.

Xie et al. have described the construction of a PEG containing nonfouling flower-shaped Au−Fe_3O_4 based nanoprobe (D_h ∼40 nm ideally define for all particle cases) that can be injected into mice for optically sensing matrix metalloproteinase (MMP) expression *in vivo*.[240] MMP is a protease related to tumor invasion and metastasis and is heavily secreted by malignant tumor cells, making it a valuable biomarker of cancer. As illustrated in Figure 23, the presynthesized Au−Fe_3O_4 nanoparticles were modified with a Cy5.5-labeled GPLGVRG peptide containing a tridihydroxyphenylalanine (TDOPA) anchor (Cy5.5-GPLGVRG-TDOPA), and PEG_{5000}-SH. Cy5.5 serves as a NIR optical reporter, which is linked to the particle by the enzyme substrate (GPLGVRG) spacer. Because of the quenching of the Cy5.5 emission by the underlying gold substrate, the fluorescence of the sensor is turned off in its native state. Upon cleavage of the peptide spacer by MMP, the fluorophore is released and the fluorescence restored. The nanoprobes were injected intravenously in SCC-7 (head and neck squamous cell carcinoma) tumor xenograft mouse models, which are known to express high levels of MMP, and subsequent NIR imaging demonstrated a 10-times stronger signal than control experiments in which a MMP inhibitor was used. Notably, almost no fluorescence signal was observed in blood while control particles without PEG were strongly fluorescent due to nonspecific activation of the sensor upon fouling.[106,240] Importantly, this platform could also be applicable to detect other proteases implicated in cancer pathogenesis if their respective enzymatic substrates are incorporated into this platform.

Despite these promising works, it should be noted that recent reports indicate that PEG may induce immunogenicity and subsequently produce anti-PEG antibodies, which may limit the application of PEG coatings for *in vivo* sensing or drug delivery, prompting the exploration of other antifouling chemistries (Table 4).[241−243]

2.3.3.2. Zwitterions. In taking advantage of the discussed properties of zwitterionic interfaces, Liu et al. have recently reported an amperometric sensor for *in vivo* tracking of DA by electropolymerizing a EDOT-PC composite on carbon fiber electrode (CFEs) (Figure 24A).[244] Fast scan CV was then used to record the electrically stimulated DA release in the rat nucleus accumbens. Notably, the authors demonstrated that the amperometric response toward DA was almost completely maintained at the PEDOT−PC/CFE after *in vivo* implantation

https://dx.doi.org/10.1021/acs.chemrev.9b00739
Chem. Rev. XXXX, XXX, XXX−XXX

Table 3. Summary of Antifouling Durable (Implantable) Sensors[a]

antifouling chemistry	sensor	detection mode	operation site	lifetime	analyte	ref
PEG	CFE	voltammetry	rat brain	~1 year	dopamine	226
PEG	semiconducting polymer nanoparticle based nanosensor	CRET	mouse peritoneal cavity	~4 h	H_2O_2	238
PEG	Au@Fe_3O_4 based nanosensor	fluorescence	mouse venous blood	~8 h	MMP	240
PEG	organosilica core−shell NP based nanosensor	fluorescence	mouse venous blood	~15 min	pH	233
PEG	carbon dot based nanosensor	fluorescence	mouse vein	~10 d	cancer cell	251
PEG	semiconducting polymer nanoparticle based nanosensor	FRET	mouse vein	~24 h	RONS	252
PEG	DNA-CNT based nanosensor	fluorescence	mouse vein	~40 h	NO	253
PEG	Pt nanosensor	phosphorescence	mouse venous blood	~2 h	histamine	235
PEG	semiconducting polymer dot based nanosensor	FRET	mouse vein	~24 h	cancer cell	254
PEG	hydrogel microbeads	fluorescence	mouse vein	~3.5 h	glucose	218
OEG	gold electrode	EIS	mouse brain	~6 min	K^+	231
cysteine	CdTeS QD based nanosensor	FRET	mouse venous blood	~36 h	MMP-2	250
PEOT−PC	CFE	amperometry	rat striatum	~50 min	dopamine	244
Phosphatidylcholine	gold wire	amperometry	rat vein	~3 h	doxorubicin	246
PVA-CS	silicon microneedle	colorimetry	rabbit skin	~17 days	glucose	255
silica nanoporous membrane	CFE	amperometry	rat brain	~2 h	O_2	256
ion-selective membrane	CFE	potentiometry	rat brain	~50 min	pH	257
nanoporous polymer membrane	CFE	amperometry	rat brain	~1 h	dopamine	258
continuos-flow diffusion filter	CFE	SWV	rat jugular vein	~4 h	doxorubicin	259
polysulfone membrane	gold wire	amperometry	rat external jugulars	~12 h	doxorubicin	260
Nafion membrane	Pt wire	amperometry	rabbit femoral quadriceps muscle	~15 min	O_2	261
Nafion membrane	CFE	amperometry	rat brain	~6 h	dopamine	262

[a]Abbreviations: CFE, carbon-fiber electrode; PEDOT−PC, polyethylenedioxythiophene-phosphorylcholine; PVA, poly(vinyl alcohol); CS, chitosan; MPA, 3-mercaptopropionic acid; FSCV, fast-scan cyclic voltammetry; MMP, matrix metalloproteinase; CRET, chemiluminescence resonance energy; RONS, reactive oxygen and nitrogen species; FRET, fluorescence resonance energy transfer.

in the striatum of the rat brain compared to *in vitro* detection in cerebral spinal fluid (CSF), indicating a high resistance to nonspecific adsorption. Moreover, DA could be monitored within 400 s after local injection of KCl (to evoke DA release) with good sensitivity. In a recent study, Qi et al. presented another phosphorylcholine decorated electrochemical sensor for amperometric monitoring secretion of Interleukin-6 (IL-6, a major cytokine in the central nervous system) in mouse brain.[245] They introduced a sandwich assay consisting of a capture antibody and electrografted zwitterionic PPC-modified graphene oxide on gold wire electrodes together with a detection antibody and Nile blue-modified GO (Figure 24B). In *in vitro* tests, this platform was capable of the highly selective amperometric detection of IL-6 down to sub pM levels. The developed sensor was also capable of monitoring IL-6 secretion in live mice after intraperitoneal injection of lipopolysaccharide (LPS), without inducing an inflammatory response.[245] Although this study was not designed for continuous real time and long-term monitoring, it presents a pioneering exploration in translating *in vitro* surface chemistry design (zwitterion-GO composite) into an *in vivo* application.

Another phosphatidylcholine (PC) based electrochemical *in vivo* sensor has been reported by the Plaxco group, who utilized mixed SAMs of a biomimetic PC-thiol and a methylene-blue tagged aptamer for sensing of doxorubicin in the external jugular vein of an anesthetized rat.[246] The working principle of this system is akin to *in vitro* aptamer sensors discussed in Section 2.3.2.4 (Figure 21), where target binding triggers conformation changes that affect electric communications between a redox-labeled capture probe and the underlying electrode.[247,248] The incorporation of the cell-membrane mimetic PC antifouling system allowed successful translational to *in vivo* monitoring of doxorubicin (DOX). On the basis of this system, the authors demonstrated significantly improved baseline stability, with a stable current response over 12 h. In contrast, control interfaces based on MCH or 1-mercapto-1-undecanol (MCU) diluents suffered significant signal loss due to fouling. This platform thus enabled a stable real-time monitoring of pharmacokinetic information, potentially of value in disease management.[249]

The discussed physicochemical characteristics of amino acid interfaces have been exploited in a recent study, where a cysteine-modified quantum dot based FRET nanosensor was developed by Li and co-workers to detect matrix metalloproteinase-2 (MMP-2) *in vivo*.[250] Specifically, cysteine-decorated NIR emitting (720 nm) CdTeS QDs (donor) were linked to an NIR organic dye (ICG-Der02, acceptor) *via* a MMP-2-specific peptide substrate (GPLGVRGKGG) to form a QD−peptide−dye nanoassembly. Exposure of the sensor to MMP-2 in the tumor environment *via* intratumoral injection led to selective cleavage of the peptide (due to specific recognition by the MMP-2), resulting in the recovery of fluorescence from QDs. These particles were reported to show high colloidal stability with no precipitation in MCF-7 cancer cell medium. The authors then successfully examined MMP-2 expression in tumors on nude mice noting a clear

https://dx.doi.org/10.1021/acs.chemrev.9b00739
Chem. Rev. XXXX, XXX, XXX−XXX

difference between tumor and symmetrical muscles in the two upper arms as tracked by fluorescence for up to 36 h.

In summary, *in vivo* sensors need to satisfy the target selective criteria that *in vitro* sensors must operate with when applied within (usually diluted) biological samples but additionally require high levels of biocompatibility, low toxicity, and need to be miniaturizable/machinable to enable effective operation in harsh, spatially confined and often dynamic conditions. The presented examples largely rely on the use of an appropriate combination of a solid support (e.g., QDs, fiber or microelectrodes with an antifouling protection, often PEG-based). The application of these designs can not only minimize fouling but also decrease host immunoresponse and thrombus formation and can stabilize colloidal nanosensors as well as reduce their clearance (thus increasing the sensor lifetime). Though the highlighted examples hold great promise for monitoring internal body dynamics, and thus supporting both health management and disease theranostics, routine applications remain some way off. More detailed studies are required to assess the long-term stability, safety, and biocompatibility of these *in vivo* agents, but there remains enormous bandwidth in chemical and physical tailoring (as detailed in Sections 2 and 4) in a manner that might, 1 day support routine automated monitoring of a wide range of relevant analytes. Of particular importance in the design of *in vivo* sensors is their lifetime, as highlighted throughout this review (see, for example, Tables 1 and 3). The requirements here are very application specific; the monitoring of pharmacokinetics is typically envisioned to be over comparatively short time spans (hours to days), while, for example, continuous glucose sensing may be sought over many weeks. The challenges of long-term stability and antifouling character scale, of course, with time but are also a factor of the analytical mode. In "reagentless" or immunorecognition configurations, this can be a very substantial challenge, markedly more so than when analyte capture and signal generation is enzymic. As indicated in Table 3, there remains much work to be done before academic work can be robustly translated into clinical application.

3. SENSORS BASED ON PHYSICAL ANTIFOULING STRATEGIES

3.1. Porous Transducer Topographies

Apart from the previously discussed sensors that rely on highly hydrated interfacial chemistries to resist nonspecific adsorption, alternative strategies to alleviate the impediments associated with interfacial fouling have also been explored. One such approach is the direct physical manipulation of sensory interfaces. For example, the engineering of porous electrodes or the use of membrane filters are promising approaches to alleviate fouling by large molecules or cells by presenting a diffusional barrier (sieving) that restricts access of these large molecules to the underlying sensor while still allowing diffusive access to smaller analytes. To this end Patel et al. have explored the relationship between electrode pore size and antifouling performance (Figure 25A).[263] In this work it was found that nanoporous (<50 nm pore size) electrodes possess greater fouling resistance compared to planar, macroporous (1200 nm pore size) or hierarchical (60 nm–1200 pore size) gold electrodes in the presence of BSA (2 mg mL^{-1}) and fibrinogen (1 mg mL^{-1}). Cyclic voltammetry in a solution containing a redox probe ($[Fe(CN)_6]^{3-/4-}$) indicated

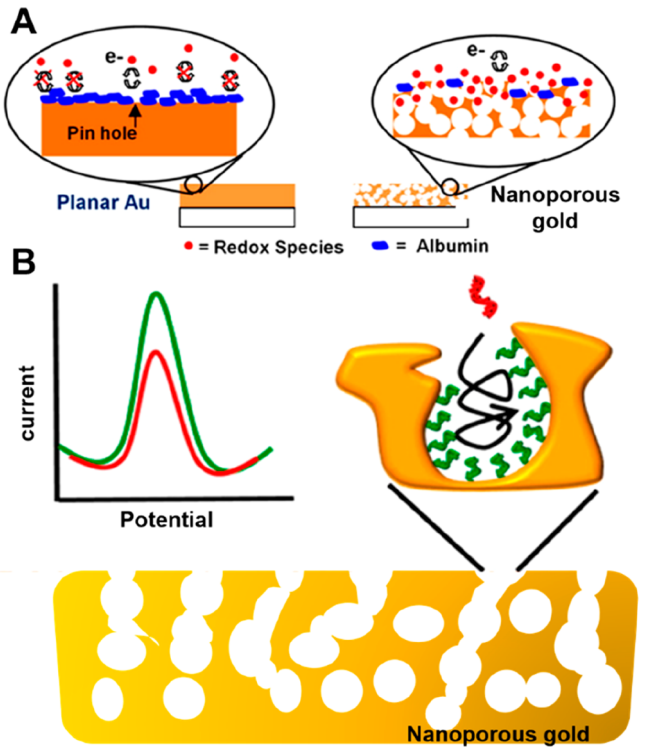

Figure 25. (A) Graphical representation of the surface of nanoporous gold and planar gold in the presence of albumin and a small redox molecule in solution. Electron transfer is hindered at planar gold but not at nanoporous gold. Reproduced with permission from ref 263. Copyright 2013 American Chemical Society. (B) Schematised summary of the use of a porous gold thin film morphology for electrochemical DNA Sensing. Adapted with permission from ref 264. Copyright 2015 American Chemical Society.

negligible fouling at the nanoporous electrode. It was proposed that restricted mass transport through small pores was key to this attenuation, an operational feature that can be feasibly exploited for sensing of small analytes.

The same group investigated a similar strategy that utilizes porous gold electrodes obtained via dealloying.[263] No significant loss in voltammetric response of ferricyanide was observed when the nanoporous gold (np-Au) was immersed in serum or heparinized blood while a significant reduction in Faradaic peak currents occurred at planar gold. The high receptive loading possible with these large surface area supports has also been shown to enable an approximately 10-fold higher electrochemical current upon probe-target hybridization as compared to the planar Au electrodes (Figure 25B).[264] On the basis of these discoveries, the Seker group have applied porous gold based sensors for assaying DNA in complex biological media.[264−266] In one example, they reported using np-Au electrodes onto which MB functionalized DNA probes where self-assembled. This allowed detection of target DNA in the presence of BSA and FBS.[266] The np-Au electrodes enabled sensitive detection with a dynamic range of 10 to 100 nM that improves by 1 order of magnitude for coarsened np-Au morphology due to increased target penetration into the porous network and hence enhanced hybridization efficiency. In comparison with planar Au and annealed np-Au electrodes, unannealed porous Au electrodes suffered least signal suppression in the presence of BSA or FBS, with highest suppression observed at planar Au electrodes

https://dx.doi.org/10.1021/acs.chemrev.9b00739
Chem. Rev. XXXX, XXX, XXX−XXX

indicating that the pores act as efficient sieves for larger (fouling) biomolecules. Importantly, a tuning of the pore size may allow the design of sensors in which molecules of specific sizes are restricted from accessing the sensory (electrode) interface. Nanoporous gold has also been applied to electrochemical detection of L-cysteine in urine[267] while in another recent study, simultaneous amperometric electrochemical sensing of ascorbic acid and uric acid in FBS was achieved with a LoD of 63.0 and 9.0 μM, respectively.[268]

3.2. Filtration Methodologies

An alternative physical approach, the application of membrane filters to transducer, has received considerable attention recently. For example, a drop-cast nanocomposite of graphene nanoribbons and a Nafion-modified electrode for the selective detection of cysteine in serum, was reported by Wu et al.[269] The graphene nanoribbons impart high conductivity and extremely highly electrocatalytic activity toward the electrochemical oxidation of cysteine at +0.025 V while the negatively charged Nafion can not only apparently prevent the aggregation of graphene nanoribbons, but also prevent electroactive interference from ascorbic acid and uric acid allowing an *in vitro* assay of cysteine in serum samples without any pretreatment. A different filtering approach was utilized by Su's group in preparing isoporous silica micelle membranes (iSMM) and used them for the electrochemical detection of drug molecules (chloramphenicol, CAP) in 10% heparinized whole blood.[270] The interfaces were formed by immersion of ITO into tetraethoxysilane solution forming small channels in the silica support that facilitate access of small molecules to the underlying electrode while blocking (sieving) large biointerferents, preventing fouling and passivation. By monitoring CAP's direct reduction peak current using DPV, this electrochemical sensor enabled the quantification of CAP in whole blood with a 100 nM LoD substantially lower than that achieved at a bare ITO electrodes.

Membrane filtration based sensors have also been applied for *in vivo* sensing. For example, for the sensitive *in vivo* monitoring of pH (important marker for physiological function) in a live rat brain,[271] Mao's group developed a H^+ selective electrode based on a carbon fiber coated with a polyvinyl chloride (pVC) based H^+ selective membrane (H^+ ISM) containing the H^+ ionophore tridodecylamine.[257] Both *in vitro* and *in vivo* studies demonstrated that the resultant membrane-coated potentiometric pH sensor possessed strong antifouling properties against protein adsorption without loss of sensitivity when exposing to BSA (up to 70 mg mL^{-1}) or cerebrospinal fluid (CSF) containing 40 mg mL^{-1} BSA. Moreover, this sensor was reported to exhibit a fast response (<1 s) to pH change within the narrow physiological pH range (pH 6.0 to 8.0) with high reversibility and selectivity when animals were subjected to CO_2 inhalation or injection of sodium bicarbonate to evoke acid–base disturbance. The translation of such ISMs for *in vivo* monitoring of other ions could be achieved if suitable ionophores are incorporated into these architectures. Recently, Maós group demonstrated *in vivo* monitoring of oxygen in rat brain with carbon fiber microelectrode (CFME)-modified with an antifouling silica nanoporous membrane. Specifically, a silica nanoporous membrane (SNM) consisting of uniform, closely packed, and vertically aligned nanochannels was electrografted (from a silane solution containing CTAB as a surfactant) onto the CFME surface, which was permeable to O_2 while nonfouling (Figure 26).[256] Continuous monitoring of O_2 for up to 2 h was achieved with this sensor in the mouse brain with retained

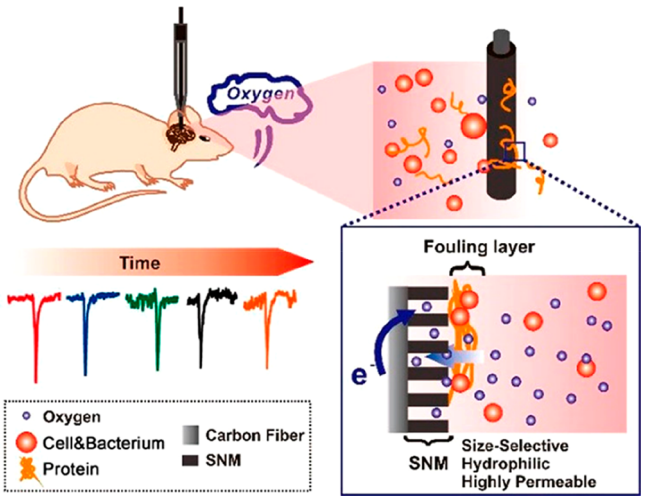

Figure 26. Illustration of hydrophilic, highly permeable and antibiofouling SNM-coated CFME for continuous monitoring of O_2 in rat brain. Reproduced with permission from ref 256. Copyright 2019 American Chemical Society.

current stability. A similar strategy using silica porous membrane has also been applied as antifouling coating for electrochemical sensing of dopamine[272] or chloramphenicol[273] in human blood.

Another filtration-based methodology to prevent electrode surface biofouling has been utilized by Soh and Plaxco to facilitate the amperometric electrochemical sensing of small molecules.[259] In an example of an off-surface filter, a continuous monitoring of the pharmacokinetics of DOX, was enabled. A "continuous diffusion filter" (CDF) was specifically utilized to block access of large molecules or blood cells while enabling diffusion of small analytes to the underlying electrode (Figure 27). Amperometric detection was achieved through the use of a conformationally responsive DOX binding methylene blue-tagged specific aptamer. It was demonstrated that this sensor allowed continuous DOX monitoring in live rats over 4.5 h with good sensitivity and a highly selective performance ultimately relying on the ~100 times higher

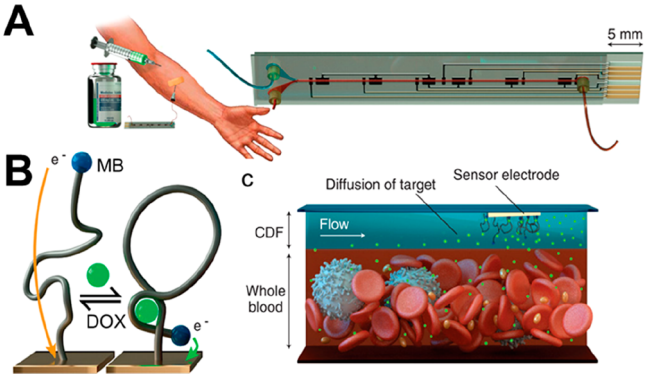

Figure 27. Microfluidic electrochemical sensor incorporating a continuous diffusion filter (CDF) allowing real-time quantitative measurement of small molecules in the blood flow of humans. Adapted with permission from ref 259. Copyright 2017 American Association for the Advancement of Science (AAAS).

https://dx.doi.org/10.1021/acs.chemrev.9b00739
Chem. Rev. XXXX, XXX, XXX−XXX

diffusivity of the DOX analyte in comparison to background HSA, IgG and Fib. Though conceptually simple, and inherently limiting, this strategy might be generally applicable to the sensing of a wide range of small-molecule analytes. In a recent study, the Plaxo group applied an alternative approach to produce an electrode that could be inserted directly into a catheter to monitor blood flow in the jugular vein.[260] Rather than using the off-surface filter, the authors integrated a biocompatible polysulfone membrane (0.2 μm pore size) onto the electrode. The system was used to measure the real-time concentrations and pharmacokinetics of DOX and several aminoglycoside antibiotics (intravenous or intramuscular injection) using redox-tagged aptamer films. The sensor was able to identify pharmacokinetic characteristics across multiple injection cycles and on both awake and mobile rats. These *in vivo* sensing systems are applicable for many small molecule therapeutic drugs but are ultimately limited to the detection of analytes that can penetrate through the filtering membrane. It is also highly unlikely this purely physical approach would be effective as coexisting nontarget small molecules may also access and disturb the sensing interface. Taking this into account, the concurrent integration of a chemically antifouling system in a manner perhaps analogous to the zwitterionic membranes, which have been widely applied in water desalination, might further improve these systems.[274] Such an approach was recently reported by Feng et al., who utilized a polytannic acid-doped nanoporous conductive PANI membrane on CFEs through potential-static electropolymerization.[258] The concurrent integration of physical (porous membrane) and chemical antifouling strategies (polytannic acid/PANI) resulted in excellent antifouling performance, enabling *in vivo* DA quantification in mouse brain, where high sensitivity was retained pre- and postcalibration.

These physical antifouling approaches present (Table 3) a promising new approach to circumvent fouling by restricting access of large biomolecules to the underlying sensory interface. They are, however, inherently restricted to the sensing of small analytes. Through the tuning of the pore size of a filter or the porous support, a relatively distinct cutoff size/molecular weight can be achieved. This will not only reduce any fouling from larger molecules, but also inherently impact the selectivity of the sensor in a manner that needs to be carefully considered.

4. SENSORS BASED ON BIOLOGICAL ANTIFOULING APPROACHES

4.1. Affinity Depletion

Another approach to the detection of analytes in complex samples is off-sensor depletion. In contrast to chemical and physical strategies, this methodology serves to directly reduce the concentration of interfering (bio)molecules. Such a sample prepurification can also be carried out via other "conventional" techniques such as liquid chromatography, although these are time-consuming or considerably dilute the sample. To circumvent this, antibody-modified magnetic beads can directly and conveniently capture and remove abundant coexisting proteins, such as HSA or IgG in blood, thereby reducing the fouling capabilities of the sample. For example, Kongsuphol et al. have used two types of magnetic beads (MBs) decorated with anti-HSA/anti-IgG and anti-TNF-α.[275] The former was used to deplete highly abundant HSA and IgG from serum to generate precleared serum, followed by specific capture of TNF-α by the latter beads (Figure 28). The captured TNF-α was then eluted from the beads and assayed

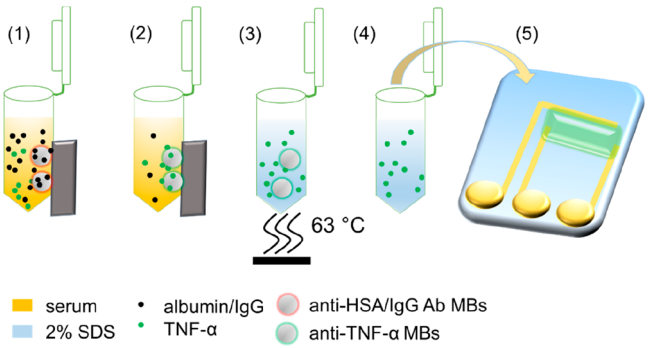

Figure 28. Schematic depiction of a TNF-α impedimetric sensor with an integrated background depletion strategy. (1) Removal of the main serum background interferents (HSA and IgG). (2) The background depleted sample is collected for TNF-α capture. (3) The captured TNF-α is eluted from the magnetic beads using 2% sodium dodecyl sulfate (SDS) at 63 °C and (4) the magnetic beads are separated from the eluted sample. (5) Eluted TNF-α is detected at gold array electrode via EIS. Adapted with permission from ref 275. Copyright 2014 Elsevier.

by impedance spectroscopy at bare gold microelectrode arrays in a manner that was reportedly able to detect TNF-α with a fM sensitivity in undiluted serum samples. The assay is small sample volume only as the total protein level in serum (~50–60 mg mL^{-1}) is usually significantly higher than specific target concentrations requiring large input quantities of antibody-modified depletion beads (Table 4) and this remains a time-consuming two-step process. It does, though, allow specific depletion and could be combined with traditional chemical nonfouling approaches (i.e., decoration of bead/sensory interface with antifouling chemistries). It is also likely to be more efficient if applied within an integrated fluidic device where more efficient (and designed) mixing of low sample volumes is possible. An early example of this was reported by Oleschuk and co-workers who developed a microfluidic platform in which three depletion beads (anti-HSA, protein A, and protein G) purified up to four human serum samples simultaneous depleting up to 95% of IgG and HSA within 10 min. This enabled a 4-fold increase in signal-to-noise ratio in the subsequent mass spectrometric detection of hemopexin, a low abundance protein biomarker.[276]

4.2. Degradation by Enzyme Catalysis

An entirely different biological antifouling strategy has been developed based on the use of enzymes capable of actively degrading (physisorbed) biomolecules thus reducing fouling. This has been widely utilized for the modification of membranes utilized in the water treatment industry.[277,278] For example, in the construction of an antifouling and self-cleaning membrane based on the covalent attachment of trypsin on a poly(methacrylic acid)-*graft*-poly(ether sulfone) (PMAA-*g*-PES) membrane via EDC/NHS coupling.[279] This suppressed protein fouling under dynamic flow where 95.0% of the initial flux of BSA solution (through the membrane) was maintained after multicycle BSA filtration over a 15-day period. A control PES membrane suffered more significantly from fouling (<35% flux recovery) within a shorter time span of 50 h. In another example, Koseoglu-Imer et al. reported the successful modification of a cellulose acetate membrane with a

https://dx.doi.org/10.1021/acs.chemrev.9b00739
Chem. Rev. XXXX, XXX, XXX−XXX

Table 4. Summary of Different Antifouling Strategies for Sensors

Antifouling Strategies		Principle	Advantages	Limitations	Future efforts	References
Chemical	EG based nonfouling systems	hydration layer induced energetic and physical barrier to prevent fouling	effective protein resistance and good biocompatibility	suffers from oxidative damage and generation of reactive oxygen species, may trigger adverse immune response	(1) Build-up of data analytics based criteria for new antifouling agents and antifouling sensor screening and optimization	31,121,242
	Zwitterionic nonfouling systems (PC/SB/CB/peptide)			antifouling behavior may be compromised/alerted in case of pH sensitive or electric field sensitive zwitterions. Peptides can suffer from oxidative damage or protease degradation	(2) Composite antifouling systems (e.g., hybrid antifouling chemistries, combined chemical/physical strategies)	84,281,282
	Other hydrophilic systems (e.g., hyaluronic acid)			biodegradation by free radicals or hyaluronidase in the *in vivo* environment		169,283
Physical	membrane filtration (e.g., Nafion, polysulfone, ISM)	pore-size restricted pass through and diffusion control	biocompatible, effective blocking of large fouling molecules/cells	low diffusion coefficient may lead to slow response times, not applicable to larger analytes	(3) Exploration of new antifouling chemistries/approaches and their improved synthesis/construction/integration	259,260,262
	porous electrode	size-exclusion based on the porous morphology	efficient transport of small molecules in the presence of larger biomolecules, highly repeatable and scalable	slow mass transportation kinetics, mainly limited to electrochemical sensors		263,265,284
Biological	affinity depletion	immunoaffinity based binding and removal of interferents	significant depletion of interfering proteins from small input volume	low depletion capacity and low throughput operation, high cost of antibodies, not applicable for *in vivo* sensing	(4) Highly integrated devices	275

serine protease enzyme (Savinase) in retaining higher flux value and protein (BSA) rejection during filtration in comparison to the unmodified membrane.[280] This approach could be incorporated into a variety of existing microfluidic devices or sensors relying on chemical or physical antifouling approaches. One note of caution is that, in addition to an appropriate selection and immobilization of the enzyme, the degradation products must not interfere with the operation of the sensor.

5. CONCLUSIONS AND PERSPECTIVES

The development of nonfouling sensors for the detection of target analytes in complex fluids has witnessed great progress in recent years as shown in Figure 29. This review has attempted to systematically summarize the comprehensive spectrum on the antifouling interface construction, characterization, incorporation strategies with receptor to form final antifouling sensors, and comment on the key antifouling strategies that facilitate sensitive and selective sensing under such demanding conditions (*in vitro* or *in vivo*). The chemical modification of sensory interfaces (flat or spherical) with suitably designed hydrated molecular systems (such as PEG, zwitterions or peptides) is undoubtedly an accessible and thus common approach that is increasing in its sophistication.

Physical or biological approaches to circumvent fouling have recently gained significant attention as an alternative or complementary approach to more established chemical formats. All approaches bring specific advantages to the table and inherently possess limitations (Table 4) that may have to be improved if robust real-world applications, at scale, are to be viable. We thus believe that future efforts within the field will focus on the following (see also Table 4):

5.1. Exploration of New Antifouling Materials and Approaches for Sensing

As discussed within this review, the majority of sensors operating in complex fluids rely on chemical barriers and currently these are largely limited to those based on PEG or accessible zwitterions. Though demonstrably effective, these have identified specific disadvantages (Table 4), for example zwitterionic systems can be field- or pH-dependent, peptides or natural polymers can be prone to hydrolysis (degradation) while PEG suffers from oxidative damage in the presence of oxygen and transition and may cause adverse immune responses *in vivo*.[242] It should also be noted that these problems are especially amplified when continuous, long-term sensing is carried out or derived devices are expected to have a tenable shelf life.

The exploration of novel chemical architectures or hybrid synergic systems as antifouling interfaces is also likely to be very important as real world applications become increasingly relevant. This is all the more apparent when considering that in most applications these interfaces must perform well diagnostically and be nontoxic. For example, as an alternative to traditional zwitterions, polyampholytes (polyelectrolytes comprising mixed charge component polymers) are both highly tunable and potentially very potent.[290] Moreover, zwitterionic inorganic/organic hybrid polymers with high stability to degradation have been increasingly explored in the material sciences (for example for the removal of heavy metal ions from environmental samples) but have not yet been applied in a sensor format.[291,292] Inspired by trimethylamine N-oxide (TMAO), a natural zwitterionic osmolyte, Jiang's

https://dx.doi.org/10.1021/acs.chemrev.9b00739
Chem. Rev. XXXX, XXX, XXX−XXX

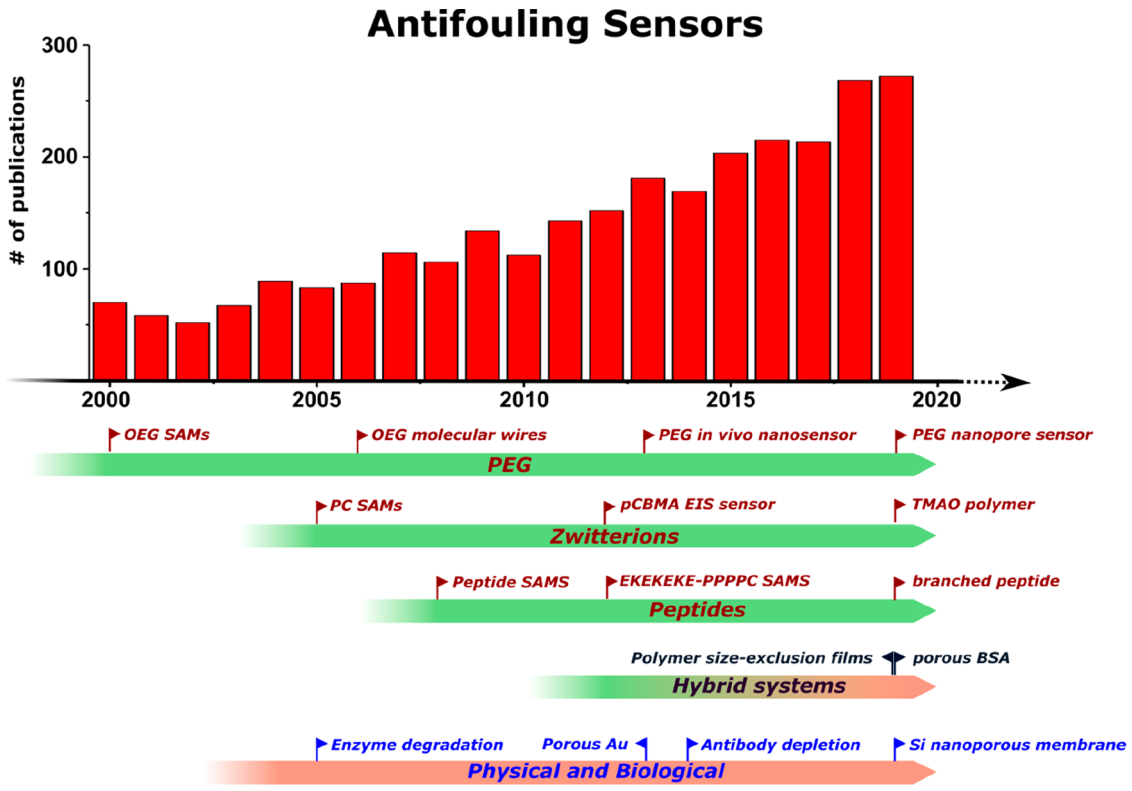

Figure 29. Overview of developments in the field of antifouling sensors. The histogram displays the number of publications per year containing the search terms ("fouling" OR "antifouling" OR "antifouling" OR "nonfouling OR "nonfouling") AND ("sensing" OR sensor" OR "detection") as analyzed by Web of Science (on 24.02.2020). This search found 3116 articles published with these keywords (since 1945) with a total of 79299 citations. Displayed underneath is an approximate timeline of the emergence of the most commonly employed antifouling materials/approaches in the context of sensor development as well as selected milestone examples. These are the introductions of PEG and related systems,[142,235,285,286] zwitterionic systems,[60,102,287] peptides,[34,168,288] hybrid systems[117,289] as well as physical[256,263] and biological approaches.[275,277]

group recently developed TMAO-based zwitterionic polymers (PTMAO) as a new class of ultralow fouling materials with promising *in vitro* and *in vivo* performance.[287] An interesting observation with potential ramifications in sensing applications is a recent report by Yeon et al., demonstrating that supraparticles (clusters of NPs) decorated with cysteine moieties of different chirality display a significantly different interaction with serum proteins (as well as cellular uptake).[293] Specifically, the *D*-cysteine-modified particles displayed a 3−4 fold enhanced cell internalization as well as increased stability against enzymatic degradation and longer biological half-life. The latter was attributed to the incompatibility of natural proteins and enzymes with the D-enantiomer-capped particles. This then potentially offers a new consideration in tuning biofouling, an approach which may be particularly promising in peptide based interfaces.

Apart from these chemical antifouling approaches, physical approaches such as bioinspired topographies, for example, shark skin patterns[268,269] or mollusc shell mimics,[190,294,295] have been used to resist marine fouling and control cell adhesion but have, again, rarely found application in sensors.

In another recent study, Yang et al. developed an injectable antibiofouling "spiky microparticle" where a commercial fluorosilane was used to entrap a fluorinated lubricant on the surface.[296] Interestingly, these particles could be stably dispersed in water and retained excellent long-term (>14 days) antiadhesive properties to proteins, cells (both *in vitro* and *in vivo*) and bacterial adsorption (e.g., *E. coli* and *S. aureus*). A similar approach was previously developed by Badv et al. where, in addition to the nonfouling fluorosilanes, aminosilanes were introduced allowing bioconjugation of cell-binding ligands or receptors.[297] A strong adhesion of endothelial cells with concurrent low levels of fouling in human whole blood was achieved with the mixed film. These discoveries highlight the potential of fluorinated, "slippery surfaces" as a new class of antifouling interfaces with promising improved or complementary performance to traditional (hydrated) nonfouling chemistries.[298,299]

In another nice example of a potential new way forward, Wang et al. have recently reported a proof-of-concept approach in which electrodes were coated with a commercial transient polymer (Eudragit L100) for glucose sensing in undiluted serum and saliva.[300] This protective and dissolvable coating can be programmed (by adjusting adlayer density or thicknesses) to expose fresh sensor surface at preselected times (up to 6 h) (Figure 30). This delayed actuation concept holds considerable promise for adaption to other electrochemical sensing platforms (e.g., sequential activation of different electrodes within an array) as well as for the protection of sensing interfaces based on other transduction modes.

In a very recent example of a combined physical and chemical approach, Ingber and co-workers have reported the generation of a cross-linked BSA-nanowire composite interface with apparent excellent long-term antifouling performance.[289] The cross-linked BSA matrix in this work presents not only a strongly hydrated interface but also acts as a physical porous filter preventing (fouling) access to the embedded electrode

https://dx.doi.org/10.1021/acs.chemrev.9b00739
Chem. Rev. XXXX, XXX, XXX−XXX

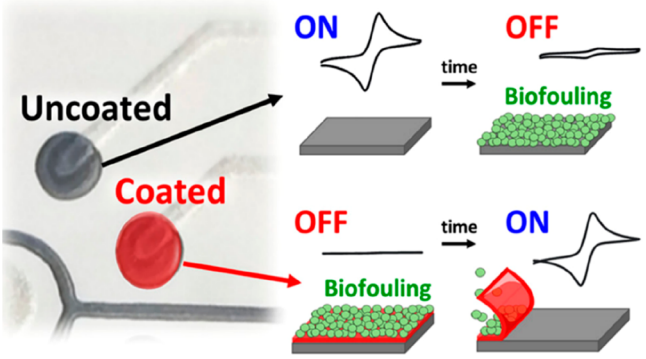

Figure 30. Antibiofouling approach using a delayed sensor activation system exploiting a dissolvable coating which can expose fresh sensor surface at designed times and thus actively remove adsorbed interferents. Reproduced with permission from ref 300. Copyright 2018 American Chemical Society.

materials. This was exploited to indirectly sense IL-6 in human plasma. Composite interfaces such as these are likely to offer much to the development of scalable *in vitro* and *in vivo* sensory applications.

Another similar example was reported by Paloni et al., in which immobilized lamellae of protein−polymer conjugates (based on poly(*N*-isopropylacrylamide) (PNIPAM)) were able to allow the access (and subsequent detection) of the small monomeric streptavidin (15.6 kDa) to the embedded receptive sites, while sterically blocking larger proteins (e.g., streptavidin (52.8 kDa)).[117] Importantly, a tuning of the polymer length facilitates some control over the protein size the film is pervious to.

5.2. Simulation Assisted Sensory Design and Data Analytics

While various computational methods have been utilized to elucidate interfacial processes associated with fouling, many designs have not been analyzed computationally. With the advent of ever stronger computational methods the simulation-assisted design of chemically complex or chemical-physical antifouling composite-based sensing interfaces will become more routine in supporting highly specific sensor design.[301] For example, in a recent study simulations were carried out on the performance of polymer coatings on nanoparticles with respect to their antifouling and cellular uptake properties.[302] Analyte diffusion across fluidic channels has also been intensively scrutinized by simulations,[303−305] and models developed within this could be expanded to elucidate the diffusion of analytes through porous antifouling architectures. This would then offer a more rational sensory design pathway.

An additionally important consideration in the construction of sensors is the number of parameters (e.g., see Table 1) that are (ideally) optimized and monitored, particularly for in vivo applications. For any viable demonstration of scalability, the use of advanced data and statistical analyses is critical. One important parameter in almost all sensory applications is the transducing signal baseline stability; any drift here has a very direct impact on signal/noise and thus analytical sensitivity. An ability to track and mathematically correct for such drift can potentially mitigate deleterious effects. Data analysis via optimized algorithms can also identify the parameters which are most analytically useful, as demonstrated via an immittance function analysis of impedimetric data (see Figure 11).[125] Though applied here to an impedance configuration, such analysis is applicable to a variety of different sensors, especially when complex signal outputs are encountered. Another data analytical tool that has received increasing attention is machine learning (ML). ML algorithms can potentially aid in in the design of improved sensory (antifouling) interfaces optimizing for desired sensory performance based on existing data sets.[306,307] These, and related, mathematical and statistical tools become increasingly important when analyzing a large number of repeat measurements (e.g., to assess reproducibility) or when sensing is performed in a multiplexed manner or on sensing arrays.

5.3. Highly Integrated PoC Sensing Devices

There are many emerging technologies based on advanced micro/nanofabrication, 3-D printing, self-powered devices and soft electronic techniques with significant potential for a myriad of sensing applications.[308,309] The integration of the antifouling technologies detailed herein (especially chemical/physical strategies) could further enhance their long-term stability and application most notably for *in vitro* and *in vivo* diagnostics/theranostics. Such integrated approaches will also find home in stimuli-responsive (intelligent) biointerfaces in, for example, improved wearable sensors,[310,311] organ-on-a-chip applications[312] and cell-based sensors for drug screening.[313,314]

AUTHOR INFORMATION

Corresponding Authors

Xiliang Luo − *Key Laboratory of Optic-electric Sensing and Analytical Chemistry for Life Science, MOE, Shandong Key Laboratory of Biochemical Analysis, College of Chemistry and Molecular Engineering, Qingdao University of Science and Technology, Qingdao 266042, China;* orcid.org/0000-0001-6075-7089; Email: xiliangluo@qust.edu.cn

Jason J. Davis − *Department of Chemistry, University of Oxford, Oxford OX1 3QZ, United Kingdom;* orcid.org/0000-0001-7734-1709; Email: jason.davis@chem.ox.ac.uk

Authors

Cheng Jiang − *Department of Chemistry and Nuffield Department of Clinical Neurosciences, University of Oxford, Oxford OX1 3QZ, United Kingdom*

Guixiang Wang − *Key Laboratory of Optic-electric Sensing and Analytical Chemistry for Life Science, MOE, Shandong Key Laboratory of Biochemical Analysis, College of Chemistry and Molecular Engineering, Qingdao University of Science and Technology, Qingdao 266042, China; College of Chemistry and Chemical Engineering, Taishan University, Taian 271021, China*

Robert Hein − *Department of Chemistry, University of Oxford, Oxford OX1 3QZ, United Kingdom;* orcid.org/0000-0001-8567-0924

Nianzu Liu − *Key Laboratory of Optic-electric Sensing and Analytical Chemistry for Life Science, MOE, Shandong Key Laboratory of Biochemical Analysis, College of Chemistry and Molecular Engineering, Qingdao University of Science and Technology, Qingdao 266042, China*

Complete contact information is available at: https://pubs.acs.org/10.1021/acs.chemrev.9b00739

Author Contributions

[¶]These authors contributed equally to this work.

https://dx.doi.org/10.1021/acs.chemrev.9b00739
Chem. Rev. XXXX, XXX, XXX−XXX

Notes

The authors declare no competing financial interest.

Biographies

Cheng Jiang received his PhD degree in chemistry from the University of New Souths Wales (Australia) in 2016. He was then recruited in a joint programme between Nuffield Department of Clinical Neurosciences (NDCN) and the Department of Chemistry as a postdoctoral fellow at the University of Oxford. His main research interests include the screening and validation of circulating biomarkers using high-throughput multiplexed sensing platforms towards disease diagnostics, stratification, and heath management.

Guixiang Wang received a Bachelor's degree in Chemistry from Liaocheng University in 2002, a Master's degree in analytical chemistry from Liaocheng University in 2005, and a PhD degree in Applied Chemistry from Qingdao University of Science and Technology in 2018. She joined the Taishan University in 2005 and was promoted to lecturer in 2007. She currently serves as lecturer of College of Chemistry and Chemical Engineering, Taishan University. Her scientific research interests mainly focus on conducting polymers and antifouling biosensing.

Robert Hein obtained his B.Sc. from Jacobs University Bremen, Germany in 2016, where he worked in the field of supramolecular chemistry under the supervision of Prof. Werner M. Nau. During his studies, he spent a semester abroad at Cornell University (with Prof. Geoffrey W. Coates). He is currently pursuing a PhD at the University of Oxford under the guidance of Prof. Paul D. Beer and Prof. Jason J. Davis working on electrochemical, supramolecular anion sensors. Other research interests include the development of novel antifouling interfaces for electrochemical (bio)sensors, surface functionalization via diazonium chemistry, and host−guest chemistry.

Nianzu Liu received her B.S. degree in Marine Science from Qingdao University of Science and Technology in 2016. She is currently a PhD candidate majoring in Applied Chemistry of the College of Chemistry and Molecular Engineering, Qingdao University of Science and Technology, under the supervision of Prof. Xiliang Luo. Her scientific research interests focus on biochemical analysis, nanobiosensing, and electrochemistry.

Xiliang Luo received his PhD degree from Nanjing University in 2005. He then worked as a postdoctoral fellow at Dublin City University, Arizona State University, and the University of Pittsburgh successively. In 2011, he became a research assistant professor in the Department of Bioengineering, University of Pittsburgh and a senior Marie Curie Fellow in the Department of Chemistry, University of Oxford. He then joined the Qingdao University of Science and Technology at the end of 2011 as a Taishan Scholar professor. His scientific interests are focused on biochemical analysis, electrochemistry, and conducting polymers.

Jason Davis is a Professor of Chemistry and a Tutorial Fellow and Dr. Lee's Reader in Chemistry at Christ Church, Oxford. He studied Chemistry at Kings College London, where he was awarded a First Class honours degree in 1993. He then undertook a DPhil in Chemistry at Oxford (1998) prior to being elected to an Extraordinary Junior Research Fellowship at The Queens College in 1998, a Royal Society University Research Fellowship in 1999, and a Lectureship in Chemistry at Jesus College, Oxford, in 2001. He was made a University Lecturer and Official Student and Tutor in Chemistry at Christ Church in 2003. He was made a full professor in 2014. His research interests are broad and primarily focussed on the design and utilization of advanced functional interfaces, particularly those associated with diagnostics, sensing, molecular switches, and imaging.

ACKNOWLEDGMENTS

We acknowledge financial support from the National Natural Science Foundation of China (21974075, 21675093), the Taishan Scholar Program of Shandong Province of China (ts20110829), the Shandong Provincial Natural Science Foundation (ZR2019MB039), the Shandong Key Laboratory of Biochemical Analysis (SKLBA1905), and Doctoral Research Initiation Project of Taishan University (Y-01-2018018). J.J.D. wishes to acknowledge support from the EPSRC, Weston Foundation, CRUK, and the Royal Society and Osler Diagnostics. The authors would like to thank Dr. Clare F. Megarity and Dr. Amol V. Patil for their helpful comments.

REFERENCES

(1) Wu, L.; Qu, X. G. Cancer Biomarker Detection: Recent Achievements and Challenges. *Chem. Soc. Rev.* **2015**, *44*, 2963−2997.
(2) Sawyers, C. L. The Cancer Biomarker Problem. *Nature* **2008**, *452*, 548−552.
(3) Wulfkuhle, J. D.; Liotta, L. A.; Petricoin, E. F. Proteomic Applications for the Early Detection of Cancer. *Nat. Rev. Cancer* **2003**, *3*, 267.
(4) Luo, X.; Davis, J. J. Electrical Biosensors and the Label Free Detection of Protein Disease Biomarkers. *Chem. Soc. Rev.* **2013**, *42*, 5944−5962.
(5) Gooding, J. J. What Is a "Real Sample"? *ACS. Sens.* **2018**, *3*, 1609−1609.
(6) Barfidokht, A.; Gooding, J. J. Approaches toward Allowing Electroanalytical Devices to Be Used in Biological Fluids. *Electroanalysis* **2014**, *26*, 1182−1196.
(7) Jiang, C. *Protein-resistant Electrodes for Biosensing*, PhD thesis, University of New Souths Wales, 2016.
(8) Harding, J. L.; Reynolds, M. M. Combating Medical Device Fouling. *Trends Biotechnol.* **2014**, *32*, 140−146.
(9) Jaffer, I. H.; Fredenburgh, J. C.; Hirsh, J.; Weitz, J. I. Medical Device-induced Thrombosis: What Causes It and How Can We Prevent It? *J. Thromb. Haemostasis* **2015**, *13*, S72−S81.
(10) Liu, B. S.; Liu, X.; Shi, S.; Huang, R. L.; Su, R. X.; Qi, W.; He, Z. M. Design and Mechanisms of Antifouling Materials for Surface Plasmon Resonance Sensors. *Acta Biomater.* **2016**, *40*, 100−118.
(11) Vaisocherová, H.; Brynda, E.; Homola, J. Functionalizable Low-Fouling Coatings for Label-Free Biosensing in Complex Biological Media: Advances and Applications. *Anal. Bioanal. Chem.* **2015**, *407*, 3927−3953.
(12) Lowe, S.; O'Brien-Simpson, N. M.; Connal, L. A. Antibiofouling Polymer Interfaces: Poly(ethylene glycol) and Other Promising Candidates. *Polym. Chem.* **2015**, *6*, 198−212.
(13) Emilsson, G.; Schoch, R. L.; Feuz, L.; Höök, F.; Lim, R. Y. H.; Dahlin, A. B. Strongly Stretched Protein Resistant Poly(ethylene glycol) Brushes Prepared by Grafting-To. *ACS Appl. Mater. Interfaces* **2015**, *7*, 7505−7515.
(14) Akbari, A.; Yegani, R.; Pourabbas, B. Synthesis of Poly (ethylene glycol)(PEG) Grafted Silica Nanoparticles with a Minimum Adhesion of Proteins via One-Pot One-Step Method. *Colloids Surf., A* **2015**, *484*, 206−215.
(15) Schlenoff, J. B. Zwitteration: Coating Surfaces with Zwitterionic Functionality to Reduce Nonspecific Adsorption. *Langmuir* **2014**, *30*, 9625−9636.
(16) Izquierdo-Barba, I.; Colilla, M.; Vallet-Regí, M. Zwitterionic Ceramics for Biomedical Applications. *Acta Biomater.* **2016**, *40*, 201−211.
(17) He, M.; Gao, K.; Zhou, L.; Jiao, Z.; Wu, M.; Cao, J.; You, X.; Cai, Z.; Su, Y.; Jiang, Z. Zwitterionic Materials for Antifouling Membrane Surface Construction. *Acta Biomater.* **2016**, *40*, 142−152.

https://dx.doi.org/10.1021/acs.chemrev.9b00739
Chem. Rev. XXXX, XXX, XXX−XXX

(18) Ham, H. O.; Park, S. H.; Kurutz, J. W.; Szleifer, I. G.; Messersmith, P. B. Antifouling Glycocalyx-Mimetic Peptoids. *J. Am. Chem. Soc.* **2013**, *135*, 13015−13022.
(19) Leng, C.; Buss, H. G.; Segalman, R. A.; Chen, Z. Surface Structure and Hydration of Sequence-Specific Amphiphilic Polypeptoids for Antifouling/Fouling Release Applications. *Langmuir* **2015**, *31*, 9306−9311.
(20) Sakala, G. P.; Reches, M. Peptide-Based Approaches to Fight Biofouling. *Adv. Mater. Interfaces* **2018**, *5*, 1800073.
(21) Huang, R.; Liu, X.; Ye, H.; Su, R.; Qi, W.; Wang, L.; He, Z. Conjugation of Hyaluronic Acid onto Surfaces via the Interfacial Polymerization of Dopamine to Prevent Protein Adsorption. *Langmuir* **2015**, *31*, 12061−12070.
(22) Zhang, C.; Liu, S. T.; Tan, L.; Zhu, H. K.; Wang, Y. M. Star-shaped Poly(2-methyl-2-oxazoline)-Based Films: Rapid Preparation and Effects of Polymer Architecture on Antifouling Properties. *J. Mater. Chem. B* **2015**, *3*, 5615−5628.
(23) Weydert, S.; Zurcher, S.; Tanner, S.; Zhang, N.; Ritter, R.; Peter, T.; Aebersold, M. J.; Thompson-Steckel, G.; Forro, C.; Rottmar, M.; et al. Easy to Apply Polyoxazoline-Based Coating for Precise and Long-Term Control of Neural Patterns. *Langmuir* **2017**, *33*, 8594−8605.
(24) Wang, W.; Jayachandran, S.; Li, M.; Xu, S.; Luo, X. Hyaluronic Acid Functionalized Nanostructured Sensing Interface for Voltammetric Determination of microRNA in Biological Media with Ultra-High Sensitivity and Ultra-Low Fouling. *Microchim. Acta* **2018**, *185*, 156.
(25) Caracciolo, G.; Farokhzad, O. C.; Mahmoudi, M. Biological Identity of Nanoparticles in Vivo: Clinical Implications of the Protein Corona. *Trends Biotechnol.* **2017**, *35*, 257−264.
(26) Bertrand, N.; Grenier, P.; Mahmoudi, M.; Lima, E. M.; Appel, E. A.; Dormont, F.; Lim, J.-M.; Karnik, R.; Langer, R.; Farokhzad, O. C. Mechanistic Understanding of in Vivo Protein Corona Formation on Polymeric Nanoparticles and Impact on Pharmacokinetics. *Nat. Commun.* **2017**, *8*, 777.
(27) Chen, S.; Cao, Z.; Jiang, S. Ultra-Low Fouling Peptide Surfaces Derived from Natural Amino Acids. *Biomaterials* **2009**, *30*, 5892−5896.
(28) Blackman, L. D.; Gunatillake, P. A.; Cass, P.; Locock, K. E. S. An Introduction to Zwitterionic Polymer Behavior and Applications in Solution and at Surfaces. *Chem. Soc. Rev.* **2019**, *48*, 757−770.
(29) Baggerman, J.; Smulders, M. M. J.; Zuilhof, H. Romantic Surfaces: A Systematic Overview of Stable, Biospecific, and Antifouling Zwitterionic Surfaces. *Langmuir* **2019**, *35*, 1072−1084.
(30) Hakobyan, S.; Rzhepishevska, O.; Barbero, D. R.; Ramstedt, M. Functionalization of Zwitterionic Polymer Brushes, Do They Remain Antifouling? *Surf. Interface Anal.* **2018**, *50*, 1001−1006.
(31) Leckband, D.; Sheth, S.; Halperin, A. Grafted Poly (ethylene oxide) Brushes as Nonfouling Surface Coatings. *J. Biomater. Sci., Polym. Ed.* **1999**, *10*, 1125−1147.
(32) Kruis, I. C.; Lowik, D.; Boelens, W. C.; van Hest, J. C. M.; Pruijn, G. J. M. An Integrated, Peptide-Based Approach to Site-Specific Protein Immobilization for Detection of Biomolecular Interactions. *Analyst* **2016**, *141*, 5321−5328.
(33) Cui, M.; Wang, Y.; Wang, H.; Wu, Y.; Luo, X. A Label-Free Electrochemical DNA Biosensor for Breast Cancer Marker BRCA1 Based on Self-Assembled Antifouling Peptide Monolayer. *Sens. Actuators, B* **2017**, *244*, 742−749.
(34) Nowinski, A. K.; Sun, F.; White, A. D.; Keefe, A. J.; Jiang, S. Sequence, Structure, and Function of Peptide Self-Assembled Monolayers. *J. Am. Chem. Soc.* **2012**, *134*, 6000−6005.
(35) Kuo, T. M.; Shen, M. Y.; Huang, S. Y.; Li, Y. K.; Chuang, M. C. Facile Fabrication of a Sensor with a Bifunctional Interface for Logic Analysis of the New Delhi Metallo-β-Lactamase (NDM)-Coding Gene. *ACS. Sens.* **2016**, *1*, 124−130.
(36) Jiang, C.; Alam, M. T.; Parker, S. G.; Darwish, N.; Gooding, J. J. Strategies To Achieve Control over the Surface Ratio of Two Different Components on Modified Electrodes Using Aryldiazonium Salts. *Langmuir* **2016**, *32*, 2509−2517.
(37) Wang, J.; Hui, N. A Nonfouling Voltammetric Immunosensor for the Carcinoembryonic Antigen based on the Use of Polyaniline Nanowires Wrapped with Hyaluronic Acid. *Microchim. Acta* **2018**, *185*, 329.
(38) Hui, N.; Sun, X. T.; Niu, S. Y.; Luo, X. L. PEGylated Polyaniline Nanofibers: Antifouling and Conducting Biomaterial for Electrochemical DNA Sensing. *ACS Appl. Mater. Interfaces* **2017**, *9*, 2914−2923.
(39) Vaisocherova-Lisalova, H.; Visova, I.; Ermini, M. L.; Springer, T.; Song, X. C.; Mrazek, J.; Lamacova, J.; Lynn, N. S.; Sedivak, P.; Homola, J. Low-Fouling Surface Plasmon Resonance Biosensor for Multi-Step Detection of Foodborne Bacterial Pathogens in Complex Food Samples. *Biosens. Bioelectron.* **2016**, *80*, 84−90.
(40) Vaisocherova-Lisalova, H.; Surman, F.; Visova, I.; Vala, M.; Springer, T.; Ermini, M. L.; Sipova, H.; Sedivak, P.; Houska, M.; Riedel, T.; et al. Copolymer Brush-Based Ultralow-Fouling Biorecognition Surface Platform for Food Safety. *Anal. Chem.* **2016**, *88*, 10533−10539.
(41) Vaisocherova, H.; Sipova, H.; Visova, I.; Bockova, M.; Springer, T.; Ermini, M. L.; Song, X.; Krejcik, Z.; Chrastinova, L.; Pastva, O.; et al. Rapid and Sensitive Detection of Multiple MicroRNAs in Cell Lysate by Low-fouling Surface Plasmon Resonance Biosensor. *Biosens. Bioelectron.* **2015**, *70*, 226−231.
(42) Riedel, T.; Surman, F.; Hageneder, S.; Pop-Georgievski, O.; Noehammer, C.; Hofner, M.; Brynda, E.; Rodriguez-Emmenegger, C.; Dostalek, J. Hepatitis B Plasmonic Biosensor for the Analysis of Clinical Serum Samples. *Biosens. Bioelectron.* **2016**, *85*, 272−279.
(43) Riedel, T.; Hageneder, S.; Surman, F.; Pop-Georgievski, O.; Noehammer, C.; Hofner, M.; Brynda, E.; Rodriguez-Emmenegger, C.; Dostálek, J. Plasmonic Hepatitis B Biosensor for the Analysis of Clinical Saliva. *Anal. Chem.* **2017**, *89*, 2972−2977.
(44) Shen, W.; Chang, Y.; Liu, G.; Wang, H.; Cao, A.; An, Z. Biocompatible, Antifouling, and Thermosensitive Core−Shell Nanogels Synthesized by RAFT Aqueous Dispersion Polymerization. *Macromolecules* **2011**, *44*, 2524−2530.
(45) Kitano, H.; Kondo, T.; Kamada, T.; Iwanaga, S.; Nakamura, M.; Ohno, K. Anti-biofouling Properties of an Amphoteric Polymer Brush Constructed on a Glass Substrate. *Colloids Surf., B* **2011**, *88*, 455−462.
(46) Lin, P.; Chuang, T.-L.; Chen, P. Z.; Lin, C.-W.; Gu, F. X. Low-Fouling Characteristics of Ultrathin Zwitterionic Cysteine SAMs. *Langmuir* **2019**, *35*, 1756−1767.
(47) Bryan, T.; Luo, X.; Forsgren, L.; Morozova-Roche, L. A.; Davis, J. J. The Robust Electrochemical Detection of a Parkinson's Disease Marker in Whole Blood Sera. *Chem. Sci.* **2012**, *3*, 3468−3473.
(48) Li, Q.; Imbrogno, J.; Belfort, G.; Wang, X.-L. Making Polymeric Membranes Antifouling via "Grafting from" Polymerization of Zwitterions. *J. Appl. Polym. Sci.* **2015**, *132*, 41781.
(49) Sin, M.-C.; Chen, S.-H.; Chang, Y. Hemocompatibility of Zwitterionic Interfaces and Membranes. *Polym. J.* **2014**, *46*, 436.
(50) Heggestad, J. T.; Fontes, C. M.; Joh, D. Y.; Hucknall, A. M.; Chilkoti, A. In Pursuit of Zero 2.0: Recent Developments in Nonfouling Polymer Brushes for Immunoassays. *Adv. Mater.* **2020**, *32*, 1903285.
(51) Cao, C.; Zhang, Y.; Jiang, C.; Qi, M.; Liu, G. Advances on Aryldiazonium Salt Chemistry Based Interfacial Fabrication for Sensing Applications. *ACS Appl. Mater. Interfaces* **2017**, *9*, 5031−5049.
(52) Pinson, J.; Podvorica, F. Attachment of Organic Layers to Conductive or Semiconductive Surfaces by Reduction of Diazonium Salts. *Chem. Soc. Rev.* **2005**, *34*, 429−439.
(53) Liu, G.; Böcking, T.; Gooding, J. J. Diazonium salts: Stable Monolayers on Gold Electrodes for Sensing Applications. *J. Electroanal. Chem.* **2007**, *600*, 335−344.
(54) Jiang, C.; Alam, M. T.; Silva, S. M.; Taufik, S.; Fan, S.; Gooding, J. J. Unique Sensing Interface That Allows the Development of an Electrochemical Immunosensor for the Detection of Tumor Necrosis Factor α in Whole Blood. *ACS. Sens.* **2016**, *1*, 1432−1438.

https://dx.doi.org/10.1021/acs.chemrev.9b00739
Chem. Rev. XXXX, XXX, XXX−XXX

(55) Khor, S. M.; Liu, G.; Fairman, C.; Iyengar, S. G.; Gooding, J. J. The Importance of Interfacial Design for the Sensitivity of a Label-free Electrochemical Immuno-Biosensor for Small Organic Molecules. *Biosens. Bioelectron.* **2011**, *26*, 2038−2044.
(56) Jiang, C.; Silva, S. M.; Fan, S.; Wu, Y.; Alam, M. T.; Liu, G.; Gooding, J. J. Aryldiazonium Salt Derived Mixed Organic Layers: From Surface Chemistry to their Applications. *J. Electroanal. Chem.* **2017**, *785*, 265−278.
(57) Jiang, C.; Tanzirul Alam, M.; Parker, S. G.; Gooding, J. J. Zwitterionic Phenyl Phosphorylcholine on Indium Tin Oxide: a Low-Impedance Protein-Resistant Platform for Biosensing. *Electroanalysis* **2015**, *27*, 884−889.
(58) Chen, S.; Li, L.; Zhao, C.; Zheng, J. Surface Hydration: Principles and Applications toward Low-Fouling/Nonfouling Biomaterials. *Polymer* **2010**, *51*, 5283−5293.
(59) Zhang, K.; Huang, H.; Hung, H.-C.; Leng, C.; Wei, S.; Crisci, R.; Jiang, S.; Chen, Z. Strong Hydration at the Poly(ethylene glycol) Brush/Albumin Solution Interface. *Langmuir* **2020**, *36*, 2030−2036.
(60) Chen, S.; Zheng, J.; Li, L.; Jiang, S. Strong Resistance of Phosphorylcholine Self-Assembled Monolayers to Protein Adsorption: Insights into Nonfouling Properties of Zwitterionic Materials. *J. Am. Chem. Soc.* **2005**, *127*, 14473−14478.
(61) Shao, Q.; Jiang, S. Molecular Understanding and Design of Zwitterionic Materials. *Adv. Mater.* **2015**, *27*, 15−26.
(62) Zhang, Y.; Liu, Y.; Ren, B.; Zhang, D.; Xie, S.; Chang, Y.; Yang, J.; Wu, J.; Xu, L.; Zheng, J. Fundamentals and Applications of Zwitterionic Antifouling Polymers. *J. Phys. D: Appl. Phys.* **2019**, *52*, 403001.
(63) Wu, J.; Lin, W.; Wang, Z.; Chen, S.; Chang, Y. Investigation of the Hydration of Nonfouling Material Poly(sulfobetaine methacrylate) by Low-Field Nuclear Magnetic Resonance. *Langmuir* **2012**, *28*, 7436−7441.
(64) Wu, J.; Chen, S. Investigation of the Hydration of Nonfouling Material Poly(ethylene glycol) by Low-Field Nuclear Magnetic Resonance. *Langmuir* **2012**, *28*, 2137−2144.
(65) Baumgartner, S.; Lahajnar, G.; Sepe, A.; Kristl, J. Quantitative Evaluation of Polymer Concentration Profile during Swelling of Hydrophilic Matrix Tablets Using 1H NMR and MRI Methods. *Eur. J. Pharm. Biopharm.* **2005**, *59*, 299−306.
(66) Perry, A.; Neipert, C.; Space, B.; Moore, P. B. Theoretical Modeling of Interface Specific Vibrational Spectroscopy: Methods and Applications to Aqueous Interfaces. *Chem. Rev.* **2006**, *106*, 1234−1258.
(67) Nagasawa, D.; Azuma, T.; Noguchi, H.; Uosaki, K.; Takai, M. Role of Interfacial Water in Protein Adsorption onto Polymer Brushes as Studied by SFG Spectroscopy and QCM. *J. Phys. Chem. C* **2015**, *119*, 17193−17201.
(68) Wang, H.-F. Sum Frequency Generation Vibrational Spectroscopy (SFG-VS) for Complex Molecular Surfaces and Interfaces: Spectral Lineshape Measurement and Analysis Plus Some Controversial Issues. *Prog. Surf. Sci.* **2016**, *91*, 155−182.
(69) Leng, C.; Hung, H.-C.; Sieggreen, O. A.; Li, Y.; Jiang, S.; Chen, Z. Probing the Surface Hydration of Nonfouling Zwitterionic and Poly(ethylene glycol) Materials with Isotopic Dilution Spectroscopy. *J. Phys. Chem. C* **2015**, *119*, 8775−8780.
(70) Leng, C.; Hung, H.-C.; Sun, S.; Wang, D.; Li, Y.; Jiang, S.; Chen, Z. Probing the Surface Hydration of Nonfouling Zwitterionic and PEG Materials in Contact with Proteins. *ACS Appl. Mater. Interfaces* **2015**, *7*, 16881−16888.
(71) Hankett, J. M.; Liu, Y.; Zhang, X.; Zhang, C.; Chen, Z. Molecular Level Studies of Polymer Behaviors at the Water Interface Using Sum Frequency Generation Vibrational Spectroscopy. *J. Polym. Sci., Part B: Polym. Phys.* **2013**, *51*, 311−328.
(72) Leng, C.; Sun, S.; Zhang, K.; Jiang, S.; Chen, Z. Molecular Level Studies on Interfacial Hydration of Zwitterionic and Other Antifouling Polymers in Situ. *Acta Biomater.* **2016**, *40*, 6−15.
(73) Leung, B. O.; Yang, Z.; Wu, S. S. H.; Chou, K. C. Role of Interfacial Water on Protein Adsorption at Cross-Linked Polyethylene Oxide Interfaces. *Langmuir* **2012**, *28*, 5724−5728.
(74) Ziemba, C.; Khavkin, M.; Priftis, D.; Acar, H.; Mao, J.; Benami, M.; Gottlieb, M.; Tirrell, M.; Kaufman, Y.; Herzberg, M. Antifouling Properties of a Self-Assembling Glutamic Acid-Lysine Zwitterionic Polymer Surface Coating. *Langmuir* **2019**, *35*, 1699−1713.
(75) Wang, R. Y.; Himmelhaus, M.; Fick, J.; Herrwerth, S.; Eck, W.; Grunze, M. Interaction of Self-Assembled Monolayers of Oligo(ethylene glycol)-Terminated Alkanethiols with Water Studied by Vibrational Sum-Frequency Generation. *J. Chem. Phys.* **2005**, *122*, 164702.
(76) Han, X.; Leng, C.; Shao, Q.; Jiang, S.; Chen, Z. Absolute Orientations of Water Molecules at Zwitterionic Polymer Interfaces and Interfacial Dynamics after Salt Exposure. *Langmuir* **2019**, *35*, 1327−1334.
(77) Zhang, C.; Parada, G. A.; Zhao, X.; Chen, Z. Probing Surface Hydration and Molecular Structure of Zwitterionic and Polyacrylamide Hydrogels. *Langmuir* **2019**, *35*, 13292−13300.
(78) Leng, C.; Huang, H.; Zhang, K.; Hung, H.-C.; Xu, Y.; Li, Y.; Jiang, S.; Chen, Z. Effect of Surface Hydration on Antifouling Properties of Mixed Charged Polymers. *Langmuir* **2018**, *34*, 6538−6545.
(79) Jeon, S. I.; Lee, J. H.; Andrade, J. D.; De Gennes, P. G. Protein—Surface Interactions in the Presence of Polyethylene Oxide: I. Simplified Theory. *J. Colloid Interface Sci.* **1991**, *142*, 149−158.
(80) Zheng, J.; Li, L.; Tsao, H.-K.; Sheng, Y.-J.; Chen, S.; Jiang, S. Strong Repulsive Forces between Protein and Oligo (ethylene glycol) Self-Assembled Monolayers: A Molecular Simulation Study. *Biophys. J.* **2005**, *89*, 158−166.
(81) He, Y.; Hower, J.; Chen, S.; Bernards, M. T.; Chang, Y.; Jiang, S. Molecular Simulation Studies of Protein Interactions with Zwitterionic Phosphorylcholine Self-Assembled Monolayers in the Presence of Water. *Langmuir* **2008**, *24*, 10358−10364.
(82) Shao, Q.; He, Y.; White, A. D.; Jiang, S. Difference in Hydration between Carboxybetaine and Sulfobetaine. *J. Phys. Chem. B* **2010**, *114*, 16625−16631.
(83) Shao, Q.; Mi, L.; Han, X.; Bai, T.; Liu, S.; Li, Y.; Jiang, S. Differences in Cationic and Anionic Charge Densities Dictate Zwitterionic Associations and Stimuli Responses. *J. Phys. Chem. B* **2014**, *118*, 6956−6962.
(84) Xie, Y.; Pan, Y.; Zhang, R.; Liang, Y.; Li, Z. Modulating Protein Behaviors on Responsive Surface by External Electric Fields: A Molecular Dynamics Study. *Appl. Surf. Sci.* **2015**, *326*, 55−65.
(85) Rabe, M.; Verdes, D.; Seeger, S. Understanding Protein Adsorption Phenomena at Solid Surfaces. *Adv. Colloid Interface Sci.* **2011**, *162*, 87−106.
(86) Zhang, Z.; Zhang, M.; Chen, S.; Horbett, T. A.; Ratner, B. D.; Jiang, S. Blood Compatibility of Surfaces with Superlow Protein Adsorption. *Biomaterials* **2008**, *29*, 4285−4291.
(87) Sun, F.; Hung, H.-C.; Sinclair, A.; Zhang, P.; Bai, T.; Galvan, D. D.; Jain, P.; Li, B.; Jiang, S.; Yu, Q. Hierarchical Zwitterionic Modification of A SERS Substrate Enables Real-Time Drug Monitoring in Blood Plasma. *Nat. Commun.* **2016**, *7*, 13437.
(88) Gui, A. L.; Luais, E.; Peterson, J. R.; Gooding, J. J. Zwitterionic Phenyl Layers: Finally, Stable, Anti-Biofouling Coatings That Do Not Passivate Electrodes. *ACS Appl. Mater. Interfaces* **2013**, *5*, 4827−4835.
(89) Darwish, N. T.; Alias, Y.; Khor, S. M. Indium Tin Oxide with Zwitterionic Interfacial Design for Biosensing Applications in Complex Matrices. *Appl. Surf. Sci.* **2015**, *325*, 91−99.
(90) Taufik, S.; Barfidokht, A.; Alam, M. T.; Jiang, C.; Parker, S. G.; Gooding, J. J. An Antifouling Electrode Based on Electrode−Organic Layer−Nanoparticle Constructs: Electrodeposited Organic Layers Versus Self-Assembled Monolayers. *J. Electroanal. Chem.* **2016**, *779*, 229−235.
(91) Parviz, M.; Darwish, N.; Alam, M. T.; Parker, S. G.; Ciampi, S.; Gooding, J. J. Investigation of the Antifouling Properties of Phenyl Phosphorylcholine-Based Modified Gold Surfaces. *Electroanalysis* **2014**, *26*, 1471−1480.
(92) Zhang, Y. X.; Islam, N.; Carbonell, R. G.; Rojas, O. J. Specific Binding of Immunoglobulin G with Bioactive Short Peptides Supported on Antifouling Copolymer Layers for Detection in Quartz

https://dx.doi.org/10.1021/acs.chemrev.9b00739
Chem. Rev. XXXX, XXX, XXX−XXX

Crystal Microgravimetry and Surface Plasmon Resonance. *Anal. Chem.* **2013**, *85*, 1106−1113.
(93) Cao, B.; Lee, C. J.; Zeng, Z. P.; Cheng, F.; Xu, F. J.; Cong, H. B.; Cheng, G. Electroactive poly(sulfobetaine-3,4-ethylenedioxythiophene) (PSBEDOT) with Controllable Antifouling and Antimicrobial Properties. *Chem. Sci.* **2016**, *7*, 1976−1981.
(94) Huang, C.-J.; Wang, L.-C.; Liu, C.-Y.; Chiang, A. S.; Chang, Y.-C. Natural Zwitterionic Organosulfurs as Surface Ligands for Antifouling and Responsive Properties. *Biointerphases* **2014**, *9*, No. 029010.
(95) Luan, Y.; Li, D.; Wei, T.; Wang, M.; Tang, Z.; Brash, J. L.; Chen, H. Hearing Loss" in QCM Measurement of Protein Adsorption to Protein Resistant Polymer Brush Layers. *Anal. Chem.* **2017**, *89*, 4184−4191.
(96) Ogi, H.; Fukunishi, Y.; Nagai, H.; Okamoto, K.; Hirao, M.; Nishiyama, M. Nonspecific-Adsorption Behavior of Polyethylenglycol and Bovine Serum Albumin Studied by 55-MHz Wireless−Electrodeless Quartz Crystal Microbalance. *Biosens. Bioelectron.* **2009**, *24*, 3148−3152.
(97) Jin, J.; Han, Y.; Zhang, C.; Liu, J.; Jiang, W.; Yin, J.; Liang, H. Effect of Grafted PEG Chain Conformation on Albumin and Lysozyme Adsorption: A Combined Study Using QCM-D and DPI. *Colloids Surf., B* **2015**, *136*, 838−844.
(98) Li, B.-R.; Shen, M.-Y.; Yu, H.-h.; Li, Y.-K. Rapid Construction of An Effective Antifouling Layer on a Au Surface via Electrodeposition. *Chem. Commun.* **2014**, *50*, 6793−6796.
(99) Cui, J.; Ju, Y.; Liang, K.; Ejima, H.; Lörcher, S.; Gause, K. T.; Richardson, J. J.; Caruso, F. Nanoscale Engineering of Low-Fouling Surfaces through Polydopamine Immobilisation of Zwitterionic Peptides. *Soft Matter* **2014**, *10*, 2656−2663.
(100) Bahadır, E. B.; Sezgintürk, M. K. A Review on Impedimetric Biosensors. *Artif. Cells, Nanomed., Biotechnol.* **2016**, *44*, 248−262.
(101) Xu, Q.; Cheng, H.; Lehr, J.; Patil, A. V.; Davis, J. J. Graphene Oxide Interfaces in Serum Based Autoantibody Quantification. *Anal. Chem.* **2015**, *87*, 346−350.
(102) Luo, X.; Xu, M.; Freeman, C.; James, T.; Davis, J. J. Ultrasensitive Label Free Electrical Detection of Insulin in Neat Blood Serum. *Anal. Chem.* **2013**, *85*, 4129−4134.
(103) Piccoli, J.; Hein, R.; El-Sagheer, A. H.; Brown, T.; Cilli, E. M.; Bueno, P. R.; Davis, J. J. Redox Capacitive Assaying of C-Reactive Protein at a Peptide Supported Aptamer Interface. *Anal. Chem.* **2018**, *90*, 3005−3008.
(104) Wang, G.; Xu, Q.; Liu, L.; Su, X.; Lin, J.; Xu, G.; Luo, X. Mixed Self-Assembly of Polyethylene Glycol and Aptamer on Polydopamine Surface for Highly Sensitive and Low-Fouling Detection of Adenosine Triphosphate in Complex Media. *ACS Appl. Mater. Interfaces* **2017**, *9*, 31153−31160.
(105) Wang, G.; Su, X.; Xu, Q.; Xu, G.; Lin, J.; Luo, X. Antifouling Aptasensor for the Detection of Adenosine Triphosphate in Biological Media Based on Mixed Self-Assembled Aptamer and Zwitterionic Peptide. *Biosens. Bioelectron.* **2018**, *101*, 129−134.
(106) Howes, P. D.; Chandrawati, R.; Stevens, M. M. Colloidal Nanoparticles as Advanced Biological Sensors. *Science* **2014**, *346*, 1247390.
(107) Wang, H.; Cheng, F.; Shen, W.; Cheng, G.; Zhao, J.; Peng, W.; Qu, J. Amino Acid-Based Anti-fouling Functionalization of Silica Nanoparticles Using Divinyl Sulfone. *Acta Biomater.* **2016**, *40*, 273−281.
(108) Sanchez-Salcedo, S.; Vallet-Regí, M.; Shanin, S. A.; Glackin, C. A.; Zink, J. I. Mesoporous Core-shell Silica Nanoparticles with Antifouling Properties for Ovarian Cancer Therapy. *Chem. Eng. J.* **2018**, *340*, 114−124.
(109) Affonso de Oliveira, J. F.; Scheffer, F. R.; Landis, R. F.; Teixeira Neto, É.; Rotello, V. M.; Cardoso, M. B. Dual Functionalization of Nanoparticles for Generating Corona-Free and Noncytotoxic Silica Nanoparticles. *ACS Appl. Mater. Interfaces* **2018**, *10*, 41917−41923.
(110) Cheng, F.; Zhu, C.; He, W.; Zhao, J.; Qu, J. pSBMA-Conjugated Magnetic Nanoparticles for Selective IgG Separation. *Langmuir* **2019**, *35*, 1111−1118.
(111) Kang, S.; Lee, M.; Kang, M.; Noh, M.; Jeon, J.; Lee, Y.; Seo, J.-H. Development of Anti-biofouling Interface on Hydroxyapatite Surface by Coating Zwitterionic MPC Polymer Containing Calcium-Binding Moieties to Prevent Oral Bacterial Adhesion. *Acta Biomater.* **2016**, *40*, 70−77.
(112) Estupiñán, D.; Bannwarth, M. B.; Mylon, S. E.; Landfester, K.; Muñoz-Espí, R.; Crespy, D. Multifunctional Clickable and Protein-Repellent Magnetic Silica Nanoparticles. *Nanoscale* **2016**, *8*, 3019−3030.
(113) Hu, F.; Chen, K.; Xu, H.; Gu, H. Design and Preparation of Bi-Functionalized Short-Chain Modified Zwitterionic Nanoparticles. *Acta Biomater.* **2018**, *72*, 239−247.
(114) Rodriguez-Emmenegger, C.; Hasan, E.; Pop-Georgievski, O.; Houska, M.; Brynda, E.; Alles, A. B. Controlled/Living Surface-Initiated ATRP of Antifouling Polymer Brushes from Gold in PBS and Blood Sera as a Model Study for Polymer Modifications in Complex Biological Media. *Macromol. Biosci.* **2012**, *12*, 525−532.
(115) Hui, N.; Sun, X.; Song, Z.; Niu, S.; Luo, X. Gold Nanoparticles and Polyethylene Glycols Functionalized Conducting Polyaniline Nanowires for Ultrasensitive and Low fouling Immunosensing of Alpha-Fetoprotein. *Biosens. Bioelectron.* **2016**, *86*, 143−149.
(116) Chen, C.-H.; Luo, S.-C. Tuning Surface Charge and Morphology for the Efficient Detection of Dopamine under the Interferences of Uric Acid, Ascorbic Acid, and Protein Adsorption. *ACS Appl. Mater. Interfaces* **2015**, *7*, 21931−21938.
(117) Paloni, J. M.; Dong, X.-H.; Olsen, B. D. Protein−Polymer Block Copolymer Thin Films for Highly Sensitive Detection of Small Proteins in Biological Fluids. *ACS. Sens.* **2019**, *4*, 2869−2878.
(118) Liu, D.; Xie, Y.; Shao, H.; Jiang, X. Using Azobenzene-Embedded Self-Assembled Monolayers To Photochemically Control Cell Adhesion Reversibly. *Angew. Chem., Int. Ed.* **2009**, *48*, 4406−4408.
(119) Ng, C. C. A.; Magenau, A.; Ngalim, S. H.; Ciampi, S.; Chockalingham, M.; Harper, J. B.; Gaus, K.; Gooding, J. J. Using an Electrical Potential to Reversibly Switch Surfaces between Two States for Dynamically Controlling Cell Adhesion. *Angew. Chem.* **2012**, *124*, 7826−7830.
(120) Demirci, S.; Kinali-Demirci, S.; Jiang, S. A Switchable Polymer Brush System for Antifouling and Controlled Detection. *Chem. Commun.* **2017**, *53*, 3713−3716.
(121) Ostuni, E.; Chapman, R. G.; Holmlin, R. E.; Shuichi Takayama, A.; Whitesides, G. M. A Survey of Structure−Property Relationships of Surfaces that Resist the Adsorption of Protein. *Langmuir* **2001**, *17*, 5605−5620.
(122) Castiello, F. R.; Tabrizian, M. Multiplex Surface Plasmon Resonance Imaging-Based Biosensor for Human Pancreatic Islets Hormones Quantification. *Anal. Chem.* **2018**, *90*, 3132−3139.
(123) Xu, M.; Luo, X.; Davis, J. J. The Label Free Picomolar Detection of Insulin in Blood Serum. *Biosens. Bioelectron.* **2013**, *39*, 21−25.
(124) Xu, Q.; Evetts, S.; Hu, M.; Talbot, K.; Wade-Martins, R.; Davis, J. J. An Impedimetric Assay of α-Synuclein Autoantibodies in Early Stage Parkinson's Disease. *RSC Adv.* **2014**, *4*, 58773−58777.
(125) Patil, A. V.; Bedatty Fernandes, F. C.; Bueno, P. R.; Davis, J. J. Immittance Electroanalysis in Diagnostics. *Anal. Chem.* **2015**, *87*, 944−950.
(126) Bryan, T.; Luo, X.; Bueno, P. R.; Davis, J. J. An Optimised Electrochemical Biosensor for the Label-Free Detection of C-Reactive Protein in Blood. *Biosens. Bioelectron.* **2013**, *39*, 94−98.
(127) Johnson, A.; Song, Q.; Ko Ferrigno, P.; Bueno, P. R.; Davis, J. J. Sensitive Affimer and Antibody Based Impedimetric Label-Free Assays for C-Reactive Protein. *Anal. Chem.* **2012**, *84*, 6553−6560.
(128) Bedatty Fernandes, F. C.; Patil, A. V.; Bueno, P. R.; Davis, J. J. Optimized Diagnostic Assays Based on Redox Tagged Bioreceptive Interfaces. *Anal. Chem.* **2015**, *87*, 12137−12144.

https://dx.doi.org/10.1021/acs.chemrev.9b00739
Chem. Rev. XXXX, XXX, XXX−XXX

(129) Li, Q.; Tofaris, G. K.; Davis, J. J. Concentration-Normalized Electroanalytical Assaying of Exosomal Markers. *Anal. Chem.* **2017**, *89*, 3184−3190.
(130) Santos, A.; Bueno, P. R.; Davis, J. J. A Dual Marker Label Free Electrochemical Assay for Flavivirus Dengue Diagnosis. *Biosens. Bioelectron.* **2018**, *100*, 519−525.
(131) Luo, X.; Xu, Q.; James, T.; Davis, J. J. Redox and Label-Free Array Detection of Protein Markers in Human Serum. *Anal. Chem.* **2014**, *86*, 5553−5558.
(132) Liu, G.; Khor, S. M.; Iyengar, S. G.; Gooding, J. J. Development of an Electrochemical Immunosensor for the Detection of HbA1c in Serum. *Analyst* **2012**, *137*, 829−832.
(133) Kaur, J.; Jiang, C.; Liu, G. Different Strategies for Detection of HbA1c Emphasizing on Biosensors and Point-of-Care Analyzers. *Biosens. Bioelectron.* **2019**, *123*, 85−100.
(134) Wang, W.; Fan, X.; Xu, S.; Davis, J. J.; Luo, X. Low Fouling Label-Free DNA Sensor Based on Polyethylene Glycols Decorated with Gold Nanoparticles for the Detection of Breast Cancer Biomarkers. *Biosens. Bioelectron.* **2015**, *71*, 51−56.
(135) Chen, L.; Liu, X.; Chen, C. Impedimetric Biosensor Modified with Hydrophilic Material of Tannic Acid/Polyethylene Glycol and Dopamine-Assisted Deposition for Detection of Breast Cancer-Related BRCA1 Gene. *J. Electroanal. Chem.* **2017**, *791*, 204−210.
(136) Chen, L.; Lv, S.; Liu, M.; Chen, C.; Sheng, J.; Luo, X. Low-Fouling Magnetic Nanoparticles and Evaluation of Their Potential Application as Disease Markers Assay in Whole Serum. *ACS. Appl. Nano. Mater.* **2018**, *1*, 2489−2495.
(137) Rana, S.; Le, N. D. B.; Mout, R.; Duncan, B.; Elci, S. G.; Saha, K.; Rotello, V. M. A Multichannel Biosensor for Rapid Determination of Cell Surface Glycomic Signatures. *ACS Cent. Sci.* **2015**, *1*, 191−197.
(138) Geng, Y.; Peveler, W. J.; Rotello, V. M. Array-Based "Chemical Nose" Sensing in Diagnostics and Drug Discovery. *Angew. Chem., Int. Ed.* **2019**, *58*, 5190−5200.
(139) De, M.; Rana, S.; Akpinar, H.; Miranda, O. R.; Arvizo, R. R.; Bunz, U. H. F.; Rotello, V. M. Sensing of Proteins in Human Serum Using Conjugates of Nanoparticles and Green Fluorescent Protein. *Nat. Chem.* **2009**, *1*, 461−465.
(140) Miranda, O. R.; Li, X.; Garcia-Gonzalez, L.; Zhu, Z.-J.; Yan, B.; Bunz, U. H. F.; Rotello, V. M. Colorimetric Bacteria Sensing Using a Supramolecular Enzyme−Nanoparticle Biosensor. *J. Am. Chem. Soc.* **2011**, *133*, 9650−9653.
(141) Rana, S.; Le, N. D. B.; Mout, R.; Saha, K.; Tonga, G. Y.; Bain, R. E. S.; Miranda, O. R.; Rotello, C. M.; Rotello, V. M. A Multichannel Nanosensor for Instantaneous Readout of Cancer Drug Mechanisms. *Nat. Nanotechnol.* **2015**, *10*, 65.
(142) Chuah, K.; Wu, Y.; Vivekchand, S. R. C.; Gaus, K.; Reece, P. J.; Micolich, A. P.; Gooding, J. J. Nanopore Blockade Sensors for Ultrasensitive Detection of Proteins in Complex Biological Samples. *Nat. Commun.* **2019**, *10*, 2109.
(143) Wu, Y.; Bennett, D.; Tilley, R. D.; Gooding, J. J. How Nanoparticles Transform Single Molecule Measurements into Quantitative Sensors. *Adv. Mater.* **2019**, *0*, 1904339.
(144) Wu, Y.; Tilley, R. D.; Gooding, J. J. Challenges and Solutions in Developing Ultrasensitive Biosensors. *J. Am. Chem. Soc.* **2019**, *141*, 1162−1170.
(145) Giamblanco, N.; Coglitore, D.; Janot, J.-M.; Coulon, P. E.; Charlot, B.; Balme, S. Detection of Protein Aggregate Morphology through Single Antifouling Nanopore. *Sens. Actuators, B* **2018**, *260*, 736−745.
(146) Pidhatika, B.; Rodenstein, M.; Chen, Y.; Rakhmatullina, E.; Mühlebach, A.; Acikgöz, C.; Textor, M.; Konradi, R. Comparative Stability Studies of Poly(2-methyl-2-oxazoline) and Poly(ethylene glycol) Brush Coatings. *Biointerphases* **2012**, *7*, 1.
(147) Du, Y.; Gao, J. Y.; Chen, T. T.; Zhang, C.; Ji, J.; Xu, Z. K. Understanding the Oxidative Stability of Antifouling Polymer Brushes. *Langmuir* **2017**, *33*, 7298−7304.
(148) Li, L.; Chen, S.; Jiang, S. Protein Interactions with Oligo(ethylene glycol) (OEG) Self-Assembled Monolayers: OEG Stability, Surface Packing Density and Protein Adsorption. *J. Biomater. Sci., Polym. Ed.* **2007**, *18*, 1415−1427.
(149) Ong, C. S.; Al-anzi, B.; Lau, W. J.; Goh, P. S.; Lai, G. S.; Ismail, A. F.; Ong, Y. S. Anti-Fouling Double-Skinned Forward Osmosis Membrane with Zwitterionic Brush for Oily Wastewater Treatment. *Sci. Rep.* **2017**, *7*, 6904.
(150) Bai, T.; Sun, F.; Zhang, L.; Sinclair, A.; Liu, S. J.; Ella-Menye, J. R.; Zheng, Y.; Jiang, S. Y. Restraint of the Differentiation of Mesenchymal Stem Cells by a Nonfouling Zwitterionic Hydrogel. *Angew. Chem., Int. Ed.* **2014**, *53*, 12729−12734.
(151) Estephan, Z. G.; Schlenoff, P. S.; Schlenoff, J. B. Zwitteration as an Alternative to PEGylation. *Langmuir* **2011**, *27*, 6794−6800.
(152) Rodriguez Emmenegger, C.; Brynda, E.; Riedel, T.; Sedlakova, Z.; Houska, M.; Alles, A. B. Interaction of Blood Plasma with Antifouling Surfaces. *Langmuir* **2009**, *25*, 6328−6333.
(153) Konai, M. M.; Bhattacharjee, B.; Ghosh, S.; Haldar, J. Recent Progress in Polymer Research to Tackle Infections and Antimicrobial Resistance. *Biomacromolecules* **2018**, *19*, 1888−1917.
(154) Le, N. L.; Ulbricht, M.; Nunes, S. P. How Do Polyethylene Glycol and Poly(sulfobetaine) Hydrogel Layers on Ultrafiltration Membranes Minimize Fouling and Stay Stable in Cleaning Chemicals? *Ind. Eng. Chem. Res.* **2017**, *56*, 6785−6795.
(155) Chang, Y.; Shih, Y. J.; Lai, C. J.; Kung, H. H.; Jiang, S. Y. Blood-Inert Surfaces via Ion-Pair Anchoring of Zwitterionic Copolymer Brushes in Human Whole Blood. *Adv. Funct. Mater.* **2013**, *23*, 1100−1110.
(156) Zhu, Y.; Xu, X.; Brault, N. D.; Keefe, A. J.; Han, X.; Deng, Y.; Xu, J.; Yu, Q.; Jiang, S. Cellulose Paper Sensors Modified with Zwitterionic Poly(carboxybetaine) for Sensing and Detection in Complex Media. *Anal. Chem.* **2014**, *86*, 2871−2875.
(157) Sam, S.; Touahir, L.; Salvador Andresa, J.; Allongue, P.; Chazalviel, J. N.; Gouget-Laemmel, A. C.; Henry de Villeneuve, C.; Moraillon, A.; Ozanam, F.; Gabouze, N.; et al. Semiquantitative Study of the EDC/NHS Activation of Acid Terminal Groups at Modified Porous Silicon Surfaces. *Langmuir* **2010**, *26*, 809−814.
(158) Wang, Y.-S.; Yau, S.; Chau, L.-K.; Mohamed, A.; Huang, C.-J. Functional Biointerfaces Based on Mixed Zwitterionic Self-Assembled Monolayers for Biosensing Applications. *Langmuir* **2019**, *35*, 1652−1661.
(159) Brault, N. D.; White, A. D.; Taylor, A. D.; Yu, Q.; Jiang, S. Directly Functionalizable Surface Platform for Protein Arrays in Undiluted Human Blood Plasma. *Anal. Chem.* **2013**, *85*, 1447−1453.
(160) Qi, M.; Zhang, Y.; Cao, C.; Zhang, M.; Liu, S.; Liu, G. Decoration of Reduced Graphene Oxide Nanosheets with Aryldiazonium Salts and Gold Nanoparticles toward a Label-Free Amperometric Immunosensor for Detecting Cytokine Tumor Necrosis Factor-α in Live Cells. *Anal. Chem.* **2016**, *88*, 9614−9621.
(161) Wei, H.; Ni, S.; Cao, C.; Yang, G.-F.; Liu, G. Graphene Oxides Signal Reporters Based Multifunctional Immunosensing Platform for Amperometric Profiling of Multiple Cytokines in Serum. *ACS. Sens.* **2018**, *3*, 1553−1561.
(162) Ederth, T.; Lerm, M.; Orihuela, B.; Rittschof, D. Resistance of Zwitterionic Peptide Monolayers to Biofouling. *Langmuir* **2019**, *35*, 1818−1827.
(163) Lin, P.; Ding, L.; Lin, C. W.; Gu, F. Nonfouling Property of Zwitterionic Cysteine Surface. *Langmuir* **2014**, *30*, 6497−6507.
(164) Liu, N.; Hui, N.; Davis, J. J.; Luo, X. Low Fouling Protein Detection in Complex Biological Media Supported by a Designed Multifunctional Peptide. *ACS. Sens.* **2018**, *3*, 1210−1216.
(165) Ye, H.; Wang, L.; Huang, R.; Su, R.; Liu, B.; Qi, W.; He, Z. Superior Antifouling Performance of a Zwitterionic Peptide Compared to an Amphiphilic, Non-Ionic Peptide. *ACS Appl. Mater. Interfaces* **2015**, *7*, 22448−22457.
(166) Qian, H.; Huang, Y.; Duan, X.; Wei, X.; Fan, Y.; Gan, D.; Yue, S.; Cheng, W.; Chen, T. Fiber Optic Surface Plasmon Resonance Biosensor for Detection of PDGF-BB in Serum Based on Self-Assembled Aptamer and Antifouling Peptide Monolayer. *Biosens. Bioelectron.* **2019**, *140*, 111350.

https://dx.doi.org/10.1021/acs.chemrev.9b00739
Chem. Rev. XXXX, XXX, XXX−XXX

(167) Wang, G.; Han, R.; Su, X.; Li, Y.; Xu, G.; Luo, X. Zwitterionic Peptide Anchored to Conducting Polymer PEDOT for the Development of Antifouling and Ultrasensitive Electrochemical DNA Sensor. *Biosens. Bioelectron.* **2017**, *92*, 396−401.
(168) Liu, N.; Song, J.; Yanwei, L.; Davis, J. J.; Gao, F.; Luo, X. Electrochemical Aptasensor for Ultralow Fouling Cancer Cell Quantification in Complex Biological Media Based on Designed Branched Peptides. *Anal. Chem.* **2019**, *91*, 8334−8340.
(169) Liu, X.; Huang, R.; Su, R.; Qi, W.; Wang, L.; He, Z. Grafting Hyaluronic Acid onto Gold Surface to Achieve Low Protein Fouling in Surface Plasmon Resonance Biosensors. *ACS Appl. Mater. Interfaces* **2014**, *6*, 13034−13042.
(170) Niu, Y. L.; Chu, M. L.; Xu, P.; Meng, S. S.; Zhou, Q.; Zhao, W. B.; Zhao, B.; Shen, J. An Aptasensor Based on Heparin-Mimicking Hyperbranched Polyester with Anti-biofouling Interface for Sensitive Thrombin Detection. *Biosens. Bioelectron.* **2018**, *101*, 174−180.
(171) Moore, E.; Delalat, B.; Vasani, R.; McPhee, G.; Thissen, H.; Voelcker, N. H. Surface-Initiated Hyperbranched Polyglycerol as an Ultralow-Fouling Coating on Glass, Silicon, and Porous Silicon Substrates. *ACS Appl. Mater. Interfaces* **2014**, *6*, 15243−15252.
(172) Moore, E.; Delalat, B.; Vasani, R.; Thissen, H.; Voelcker, N. H. Patterning and Biofunctionalization of Antifouling Hyperbranched Polyglycerol Coatings. *Biomacromolecules* **2014**, *15*, 2735−2743.
(173) Chen, P. R.; Wang, T. C.; Chen, S. T.; Chen, H. Y.; Tsai, W. B. Development of Antifouling Hyperbranched Polyglycerol Layers on Hydroxyl Poly-p-xylylene Coatings. *Langmuir* **2017**, *33*, 14657−14662.
(174) Liu, Z.; An, X.; Dong, C.; Zheng, S.; Mi, B.; Hu, Y. Modification of Thin Film Composite Polyamide Membranes with 3D Hyperbranched Polyglycerol for Simultaneous Improvement in Their Filtration Performance and Antifouling Properties. *J. Mater. Chem. A* **2017**, *5*, 23190.
(175) Ma, L.; Jayachandran, S.; Li, Z.; Song, Z.; Wang, W.; Luo, X. Antifouling and Conducting PEDOT Derivative Grafted with Polyglycerol for Highly Sensitive Electrochemical Protein Detection in Complex Biological Media. *J. Electroanal. Chem.* **2019**, *840*, 272−278.
(176) Qi, H.; Li, S.; Li, C.; Li, X.; Gao, Q.; Zhang, C. Sensitive and Antifouling Impedimetric Aptasensor for the Determination of Thrombin in Undiluted Serum Sample. *Biosens. Bioelectron.* **2013**, *39*, 324−328.
(177) McQuistan, A.; Zaitouna, A. J.; Echeverria, E.; Lai, R. Y. Use of Thiolated Oligonucleotides as Anti-Fouling Diluents in Electrochemical Peptide-Based Sensors. *Chem. Commun.* **2014**, *50*, 4690−4692.
(178) Hui, l.; Xu, A.; Liu, H. DNA-Based Nanofabrication for Antifouling Applications. *Langmuir* **2019**, *35*, 12543−12549.
(179) Subbiahdoss, G.; Zeng, G.; Aslan, H.; Ege Friis, J.; Iruthayaraj, J.; Zelikin, A. N.; Meyer, R. L. Antifouling Properties of Layer by Layer DNA Coatings. *Biofouling* **2019**, *35*, 75−88.
(180) Nie, W.; Wang, Q.; Zou, L.; Zheng, Y.; Liu, X.; Yang, X.; Wang, K. Low-Fouling Surface Plasmon Resonance Sensor for Highly Sensitive Detection of MicroRNA in a Complex Matrix Based on the DNA Tetrahedron. *Anal. Chem.* **2018**, *90*, 12584−12591.
(181) McKeating, K. S.; Hinman, S. S.; Rais, N. A.; Zhou, Z.; Cheng, Q. Antifouling Lipid Membranes over Protein A for Orientation-Controlled Immunosensing in Undiluted Serum and Plasma. *ACS. Sens.* **2019**, *4*, 1774−1782.
(182) Hu, C.-M. J.; Fang, R. H.; Wang, K.-C.; Luk, B. T.; Thamphiwatana, S.; Dehaini, D.; Nguyen, P.; Angsantikul, P.; Wen, C. H.; Kroll, A. V.; et al. Nanoparticle Biointerfacing by Platelet Membrane Cloaking. *Nature* **2015**, *526*, 118−121.
(183) Piao, J.-G.; Wang, L.; Gao, F.; You, Y.-Z.; Xiong, Y.; Yang, L. Erythrocyte Membrane Is an Alternative Coating to Polyethylene Glycol for Prolonging the Circulation Lifetime of Gold Nanocages for Photothermal Therapy. *ACS Nano* **2014**, *8*, 10414−10425.
(184) Fan, B.; Fan, Q.; Cui, M.; Wu, T.; Wang, J.; Ma, H.; Wei, Q. Photoelectrochemical Biosensor for Sensitive Detection of Soluble CD44 Based on the Facile Construction of a Poly(ethylene glycol)/Hyaluronic Acid Hybrid Antifouling Interface. *ACS Appl. Mater. Interfaces* **2019**, *11*, 24764−24770.
(185) Xia, Y.; Adibnia, V.; Shan, C.; Huang, R.; Qi, W.; He, Z.; Xie, G.; Olszewski, M.; De Crescenzo, G.; Matyjaszewski, K.; et al. Synergy between Zwitterionic Polymers and Hyaluronic Acid Enhances Antifouling Performance. *Langmuir* **2019**, *35*, 15535−15542.
(186) Chen, L.; Zhao, S.; Liu, M.; Wu, P.; Chen, C. A Novel Label-Free Electrochemical Immunosensor Modified by Glutathione and Hyaluronic Acid for the Ultrasensitive and Ultraselective Detection of Brucellosis in Dilute Serum Done. *Sens. Actuators, B* **2019**, *287*, 510−516.
(187) Kim, S.; Lee, S.; Park, J.; Lee, J. Y. Electrochemical Co-deposition of Polydopamine/Hyaluronic Acid for Anti-Biofouling Bioelectrodes. *Front. Chem.* **2019**, *7*, 262.
(188) Ye, H.; Xia, Y.; Liu, Z.; Huang, R.; Su, R.; Qi, W.; Wang, L.; He, Z. Dopamine-Assisted Deposition and Zwitteration of Hyaluronic Acid for the Nanoscale Fabrication of Low-Fouling Surfaces. *J. Mater. Chem. B* **2016**, *4*, 4084−4091.
(189) Ye, H.; Che, J.; Huang, R.; Qi, W.; He, Z.; Su, R. Zwitterionic Peptide Enhances Protein-Resistant Performance of Hyaluronic Acid-Modified Surfaces. *Langmuir* **2020**, *36*, 1923−1929.
(190) Wei, Q.; Liu, X.; Yue, Q.; Ma, S.; Zhou, F. Mussel-Inspired One-Step Fabrication of Ultralow-Friction Coatings on Diverse Biomaterial Surfaces. *Langmuir* **2019**, *35*, 8068−8075.
(191) Xia, Y.; Adibnia, V.; Huang, R.; Murschel, F.; Faivre, J.; Xie, G.; Olszewski, M.; De Crescenzo, G.; Qi, W.; He, Z.; et al. Biomimetic Bottlebrush Polymer Coatings for Fabrication of Ultralow Fouling Surfaces. *Angew. Chem.* **2019**, *131*, 1322−1328.
(192) Ye, H.; Han, M.; Huang, R.; Schmidt, T. A.; Qi, W.; He, Z.; Martin, L. L.; Jay, G. D.; Su, R.; Greene, G. W. Interactions between Lubricin and Hyaluronic Acid Synergistically Enhance Antiadhesive Properties. *ACS Appl. Mater. Interfaces* **2019**, *11*, 18090−18102.
(193) Liu, G.; Qi, M.; Zhang, Y.; Cao, C.; Goldys, E. M. Nanocomposites of Gold Nanoparticles and Graphene Oxide towards an Stable Label-free Electrochemical Immunosensor for Detection of Cardiac Marker Troponin-I. *Anal. Chim. Acta* **2016**, *909*, 1−8.
(194) Wang, G. Z.; Wang, L. G.; Lin, W. F.; Wang, Z.; Zhang, J.; Ji, F. Q.; Ma, G. L.; Yuan, Z. F.; Chen, S. F. Development of Robust and Recoverable Ultralow-Fouling Coatings Based on Poly-(carboxybetaine) Ester Analogue. *ACS Appl. Mater. Interfaces* **2015**, *7*, 16938−16945.
(195) Sharma, R.; Deacon, S. E.; Nowak, D.; George, S.; Szymonik, M.; Tang, A.; Tomlinson, D.; Davies, A.; McPherson, M.; Wälti, C. Label-Free Electrochemical Impedance Biosensor to Detect Human Interleukin-8 in Serum with Sub-pg/mL Sensitivity. *Biosens. Bioelectron.* **2016**, *80*, 607−613.
(196) Lv, S.; Sheng, J.; Zhao, S.; Liu, M.; Chen, L. The Detection of Brucellosis Antibody in Whole Serum Based on the Low-fouling Electrochemical Immunosensor Fabricated with Magnetic Fe_3O_4@ Au@ PEG@ HA Nanoparticles. *Biosens. Bioelectron.* **2018**, *117*, 138−144.
(197) Bayramoglu, G.; Ozalp, C.; Oztekin, M.; Guler, U.; Salih, B.; Arica, M. Y. Design of an Aptamer-Based Magnetic Adsorbent and Biosensor Systems for Selective and Sensitive Separation and Detection of Thrombin. *Talanta* **2019**, *191*, 59−66.
(198) Mathew, D.; Beekman, P.; Lemay, S. G.; Zuilhof, H.; Le Gac, S.; van der Wiel, W. G. Electrochemical Detection of Tumor-Derived Extracellular Vesicles on Nano-interdigitated Electrodes. *Nano Lett.* **2020**, *20*, 820−828.
(199) He, X.; Han, H.; Liu, L.; Shi, W.; Lu, X.; Dong, J.; Yang, W.; Lu, X. Self-Assembled Microgels for Sensitive and Low-Fouling Detection of Streptomycin in Complex Media. *ACS Appl. Mater. Interfaces* **2019**, *11*, 13676−13684.
(200) Cui, M.; Wang, Y.; Jiao, M.; Jayachandran, S.; Wu, Y.; Fan, X.; Luo, X. Mixed Self-Assembled Aptamer and Newly Designed Zwitterionic Peptide as Antifouling Biosensing Interface for Electrochemical Detection of alpha-Fetoprotein. *ACS. Sens.* **2017**, *2*, 490−494.

https://dx.doi.org/10.1021/acs.chemrev.9b00739
Chem. Rev. XXXX, XXX, XXX−XXX

(201) Li, Y.; Wang, L.; Ding, C.; Luo, X. Highly Selective Ratiometric Electrogenerated Chemiluminescence Assay of DNA Methyltransferase Activity via Polyaniline and Anti-Fouling Peptide Modified Electrode. *Biosens. Bioelectron.* **2019**, *142*, 111553.
(202) Wang, Y.; Cui, M.; Jiao, M.; Luo, X. Antifouling and Ultrasensitive Biosensing Interface Based on Self-Assembled Peptide and Aptamer on Macroporous Gold for Electrochemical Detection of Immunoglobulin E in Serum. *Anal. Bioanal. Chem.* **2018**, *410*, 5871−5878.
(203) Fan, G.-C.; Li, Z.; Lu, Y.; Ma, L.; Zhao, H.; Luo, X. Robust Photoelectrochemical Cytosensor in Biological Media Using Anti-fouling Property of Zwitterionic Peptide. *Sens. Actuators, B* **2019**, *299*, 126996.
(204) Song, Z.; Li, Y.; Teng, H.; Ding, C.; Xu, G.; Luo, X. Designed Zwitterionic Peptide Combined with Sacrificial Fe-MOF for Low Fouling and Highly Sensitive Electrochemical Detection of T4 Polynucleotide Kinase. *Sens. Actuators, B* **2020**, *305*, 127329.
(205) Chang, P.-H.; Weng, C.-C.; Li, B.-R.; Li, Y.-K. An Antifouling Peptide-Based Biosensor for Determination of Streptococcus Pneumonia Markers in Human Serum. *Biosens. Bioelectron.* **2020**, *151*, 111969.
(206) Xu, Q.; Wang, G.; Zhang, M.; Xu, G.; Lin, J.; Luo, X. Aptamer Based Label Free Thrombin Assay Based on the Use of Silver Nanoparticles Incorporated into Self-Polymerized Dopamine. *Microchim. Acta* **2018**, *185*, 253.
(207) Wang, W.; Cui, M.; Song, Z.; Luo, X. An Antifouling Electrochemical Immunosensor for Carcinoembryonic Antigen Based on Hyaluronic Acid Doped Conducting Polymer PEDOT. *RSC Adv.* **2016**, *6*, 88411−88416.
(208) Liu, Z.; Wang, H. An Antifouling Interface Integrated with HRP-Based Amplification to Achieve Highly Sensitive Electrochemical Aptasensor for Lysozyme Detection. *Analyst* **2019**, *144*, 5794−5801.
(209) Baradoke, A.; Hein, R.; Li, X.; Davis, J. J. Reagentless Redox Capacitive Assaying of C-Reactive Protein at a Polyaniline Interface. *Anal. Chem.* **2020**, *92*, 3508−3511.
(210) Soto, R. J.; Hall, J. R.; Brown, M. D.; Taylor, J. B.; Schoenfisch, M. H. In Vivo Chemical Sensors: Role of Biocompatibility on Performance and Utility. *Anal. Chem.* **2017**, *89*, 276−299.
(211) Rong, G.; Corrie, S. R.; Clark, H. A. In Vivo Biosensing: Progress and Perspectives. *ACS. Sens.* **2017**, *2*, 327−338.
(212) Liu, J.; Yu, M.; Ning, X.; Zhou, C.; Yang, S.; Zheng, J. PEGylation and Zwitterionization: Pros and Cons in the Renal Clearance and Tumor Targeting of Near-IR-Emitting Gold Nanoparticles. *Angew. Chem.* **2013**, *125*, 12804−12808.
(213) Ruckh, T. T.; Clark, H. A. Implantable Nanosensors: Toward Continuous Physiologic Monitoring. *Anal. Chem.* **2014**, *86*, 1314−1323.
(214) Chatard, C.; Meiller, A.; Marinesco, S. Microelectrode Biosensors for in Vivo Analysis of Brain Interstitial Fluid. *Electroanalysis* **2018**, *30*, 977−998.
(215) Dardano, P.; Rea, I.; De Stefano, L. Microneedles Based Electrochemical Sensors: New Tools for Advanced Biosensing. *Curr. Opin. Electrochem.* **2019**, *17*, 121−127.
(216) Baranwal, A.; Chandra, P. Clinical Implications and Electrochemical Biosensing of Monoamine Neurotransmitters in Body Fluids, in Vitro, in Vivo, and Ex Vivo Models. *Biosens. Bioelectron.* **2018**, *121*, 137−152.
(217) Xiao, T.; Wu, F.; Hao, J.; Zhang, M.; Yu, P.; Mao, L. In Vivo Analysis with Electrochemical Sensors and Biosensors. *Anal. Chem.* **2017**, *89*, 300−313.
(218) Shibata, H.; Heo, Y. J.; Okitsu, T.; Matsunaga, Y.; Kawanishi, T.; Takeuchi, S. Injectable Hydrogel Microbeads for Fluorescence-Based in vivo Continuous Glucose Monitoring. *Proc. Natl. Acad. Sci. U. S. A.* **2010**, *107*, 17894−17898.
(219) He, Q.; Zhang, Z.; Gao, F.; Li, Y.; Shi, J. In vivo Biodistribution and Urinary Excretion of Mesoporous Silica Nanoparticles: Effects of Particle Size and PEGylation. *Small* **2011**, *7*, 271−280.
(220) Dudani, J. S.; Jain, P. K.; Kwong, G. A.; Stevens, K. R.; Bhatia, S. N. Photoactivated Spatiotemporally-Responsive Nanosensors of in Vivo Protease Activity. *ACS Nano* **2015**, *9*, 11708−11717.
(221) Wei, R.; Cai, Z.; Ren, B. W.; Li, A.; Lin, H.; Zhang, K.; Chen, H.; Shan, H.; Ai, H.; Gao, J. Biodegradable and Renal-Clearable Hollow Porous Iron Oxide Nanoboxes for In Vivo Imaging. *Chem. Mater.* **2018**, *30*, 7950−7961.
(222) Liu, W.; Choi, H. S.; Zimmer, J. P.; Tanaka, E.; Frangioni, J. V.; Bawendi, M. Compact Cysteine-Coated CdSe(ZnCdS) Quantum Dots for in Vivo Applications. *J. Am. Chem. Soc.* **2007**, *129*, 14530−14531.
(223) Soo Choi, H.; Liu, W.; Misra, P.; Tanaka, E.; Zimmer, J. P.; Itty Ipe, B.; Bawendi, M. G.; Frangioni, J. V. Renal Clearance of Quantum Dots. *Nat. Biotechnol.* **2007**, *25*, 1165.
(224) Breus, V. V.; Heyes, C. D.; Tron, K.; Nienhaus, G. U. Zwitterionic Biocompatible Quantum Dots for Wide pH Stability and Weak Nonspecific Binding to Cells. *ACS Nano* **2009**, *3*, 2573−2580.
(225) Kozai, T. D. Y.; Langhals, N. B.; Patel, P. R.; Deng, X.; Zhang, H.; Smith, K. L.; Lahann, J.; Kotov, N. A.; Kipke, D. R. Ultrasmall Implantable Composite Microelectrodes with Bioactive Surfaces for Chronic Neural Interfaces. *Nat. Mater.* **2012**, *11*, 1065−1073.
(226) Schwerdt, H. N.; Zhang, E.; Kim, M. J.; Yoshida, T.; Stanwicks, L.; Amemori, S.; Dagdeviren, H. E.; Langer, R.; Cima, M. J.; Graybiel, A. M. Cellular-Scale Probes Enable Stable Chronic Subsecond Monitoring of Dopamine Neurochemicals in a Rodent Model. *Commun. Biol.* **2018**, *1*, 144.
(227) Obidin, N.; Tasnim, F.; Dagdeviren, C. The Future of Neuroimplantable Devices: A Materials Science and Regulatory Perspective. *Adv. Mater.* **2019**, *0*, 201901482.
(228) Huang, Y.; Geng, X.; Li, L.; Stein, J. F.; Aziz, T. Z.; Green, A. L.; Wang, S. Measuring Complex Behaviors of Local Oscillatory Networks in Deep Brain Local Field Potentials. *J. Neurosci. Methods* **2016**, *264*, 25−32.
(229) Huang, Y.; Luo, H.; Green, A. L.; Aziz, T. Z.; Wang, S. Characteristics of Local Field Potentials Correlate with Pain Relief by Deep Brain Stimulation. *Clin. Neurophysiol.* **2016**, *127*, 2573−2580.
(230) Huang, Y.; Green, A. L.; Hyam, J.; Fitzgerald, J.; Aziz, T. Z.; Wang, S. Oscillatory Neural Representations in the Sensory Thalamus Predict Neuropathic Pain Relief by Deep Brain Stimulation. *Neurobiol. Dis.* **2018**, *109*, 117−126.
(231) Machado, R.; Soltani, N.; Dufour, S.; Salam, M.; Carlen, P.; Genov, R.; Thompson, M. Biofouling-Resistant Impedimetric Sensor for Array High-Resolution Extracellular Potassium Monitoring in the Brain. *Biosensors* **2016**, *6*, 53.
(232) Smart, S. L.; Lopantsev, V.; Zhang, C.; Robbins, C. A.; Wang, H.; Chiu, S.; Schwartzkroin, P. A.; Messing, A.; Tempel, B. L. Deletion of the Kv1. 1 Potassium Channel Causes Epilepsy in Mice. *Neuron* **1998**, *20*, 809−819.
(233) Robinson, K. J.; Huynh, G. T.; Kouskousis, B. P.; Fletcher, N. L.; Houston, Z. H.; Thurecht, K. J.; Corrie, S. R. Modified Organosilica Core−Shell Nanoparticles for Stable pH Sensing in Biological Solutions. *ACS. Sens.* **2018**, *3*, 967−975.
(234) Miller, C. R.; Vogel, R.; Surawski, P. P. T.; Jack, K. S.; Corrie, S. R.; Trau, M. Functionalized Organosilica Microspheres via a Novel Emulsion-Based Route. *Langmuir* **2005**, *21*, 9733−9740.
(235) Cash, K. J.; Clark, H. A. Phosphorescent Nanosensors for In Vivo Tracking of Histamine Levels. *Anal. Chem.* **2013**, *85*, 6312−6318.
(236) Dubach, J. M.; Harjes, D. I.; Clark, H. A. Fluorescent Ion-Selective Nanosensors for Intracellular Analysis with Improved Lifetime and Size. *Nano Lett.* **2007**, *7*, 1827−1831.
(237) Querfurth, H. W.; LaFerla, F. M. Alzheimer's Disease. *N. Engl. J. Med.* **2010**, *362*, 329−344.
(238) Zhen, X.; Zhang, C.; Xie, C.; Miao, Q.; Lim, K. L.; Pu, K. Intraparticle Energy Level Alignment of Semiconducting Polymer Nanoparticles to Amplify Chemiluminescence for Ultrasensitive In Vivo Imaging of Reactive Oxygen Species. *ACS Nano* **2016**, *10*, 6400−6409.

https://dx.doi.org/10.1021/acs.chemrev.9b00739
Chem. Rev. XXXX, XXX, XXX−XXX

(239) Shuhendler, A. J.; Pu, K.; Cui, L.; Uetrecht, J. P.; Rao, J. Real-Time Imaging of Oxidative and Nitrosative Stress in the Liver of Live Animals for Drug-Toxicity Testing. *Nat. Biotechnol.* **2014**, *32*, 373−380.
(240) Xie, J.; Zhang, F.; Aronova, M.; Zhu, L.; Lin, X.; Quan, Q.; Liu, G.; Zhang, G.; Choi, K.-Y.; Kim, K.; et al. Manipulating the Power of an Additional Phase: A Flower-like Au−Fe_3O_4 Optical Nanosensor for Imaging Protease Expressions In Vivo. *ACS Nano* **2011**, *5*, 3043−3051.
(241) Abu Lila, A. S.; Kiwada, H.; Ishida, T. The Accelerated Blood Clearance (ABC) Phenomenon: Clinical Challenge and Approaches to Manage. *J. Controlled Release* **2013**, *172*, 38−47.
(242) Schellekens, H.; Hennink, W. E.; Brinks, V. The Immunogenicity of Polyethylene Glycol: Facts and Fiction. *Pharm. Res.* **2013**, *30*, 1729−1734.
(243) Herzenberg, L. A.; Tokuhisa, T. Epitope-specific regulation. I. Carrier-Specific Induction of Suppression for IgG Anti-Hapten Antibody Responses. *J. Exp. Med.* **1982**, *155*, 1730−1740.
(244) Liu, X.; Xiao, T.; Wu, F.; Shen, M. Y.; Zhang, M.; Yu, H. h.; Mao, L. Ultrathin Cell-Membrane-Mimic Phosphorylcholine Polymer Film Coating Enables Large Improvements for In Vivo Electrochemical Detection. *Angew. Chem., Int. Ed.* **2017**, *56*, 11802−11806.
(245) Qi, M.; Huang, J.; Wei, H.; Cao, C.; Feng, S.; Guo, Q.; Goldys, E. M.; Li, R.; Liu, G. Graphene Oxide Thin Film with Dual Function Integrated into a Nanosandwich Device for In Vivo Monitoring of Interleukin-6. *ACS Appl. Mater. Interfaces* **2017**, *9*, 41659−41668.
(246) Li, H.; Dauphin-Ducharme, P.; Arroyo-Currás, N.; Tran, C. H.; Vieira, P. A.; Li, S.; Shin, C.; Somerson, J.; Kippin, T. E.; Plaxco, K. W. A Biomimetic Phosphatidylcholine-Terminated Monolayer Greatly Improves the In Vivo Performance of Electrochemical Aptamer-Based Sensors. *Angew. Chem., Int. Ed.* **2017**, *56*, 7492−7495.
(247) Baker, B. R.; Lai, R. Y.; Wood, M. S.; Doctor, E. H.; Heeger, A. J.; Plaxco, K. W. An Electronic, Aptamer-Based Small-Molecule Sensor for the Rapid, Label-Free Detection of Cocaine in Adulterated Samples and Biological Fluids. *J. Am. Chem. Soc.* **2006**, *128*, 3138−3139.
(248) Zuo, X.; Xiao, Y.; Plaxco, K. W. High Specificity, Electrochemical Sandwich Assays Based on Single Aptamer Sequences and Suitable for the Direct Detection of Small-Molecule Targets in Blood and Other Complex Matrices. *J. Am. Chem. Soc.* **2009**, *131*, 6944−6945.
(249) Hamburg, M. A.; Collins, F. S. The Path to Personalized Medicine. *N. Engl. J. Med.* **2010**, *363*, 301−304.
(250) Li, X.; Deng, D.; Xue, J.; Qu, L.; Achilefu, S.; Gu, Y. Quantum Dots Based Molecular Beacons for In Vitro and In Vivo Detection of MMP-2 on Tumor. *Biosens. Bioelectron.* **2014**, *61*, 512−518.
(251) Choi, Y.; Kim, S.; Choi, M.-H.; Ryoo, S.-R.; Park, J.; Min, D.-H.; Kim, B.-S. Highly Biocompatible Carbon Nanodots for Simultaneous Bioimaging and Targeted Photodynamic Therapy In Vitro and In Vivo. *Adv. Funct. Mater.* **2014**, *24*, 5781−5789.
(252) Pu, K.; Shuhendler, A. J.; Rao, J. Semiconducting Polymer Nanoprobe for In Vivo Imaging of Reactive Oxygen and Nitrogen Species. *Angew. Chem., Int. Ed.* **2013**, *52*, 10325−10329.
(253) Iverson, N. M.; Barone, P. W.; Shandell, M.; Trudel, L. J.; Sen, S.; Sen, F.; Ivanov, V.; Atolia, E.; Farias, E.; McNicholas, T. P.; et al. In Vivo Biosensing via Tissue-Localizable Near-Infrared-Fluorescent Single-Walled Carbon Nanotubes. *Nat. Nanotechnol.* **2013**, *8*, 873.
(254) Xiong, L.; Shuhendler, A. J.; Rao, J. Self-Luminescing BRET-FRET Near-Infrared Dots for In Vivo Lymph-Node Mapping and Tumour Imaging. *Nat. Commun.* **2012**, *3*, 1193.
(255) He, R.; Niu, Y.; Li, Z.; Li, A.; Yang, H.; Xu, F.; Li, F. A Hydrogel Microneedle Patch for Point-of-Care Testing Based on Skin Interstitial Fluid. *Adv. Healthcare Mater.* **2020**, *9*, 1901201.
(256) Zhou, L.; Hou, H.; Wei, H.; Yao, L.; Sun, L.; Yu, P.; Su, B.; Mao, L. In Vivo Monitoring of Oxygen in Rat Brain by Carbon Fiber Microelectrode Modified with Antifouling Nanoporous Membrane. *Anal. Chem.* **2019**, *91*, 3645−3651.
(257) Hao, J.; Xiao, T.; Wu, F.; Yu, P.; Mao, L. High Antifouling Property of Ion-Selective Membrane: Toward In Vivo Monitoring of pH Change in Live Brain of Rats with Membrane-Coated Carbon Fiber Electrodes. *Anal. Chem.* **2016**, *88*, 11238−11243.
(258) Feng, T.; Ji, W.; Tang, Q.; Wei, H.; Zhang, S.; Mao, J.; Zhang, Y.; Mao, L.; Zhang, M. Low-Fouling Nanoporous Conductive Polymer-Coated Microelectrode for In Vivo Monitoring of Dopamine in the Rat Brain. *Anal. Chem.* **2019**, *91*, 10786−10791.
(259) Ferguson, B. S.; Hoggarth, D. A.; Maliniak, D.; Ploense, K.; White, R. J.; Woodward, N.; Hsieh, K.; Bonham, A. J.; Eisenstein, M.; Kippin, T. E.; et al. Real-Time, Aptamer-Based Tracking of Circulating Therapeutic Agents in Living Animals. *Sci. Transl. Med.* **2013**, *5*, 213ra165.
(260) Arroyo-Currás, N.; Somerson, J.; Vieira, P. A.; Ploense, K. L.; Kippin, T. E.; Plaxco, K. W. Real-Time Measurement of Small Molecules Directly in Awake, Ambulatory Animals. *Proc. Natl. Acad. Sci. U. S. A.* **2017**, *114*, 645−650.
(261) Rivas, L.; Dulay, S.; Miserere, S.; Pla, L.; Marin, S. B.; Parra, J.; Eixarch, E.; Gratacós, E.; Illa, M.; Mir, M.; et al. Micro-Needle Implantable Electrochemical Oxygen Sensor: Ex-Vivo and In-Vivo Studies. *Biosens. Bioelectron.* **2020**, *153*, 112028.
(262) Vreeland, R. F.; Atcherley, C. W.; Russell, W. S.; Xie, J. Y.; Lu, D.; Laude, N. D.; Porreca, F.; Heien, M. L. Biocompatible PEDOT:Nafion Composite Electrode Coatings for Selective Detection of Neurotransmitters In Vivo. *Anal. Chem.* **2015**, *87*, 2600−2607.
(263) Patel, J.; Radhakrishnan, L.; Zhao, B.; Uppalapati, B.; Daniels, R. C.; Ward, K. R.; Collinson, M. M. Electrochemical Properties of Nanostructured Porous Gold Electrodes in Biofouling Solutions. *Anal. Chem.* **2013**, *85*, 11610−11618.
(264) Daggumati, P.; Matharu, Z.; Seker, E. Effect of Nanoporous Gold Thin Film Morphology on Electrochemical DNA Sensing. *Anal. Chem.* **2015**, *87*, 8149−8156.
(265) Chapman, C. A. R.; Chen, H.; Stamou, M.; Biener, J.; Biener, M. M.; Lein, P. J.; Seker, E. Nanoporous Gold as a Neural Interface Coating: Effects of Topography, Surface Chemistry, and Feature Size. *ACS Appl. Mater. Interfaces* **2015**, *7*, 7093−7100.
(266) Daggumati, P.; Matharu, Z.; Wang, L.; Seker, E. Biofouling-Resilient Nanoporous Gold Electrodes for DNA Sensing. *Anal. Chem.* **2015**, *87*, 8618−8622.
(267) Liu, Z.; Zhang, H.; Hou, S.; Ma, H. Highly Sensitive and Selective Electrochemical Detection of L-Cysteine Using Nanoporous Gold. *Microchim. Acta* **2012**, *177*, 427−433.
(268) Silva, T. A.; Khan, M. R. K.; Fatibello-Filho, O.; Collinson, M. M. Simultaneous Electrochemical Sensing of Ascorbic Acid and Uric Acid under Biofouling Conditions Using Nanoporous Gold Electrodes. *J. Electroanal. Chem.* **2019**, *846*, 113160.
(269) Wu, S.; Lan, X.; Huang, F.; Luo, Z.; Ju, H.; Meng, C.; Duan, C. Selective Electrochemical Detection of Cysteine in Complex Serum by Graphene Nanoribbon. *Biosens. Bioelectron.* **2012**, *32*, 293−296.
(270) Sun, Q.; Yan, F.; Yao, L.; Su, B. Anti-Biofouling Isoporous Silica-Micelle Membrane Enabling Drug Detection in Human Whole Blood. *Anal. Chem.* **2016**, *88*, 8364−8368.
(271) Zhou, J.; Zhang, L.; Tian, Y. Micro Electrochemical pH Sensor Applicable for Real-Time Ratiometric Monitoring of pH Values in Rat Brains. *Anal. Chem.* **2016**, *88*, 2113−2118.
(272) Zhou, L.; Ding, H.; Yan, F.; Guo, W.; Su, B. Electrochemical Detection of Alzheimer's Disease Related Substances in Biofluids by Silica Nanochannel Membrane Modified Glassy Carbon Electrodes. *Analyst* **2018**, *143*, 4756−4763.
(273) Yan, F.; Zheng, W.; Yao, L.; Su, B. Direct Electrochemical Analysis in Complex Samples Using ITO Electrodes Modified with Permselective Membranes Consisting of Vertically Ordered Silica Mesochannels and Micelles. *Chem. Commun.* **2015**, *51*, 17736−17739.
(274) Zhang, L.; Xu, J.; Tang, Y.; Hou, J.; Yu, L.; Gao, C. A Novel Long-Lasting Antifouling Membrane Modified with Bifunctional Capsaicin-Mimic Moieties via in Situ Polymerization for Efficient water Purification. *J. Mater. Chem. A* **2016**, *4*, 10352−10362.

https://dx.doi.org/10.1021/acs.chemrev.9b00739
Chem. Rev. XXXX, XXX, XXX−XXX

(275) Kongsuphol, P.; Ng, H. H.; Pursey, J. P.; Arya, S. K.; Wong, C. C.; Stulz, E.; Park, M. K. EIS-Based Biosensor for Ultra-Sensitive Detection of TNF-α from Non-Diluted Human Serum. *Biosens. Bioelectron.* **2014**, *61*, 274−279.
(276) Mei, N.; Seale, B.; Ng, A. H. C.; Wheeler, A. R.; Oleschuk, R. Digital Microfluidic Platform for Human Plasma Protein Depletion. *Anal. Chem.* **2014**, *86*, 8466−8472.
(277) Olsen, S. M.; Pedersen, L. T.; Laursen, M.; Kiil, S.; Dam-Johansen, K. Enzyme-Based Antifouling Coatings: A Review. *Biofouling* **2007**, *23*, 369−383.
(278) Kristensen, J. B.; Meyer, R. L.; Laursen, B. S.; Shipovskov, S.; Besenbacher, F.; Poulsen, C. H. Antifouling Enzymes and the Biochemistry of Marine Settlement. *Biotechnol. Adv.* **2008**, *26*, 471−481.
(279) Shi, Q.; Su, Y.; Ning, X.; Chen, W.; Peng, J.; Jiang, Z. Trypsin-Enabled Construction of Anti-Fouling and Self-Cleaning Polyethersulfone Membrane. *Bioresour. Technol.* **2011**, *102*, 647−651.
(280) Koseoglu-Imer, D. Y.; Dizge, N.; Koyuncu, I. Enzymatic Activation of Cellulose Acetate Membrane for Reducing of Protein Fouling. *Colloids Surf., B* **2012**, *92*, 334−339.
(281) Harreither, W.; Trouillon, R.; Poulin, P.; Neri, W.; Ewing, A. G.; Safina, G. Cysteine Residues Reduce the Severity of Dopamine Electrochemical Fouling. *Electrochim. Acta* **2016**, *210*, 622−629.
(282) Zhang, L.; Cao, Z.; Bai, T.; Carr, L.; Ella-Menye, J.-R.; Irvin, C.; Ratner, B. D.; Jiang, S. Zwitterionic Hydrogels Implanted in Mice Resist the Foreign-Body Reaction. *Nat. Biotechnol.* **2013**, *31*, 553−556.
(283) Zhong, S.; Campoccia, D.; Doherty, P.; Williams, R.; Benedetti, L.; Williams, D. Biodegradation of Hyaluronic Acid Derivatives by Hyaluronidase. *Biomaterials* **1994**, *15*, 359−365.
(284) Zhang, L.; Chang, H.; Hirata, A.; Wu, H.; Xue, Q.-K.; Chen, M. Nanoporous Gold Based Optical Sensor for Sub-ppt Detection of Mercury Ions. *ACS Nano* **2013**, *7*, 4595−4600.
(285) Chapman, R. G.; Ostuni, E.; Yan, L.; Whitesides, G. M. Preparation of Mixed Self-Assembled Monolayers (SAMs) That Resist Adsorption of Proteins Using the Reaction of Amines with a SAM That Presents Interchain Carboxylic Anhydride Groups. *Langmuir* **2000**, *16*, 6927−6936.
(286) Liu; Gooding, J. J. An Interface Comprising Molecular Wires and Poly(ethylene glycol) Spacer Units Self-Assembled on Carbon Electrodes for Studies of Protein Electrochemistry. *Langmuir* **2006**, *22*, 7421−7430.
(287) Li, B.; Jain, P.; Ma, J.; Smith, J. K.; Yuan, Z.; Hung, H.-C.; He, Y.; Lin, X.; Wu, K.; Pfaendtner, J.; et al. Trimethylamine N-Oxide−Derived Zwitterionic Polymers: A New Class of Ultralow Fouling Bioinspired Materials. *Sci. Adv.* **2019**, *5*, No. eaaw9562.
(288) Chelmowski, R.; Köster, S. D.; Kerstan, A.; Prekelt, A.; Grunwald, C.; Winkler, T.; Metzler-Nolte, N.; Terfort, A.; Wöll, C. Peptide-Based SAMs that Resist the Adsorption of Proteins. *J. Am. Chem. Soc.* **2008**, *130*, 14952−14953.
(289) Sabaté del Río, J.; Henry, O. Y. F.; Jolly, P.; Ingber, D. E. An Antifouling Coating that Enables Affinity-Based Electrochemical Biosensing in Complex Biological Fluids. *Nat. Nanotechnol.* **2019**, *14*, 1143−1149.
(290) Sun, T. L.; Kurokawa, T.; Kuroda, S.; Ihsan, A. B.; Akasaki, T.; Sato, K.; Haque, M. A.; Nakajima, T.; Gong, J. P. Physical Hydrogels Composed of Polyampholytes Demonstrate High Toughness and Viscoelasticity. *Nat. Mater.* **2013**, *12*, 932−937.
(291) Dong, Q.; Liu, J.; Song, L.; Shao, G. Novel Zwitterionic Inorganic−Organic Hybrids: Synthesis of Hybrid Adsorbents and Their Applications for Cu^{2+} Removal. *J. Hazard. Mater.* **2011**, *186*, 1335−1342.
(292) Liu, J.; Ma, Y.; Xu, T.; Shao, G. Preparation of Zwitterionic Hybrid Polymer and Its Application for the Removal of Heavy Metal Ions from Water. *J. Hazard. Mater.* **2010**, *178*, 1021−1029.
(293) Yeom, J.; Guimaraes, P. P. G.; Ahn, H. M.; Jung, B.-K.; Hu, Q.; McHugh, K.; Mitchell, M. J.; Yun, C.-O.; Langer, R.; Jaklenec, A. Chiral Supraparticles for Controllable Nanomedicine. *Adv. Mater.* **2020**, *32*, 1903878.
(294) Qi, H.; Zheng, W.; Zhou, X.; Zhang, C.; Zhang, L. A Mussel-Inspired Chimeric Protein as a Novel Facile Antifouling Coating. *Chem. Commun.* **2018**, *54*, 11328−11331.
(295) Qi, H.; Zheng, W.; Zhang, C.; Zhou, X.; Zhang, L. Novel Mussel-Inspired Universal Surface Functionalization Strategy: Protein-Based Coating with Residue-Specific Post-Translational Modification in Vivo. *ACS Appl. Mater. Interfaces* **2019**, *11*, 12846−12853.
(296) Yang, C.; He, G.; Zhang, A.; Wu, Q.; Zhou, L.; Hang, T.; Liu, D.; Xiao, S.; Chen, H.-J.; Liu, F.; et al. Injectable Slippery Lubricant-Coated Spiky Microparticles with Persistent and Exceptional Biofouling-Resistance. *ACS Cent. Sci.* **2019**, *5*, 250−258.
(297) Badv, M.; Imani, S. M.; Weitz, J. I.; Didar, T. F. Lubricant-Infused Surfaces with Built-In Functional Biomolecules Exhibit Simultaneous Repellency and Tunable Cell Adhesion. *ACS Nano* **2018**, *12*, 10890−10902.
(298) Greene, G. W.; Ortiz, V.; Pozo-Gonzalo, C.; Moulton, S. E.; Wang, X.; Martin, L. L.; Michalczky, A.; Howlett, P. C. Lubricin Antiadhesive Coatings Exhibit Size-Selective Transport Properties that Inhibit Biofouling of Electrode Surfaces with Minimal Loss in Electrochemical Activity. *Adv. Mater. Interfaces* **2018**, *5*, 1701296.
(299) Silva, S. M.; Quigley, A. F.; Kapsa, R. M. I.; Greene, G. W.; Moulton, S. E. Lubricin on Platinum Electrodes: A Low-Impedance Protein-Resistant Surface Towards Biomedical Implantation. *ChemElectroChem* **2019**, *6*, 1939−1943.
(300) Ruiz-Valdepeñas Montiel, V.; Sempionatto, J. R.; Esteban-Fernández de Ávila, B.; Whitworth, A.; Campuzano, S.; Pingarrón, J. M.; Wang, J. Delayed Sensor Activation Based on Transient Coatings: Biofouling Protection in Complex Biofluids. *J. Am. Chem. Soc.* **2018**, *140*, 14050−14053.
(301) Laschewsky, A.; Rosenhahn, A. Molecular Design of Zwitterionic Polymer Interfaces: Searching for the Difference. *Langmuir* **2019**, *35*, 1056−1071.
(302) Quan, X.; Zhao, D.; Li, L.; Zhou, J. Understanding the Cellular Uptake of pH-Responsive Zwitterionic Gold Nanoparticles: A Computer Simulation Study. *Langmuir* **2017**, *33*, 14480−14489.
(303) Liu, C.; Guo, J.; Tian, F.; Yang, N.; Yan, F.; Ding, Y.; Wei, J.; Hu, G.; Nie, G.; Sun, J. Field-Free Isolation of Exosomes from Extracellular Vesicles by Microfluidic Viscoelastic Flows. *ACS Nano* **2017**, *11*, 6968−6976.
(304) Lee, K.; Shao, H.; Weissleder, R.; Lee, H. Acoustic Purification of Extracellular Microvesicles. *ACS Nano* **2015**, *9*, 2321−2327.
(305) Wu, M.; Ouyang, Y.; Wang, Z.; Zhang, R.; Huang, P.-H.; Chen, C.; Li, H.; Li, P.; Quinn, D.; Dao, M.; et al. Isolation of Exosomes from Whole Blood by Integrating Acoustics and Microfluidics. *Proc. Natl. Acad. Sci. U. S. A.* **2017**, *114*, 10584−10589.
(306) Bagheri, M.; Akbari, A.; Mirbagheri, S. A. Advanced Control of Membrane Fouling in Filtration Systems Using Artificial Intelligence and Machine Learning Techniques: A Critical Review. *Process Saf. Environ. Prot.* **2019**, *123*, 229.
(307) Ko, J.; Bhagwat, N.; Yee, S. S.; Ortiz, N.; Sahmoud, A.; Black, T.; Aiello, N. M.; McKenzie, L.; O'Hara, M.; Redlinger, C.; et al. Combining Machine Learning and Nanofluidic Technology To Diagnose Pancreatic Cancer Using Exosomes. *ACS Nano* **2017**, *11*, 11182−11193.
(308) Ohayon, D.; Nikiforidis, G.; Savva, A.; Giugni, A.; Wustoni, S.; Palanisamy, T.; Chen, X.; Maria, I. P.; Di Fabrizio, E.; Costa, P. M. F. J.; et al. Biofuel Powered Glucose Detection in Bodily Fluids with an n-Type Conjugated Polymer. *Nat. Mater.* **2019**, 1−8.
(309) Lee, H.; Hong, Y. J.; Baik, S.; Hyeon, T.; Kim, D. H. Enzyme-Based Glucose Sensor: From Invasive to Wearable Device. *Adv. Healthcare Mater.* **2018**, *7*, 1701150.
(310) Lee, H.; Song, C.; Hong, Y. S.; Kim, M. S.; Cho, H. R.; Kang, T.; Shin, K.; Choi, S. H.; Hyeon, T.; Kim, D.-H. Wearable/Disposable Sweat-Based Glucose Monitoring Device with Multistage Transdermal Drug Delivery Module. *Sci. Adv.* **2017**, *3*, No. e1601314.
(311) Chen, Y.; Lu, S.; Zhang, S.; Li, Y.; Qu, Z.; Chen, Y.; Lu, B.; Wang, X.; Feng, X. Skin-like Biosensor System via Electrochemical

https://dx.doi.org/10.1021/acs.chemrev.9b00739
Chem. Rev. XXXX, XXX, XXX−XXX

Channels for Noninvasive Blood Glucose Monitoring. *Sci. Adv.* **2017**, *3*, No. e1701629.
(312) Rivera, K. R.; Pozdin, V. A.; Young, A. T.; Erb, P. D.; Wisniewski, N. A.; Magness, S. T.; Daniele, M. Integrated Phosphorescence-Based Photonic Biosensor (iPOB) for Monitoring Oxygen Levels in 3D Cell Culture Systems. *Biosens. Bioelectron.* **2019**, *123*, 131−140.
(313) Piya, R.; Zhu, Y.; Soeriyadi, A. H.; Silva, S. M.; Reece, P. J.; Gooding, J. J. Micropatterning of Porous Silicon Bragg Reflectors With Poly (Ethylene Glycol) to Fabricate Cell Microarrays: Towards Single Cell Sensing. *Biosens. Bioelectron.* **2019**, *127*, 229−235.
(314) Parker, S. G.; Yang, Y.; Ciampi, S.; Gupta, B.; Kimpton, K.; Mansfeld, F. M.; Kavallaris, M.; Gaus, K.; Gooding, J. J. A Photoelectrochemical Platform for the Capture and Release of Rare Single Cells. *Nat. Commun.* **2018**, *9*, 2288.

https://dx.doi.org/10.1021/acs.chemrev.9b00739
Chem. Rev. XXXX, XXX, XXX−XXX